RECEIVED
LAWRENCE
RADIATION LABORATORY

DEC 8 1970

LIBRARY AND
DOCUMENTS SECTION

UCRL-20139
C.2

ELECTRON DIFFRACTION TECHNIQUE FOR THE DETERMINATION OF CRYSTALLINE STRUCTURE OF BETA GLYCINE

Wai-Kit Quon
(Ph. D. Thesis)

October 1970

AEC Contract No. W-7405-eng-48

TWO-WEEK LOAN COPY

This is a Library Circulating Copy which may be borrowed for two weeks. For a personal retention copy, call Tech. Info. Division, Ext. 5545

UCRL-20139
C.2

LAWRENCE RADIATION LABORATORY
UNIVERSITY of CALIFORNIA BERKELEY

DISCLAIMER

This document was prepared as an account of work sponsored by the United States Government. While this document is believed to contain correct information, neither the United States Government nor any agency thereof, nor the Regents of the University of California, nor any of their employees, makes any warranty, express or implied, or assumes any legal responsibility for the accuracy, completeness, or usefulness of any information, apparatus, product, or process disclosed, or represents that its use would not infringe privately owned rights. Reference herein to any specific commercial product, process, or service by its trade name, trademark, manufacturer, or otherwise, does not necessarily constitute or imply its endorsement, recommendation, or favoring by the United States Government or any agency thereof, or the Regents of the University of California. The views and opinions of authors expressed herein do not necessarily state or reflect those of the United States Government or any agency thereof or the Regents of the University of California.

ELECTRON DIFFRACTION TECHNIQUE FOR THE DETERMINATION OF THE CRYSTALLINE STRUCTURE OF β GLYCINE

By

Wai-Kit Quon

ABSTRACT

The method of electron diffraction is applied to the investigation of the crystalline structure of β glycine. The structure as determined by x-ray diffraction methods is used as a standard of the investigation. The emphasis of the research is therefore on the evaluation of the electron diffraction technique and the effects of dynamical scattering, rather than on the redetermination of the glycine structure.

It is shown that the Patterson map is similar to the inter-atomic vector map calculated from the atom coordinates of the x-ray determined standard structure. Hence it can either be interpreted kinematically, or it is not sensitive enough to show moderate dynamical effects.

A test based on the Two Beam dynamical scattering theory shows that the sample is weakly dynamical and has an estimated mean thickness of about 1300 Å.

Dynamical effects play a more important role in electron diffraction than in x-ray diffraction. The effect of dynamical scattering is not corrected for in the work reported here, and it is found that the resulting reliability

factor of the determined structure is about 0.48, which indicates a very low level of confidence. Therefore, dynamical scattering must be corrected for if an accurate determination of crystal structure is to be attempted.

Hydrogen positions are easily detectable in the difference Fourier synthesis map. This shows that scattering by hydrogen is much stronger in electron diffraction than in x-ray diffraction. It is suggested that hydrogen atoms should be included into the structural analysis at an earlier stage than that of the normal x-ray diffraction procedures.

The extent to which dynamical scattering limits the usefulness of electron diffraction intensity data for crystallographic determination has also evident significance for the interpretation of high resolution structures that might be obtained by electron optical imaging of the scattered radiation.

CONTENTS

CHAPTER		Page
ABSTRACT		ii
	PART I: INTRODUCTION AND THEORY	
I.	INTRODUCTION	2
II.	THEORY OF ELECTRON DIFFRACTION	7
	PART II: METHODS AND MATERIALS	
III.	SPECIMEN PREPARATION	16
IV.	SELECTED AREA DIFFRACTION TECHNIQUE	19
V.	DATA COLLECTION	24
VI.	DATA CONVERSION	28
VII.	STRUCTURAL DETERMINATION PROGRAMS	46
	PART III: RESULTS	
VIII.	THE PATTERSON PLOT	51
IX.	STRUCTURE OF β GLYCINE	72
X.	EXTENT OF DYNAMICAL SCATTERING	106
XI.	CONCLUSION AND SUMMARY	117
REFERENCES		121
APPENDIX A:	ATOMIC SCATTERING TABLE	124
APPENDIX B:	EXPERIMENTAL AND CALCULATED SCATTERING AMPLITUDES	125

PART I:

INTRODUCTION AND THEORY

I. INTRODUCTION

The phenomenon of electron diffraction was first discovered in 1927 by Davisson and Germer. The first photographic record of diffraction patterns was obtained by G. P. Thomson from polycrystalline films of gold and other metals [1]. Since their discovery, electron diffraction methods have constituted an important tool in solving the structure of matter, in addition to or supplementing the method of x-ray diffraction, which was first demonstrated in 1912 [2,5,4]. X-ray diffraction has of course proven to be the more powerful tool of the two in the structural determination of crystalline materials.

Electron, x-ray and neutron diffraction share the same basic scattering theory. X-ray diffraction gives the distribution of electron density, electron diffraction gives the distribution of electric potential and neutron diffraction gives the distribution of nuclear scattering potentials within the crystal. Any of these distributions, however, is able to map the locations of atoms within the molecule. All three methods compliment each other. X-ray diffraction leads substantially in both the degree of reliability and sophistication, while electron diffraction and neutron diffraction

have yet to come of age.

While x-ray diffraction has many advantages over the other techniques, electron diffraction can claim the following advantages which makes it desirable:

1. The ability to handle extremely small quantities of material (about 10^{-12}gm quite easily). X-ray diffraction in general requires considerably larger crystals to be grown.

2. Simplicity in specimen preparation.

3. The ability to observe visually the diffraction pattern before recording.

4. The intensities of reflection are much higher than in either x-ray or neutron diffraction (10^6 times higher than for x-rays and 10^8 times higher than for neutron [5]). This enables much shorter recording times.

5. With selected area diffraction techniques, an image of the specimen area under investigation can be obtained in conjunction with the recording of a diffraction pattern. Radiation damage may be the ultimate limitation to the amount of useful information that can be gotten from either diffraction or transmission data [6].

Conversely, the disadvantages at the present time are:

1. Operation in vacuum where certain crystalline structure might be disordered. Examples are specimens that must be hydrated.

2. Difficulty in determining the crystal orientation in

the preparation of specimens. This poses great problems in indexing a new structure.

3. Relative to x-ray, the interaction of electrons with matter is much stronger. While this feature ensures small specimen volumes and short exposure times it also limits the thickness of a specimen that can be used. Dynamical scattering effects are much more easily encountered [7].

The special characteristics of electron diffraction that are mentioned above makes it potentially an extremely useful tool in the investigation of biological specimens such as proteins and membrane structures because of inherently small specimen size in most cases. Part of the purpose of the work reported here is to investigate in a practical sort of way the extent to which dynamical scattering would limit the usefulness of electron diffraction intensity data for crystallographic work. The work reported here has also some evident significance for the interpretation of high resolution structures that might be obtained by electron optical imaging of the scattered radiation.

The other difficulties of specimen hydration, specimen orientation, indexing are largely of an instrumental and technical nature, and can presumably be overcome without great difficulty.

Most efforts in the application of electron diffraction have been in the studies of inorganic material [8,9]. The

application to organic materials such as the determination of the structures of paraffin by Vainshtein et al. [10], cis-dichloroethylene by Hoffman [11] and perfluorotrimethylamine and trifluoroethanol by Vaughn [12], are relatively infrequent. As far as biological structures are concerned electron diffraction is a relatively new tool [9, 13, 14, 15]. An optical diffraction technique which uses an electron micrograph of the specimen was developed by Klug and Berger [16]. Methods of reconstructing the three dimensional structure using the Fourier projection theorem have been applied to biological structures with helical and ocosahedial symmetry by Klug, DeRosier and others [17, 18, 19, 20]. Direct structural determination of biologically significant molecules is rare. An example is diketopiperazine by Vainshtein [21]. Diketopiperazine groups play an important role in the structure of proteins.

There has been no work done previously on the determination of the crystalline structures of amino acids, which have been accurately determined by x-ray, however [22].

This research sets out to investigate one of the simplest of the biologically relevant molecules, the amino acid glycine. The reason of the choice is that glycine is the smallest and simplest amino acid. Not including hydrogen atoms it has only five atoms in the molecule. This fact greatly reduces the number of parameters to be determined in the structural programs. It is very common and can easily be crystallized.

Its structure has been very accurately determined by x-ray diffraction [23, 24, 25]. The structure of beta glycine as determined by Iitaka [24] is used both as a guide as well as a standard for this investigation.

The main emphasis of this work has not been on the refinement and achievement of absolute accuracy in determining the bond lengths and bond angles, as would be the case for normal crystallography. Rather, this thesis shows the possibility and a set of procedures to do so for future work. This investigation must be viewed as a preliminary study of the application of the technique of electron diffraction to the determination of structure of amino acids and other biologically relevant structures.

This research responds to the following objectives:

1. A critical evaluation of the experimental procedure.

2. The extent of dynamical scattering.

3. Empirically testing the sensitivity of the Patterson function to the existence of dynamical effects in the diffraction intensities.

4. The characteristics of the x-ray structural determination computer programs after being adapted for electron diffraction uses.

a. To modify programs for electron diffraction work.

b. To test convergence of Least Square method using typical electron diffraction data.

II. THEORY OF ELECTRON DIFFRACTION

A. Kinematical Approximation

The motion of electrons is described by the Schroedinger wave equation,

$$\nabla^2\Psi + (8\pi^2 m/h^2)(E-V)\Psi = 0 \qquad 201$$

where Ψ is the wave function, m is the mass of the electron, h is the Planck's constant, E is the total energy of the electron, and V is the potential energy of the matter through which the electron passes. V must be equated to

$$V = e\psi \qquad 202$$

where ψ is the scattering potential within the crystal and e is the charge of one electron. The electron beam incident upon the surface of the crystal may be described by a plane monochromatic wave

$$\Psi_o = A \exp(ik_o x) \qquad 203$$

where A is the amplitude and $k_o/2\pi = 1/\lambda = (2mE/R)^{\frac{1}{2}}$ and x is the generalized coordinate. Ψ_o is the solution to eq. 201 when V = 0.

For a kinematic approximation [26], [27], [28], the problem of the electron scattering by matter may be solved by the first order perturbation method [29]. This method assumes

that Ψ is composed of two terms, the wave function Ψ_o and a scattered wave Ψ'.

$$\Psi = \Psi_o + \Psi' \qquad 204$$

The substitution of eq. 204 into 201 gives

$$\nabla^2\Psi + k_o{}^2\Psi = U(r)(\Psi_o+\Psi') \qquad 205$$

where

$$U(r) = (8\pi^2 me/h^2)\psi(r) \qquad 206$$

Eq. 205 is the general equation of the form

$$\nabla^2\Psi' + k_o{}^2\Psi = U(r)\Psi(r) \qquad 207$$

the solution of which [30], is

$$\Psi_k(r) = -(1/4\pi)\int U(r_1)\Psi(r_1)\ \frac{\exp(ikR)}{R}\partial_{r_1} \qquad 208$$

where $R = |r-r_1|$ and r_1 is a vector within the scattering volume v. Since $\Psi = \Psi_o t\Psi'$, the required solution is actually an integral for $\Psi(r_1)$.

$$\Psi'(r) = -1/4\pi \int U_{r_1}[\Psi_o(r_1)+\Psi'(r_1)]\ \frac{\exp(ikR)}{R}\partial v_{r_1} \qquad 209$$

Eq. 209 states that the scattered waves are generated by waves travelling in the scattering field $U(r_1)$ of the sample, Ψ_o being the initial wave and Ψ' the scattered wave.

The kinematic approximation or the first Born approximation assumes that the scattered waves are weak compared with the initial wave,

$$\Psi' << \Psi_o \qquad 210$$

This means that only the initial wave gives rise to new

scattered waves and that the term $U \cdot \Psi'$ representing the scattering of secondary waves is negligible. Therefore the term $\Psi_o + \Psi'$ in Eq. 209 can be replaced by $\Psi_o = A \exp(i\vec{k} \cdot \vec{r})$. Eq. 209 is then approximated to be

$$\Psi'(\vec{r}) = 1/4\pi \int U(\vec{r}_1)\ \Psi_o(\vec{r}_1)\ \frac{\exp(ikR)}{R}\, \partial v_{r_1} \qquad 211$$

which can be shown [30] to be

$$\Psi_1(\vec{r}) = -\ 1/4\pi\ \Phi(\vec{s})\ \frac{A \exp(ikr)}{r} \qquad 212$$

where

$$\Phi(\vec{s}) = \frac{2\pi me}{h^2} \int \Psi(\vec{r})\ \exp[if\vec{s} \cdot \vec{r})]\, \partial v_{r_1} \qquad 213$$

The scattered wave is then shown by Eq. 212 to be a spherical wave with an amplitude proportional to the Fourier integral over the potential of the object, Eq. 213 and Eq. 212 are valid when $\Psi_1(\vec{r})$ is viewed at a great distance from the object.

The kinematic theory of electron scattering assumes the validity of the Born approximation, which is not used in the dynamical theory, since the dynamical theory takes into account the interference of both the primary and the secondary waves, which produces a complex wave field in the crystal. This complex wave field makes the scattering potential a complex function rather than a real function.

The flow of particles through unit area, J, is determined by

$$J = (h/4\pi m)(\Psi^* \text{grad}\ \Psi - \Psi \text{grad} \Psi^*). \qquad 214$$

Thus, the substitution of Ψ_1 gives

$$J_r = (J_o/r^2)|\Phi(s)|^2, \qquad 215$$

where J_o is the intensity of the incident beam. It should be noted that r is the distance from the specimen to the screen and is a constant. Therefore, Eq. 215 goes into

$$I \sim |\Phi|^2 \qquad 216$$

which defines the important relationship between the relative scattered intensity and the structural amplitude, which in turn relates I_{hkl} to the real structure, $\psi(\vec{r})$.

Eq. 213 shows that the structure amplitude is the inverse Fourier transform of the scattering potential of the crystal. This potential is the potential of the unit cell. If this is approximated by a superposition of the potential for each of the atoms within the unit cell

$$\psi(r) = \Sigma\psi_i(r-r_i) \qquad 217$$

then upon substituting into Eq. 213, we find that the structure amplitude can be expressed as the summation of Fourier integrals over atoms, with a phase factor $\exp[U(\vec{s}\cdot\vec{r}_i)]$

$$\Phi_{hkl} = \Sigma f_{el_i} \exp[2\pi i(\vec{r}_i\cdot\vec{H})] \qquad 218$$

where $H = \vec{s}/2\pi$. In this equation f_{el_i} is the scattering factor of atom i and H = the reciprocal lattice vector. A table of the atomic scattering factors for H, C, N, and O is listed in Appendix A.

The atom scattering factor f_{el} must be modified by the

temperature function f_T to take into account the thermal vibrations of the atoms.

$$f_{el,T} = f_{el} \cdot f_T \qquad 219$$

where $$f_T = \exp[-B(\sin\theta/\lambda)^2] \qquad 220$$

B is the temperature factor.

Thus, given the atom coordinates and the atomic scattering factor, the scattering amplitude Φ_{hkl} can be calculated by Eq. 218. On the other hand, given the scattering amplitude (from experiment, by measuring I_{hkl}) and if the phases are also known an inverse Fourier transform of Eq. 218 gives the distribution of scattering potential within the unit cell.

Since $$\Phi = F^{-1}(\psi) \qquad 221$$

then $$\psi = F(\Phi) \qquad 222$$

where F represents the Fourier operator and F^{-1} the inverse Fourier operator.

B. The Patterson Function

If Eq. 222 is calculated with $|\Phi|^2$ instead of Φ, then it can sidestep the phase problem since by squaring the scattering amplitude, the phase term is equal to unity. This is the same as doing the Fourier summation over the diffraction intensity I_{hkl} as given by Eq. 216. The Fourier integral over the intensity of the diffraction pattern is called the Patterson function or

$$P = F(\Phi^2) \qquad 223$$

Because Eq. 221 shows that Φ itself is an inverse Fourier transform of ψ, the Patterson function can be interpreted as

$$P = F[F^{-1}(\psi)\cdot F^{*-1}(\psi)]$$

or $$P = \psi * \psi \qquad 224$$

where the symbol $*$ denotes the convolution operation. The Patterson function is thus seen to be the autocorrelation of the scattering potential. The Patterson function defined by Eq. 224 will show peaks for values of functional displacements which produce superposition of scattering centers. Hence, a Patterson function plot results in a plot of the interatomic vectors within the unit cell.

The Patterson function, when interpreted kinematically, can be used to find scattering centers, i.e., atoms, within the unit cell, if the number of atoms is small. If the number of atoms within the unit cell is large (above 10 for example) interpretation becomes virtually impossible [31],[32].

C. Dynamical Scattering

Most of the work done so far on the diffraction of either x-rays, neutrons, or electrons as a tool for structural determination has been based on the kinematical theory because it has a wide range of validity over most experimental conditions. Treatments based upon the dynamical theory are at best complicated exercises because a practical theory governing the range of dynamical scattering is still in want.

A dynamical approximation which has been widely applied was originally proposed by Blackman [33]. It is based on the two beam model, in which it is assumed that one scattered secondary beam besides the central beam can give rise to secondary scattering. For the case of a crystal of "medium" thickness with a weak dynamical effect, the relative intensity of diffraction can be shown [3] to be

$$I_{nkl} = \lambda^2 \left|\frac{\Phi_{hkl}}{\Omega}\right|^2 \cdot t \cdot K(t,\Phi) \qquad 225$$

where Ω is the unit cell volume, t the thickness of the crystal and K a correction factor of the form

$$K(t,\Phi) \sim \exp\left[-\frac{1}{3}\left(t\lambda\left|\frac{\Phi_{hkl}}{\Omega}\right|\right)^2\right] \qquad 226$$

Schiff [44] shows another way of treating dynamical scattering. Assuming an infinite order of multiple scattering, he arrives at the formulation

$$\Phi \sim F(1-e^{-i\psi'}) \qquad 227$$

where ψ' is the two dimensional projection of the scattering potential. This approximation is valid only at small scattering angles. That is, if the Ewald sphere is perfectly flat so that the following equation applies

$$\psi'(x,y) = \int \psi(x,y,z)\,\partial z \qquad 228$$

Cowley and Moody [34] use an approximation which corresponds to a successive increase in the number of two dimensional distribution of potentials (Eq. 228) by which the three dimensional field is approximated. If the number of

sections is one, they arrive at a pseudokinematic theory

$$\Phi \sim \exp(i\partial\psi') \qquad 229$$

with $\sigma = 2\pi m\lambda/h^2$

In the special case of a two beam approximation, they give essentially the same result as the dynamical theory of Bethe [45].

The Patterson function is difficult to interpret with the dynamical formulation, but it can be shown (9 and Ch. VIII) that it might not differ significantly from the Patterson function calculated from the kinematical model for the cases of light atoms if the dynamical effect is not too strong. This point is discussed at greater length in Chapter VIII.

PART II:

METHOD AND MATERIAL

III. SPECIMEN PREPARATION

Three polymorphic forms of glycine have been reported: (1) an ordinary form, alpha. The crystal structure was first determined by Albrecht and Corey [35] in 1939. It was redetermined very precisely by Marsh [23] in 1958. (2) An unstable form, beta. It was first described by Fischer [36] in 1905. Iitaka [24] in 1959 determined its structure by x-ray diffraction and showed that single molecular layers, whose internal arrangement is the same as in the alpha form, are held together by hydrogen bonds throughout the crystal. (3) A third form, gamma, is strongly piezoelectric and crystallizes with trigonal hemihedral symmetry. Its structure was determined by Iitaka [25] in 1959.

Iitaka reports that beta glycine crystallizes in the form of small needles and can be prepared by adding ethyl alcohol to a concentrated aqueous solution of glycine. He also reports that beta glycine readily transforms into the alpha form in air, but remains unchanged indefinitely if kept in a dry atmosphere.

However, in our experiments, beta glycine is readily crystallized by evaporating in a 60° C oven small droplets of half concentrated aqueous solution, without adding ethyl alcohol. The micro-crystals thus produced remain as far as

we can determine, indefinitely without changing into the alpha form.

Our experimental procedure is as follows: 200 mesh copper electron microscope sample holders are used. On top of the sample holder is deposited a thin film of formvar to serve as the specimen support. A small droplet of about half concentrated solution of glycine in distilled water is deposited on top of the formvar film. The sample holder is then put for a few minutes inside a dry oven heated constantly at 60° C. Micro-crystals of glycine are readily formed on the formvar film.

A thin carbon film is then evaporated in vacuum onto the specimen. This is done so that the specimen is more stable in the electron beam of the electron microscope, and to avoid electrical charging of the specimen during electron irradiation.

Specimens prepared in this way have the disadvantage that probably all three crystalline forms will be present. There is no physical way to separate them. The diffraction pattern of this specimen shows predominantly three different types of spot patterns. These have been indexed to be:

a. The hkO plane of β glycine

b. The hOl plane of β glycine

c. The hkO plane of alpha glycine

Among the three spot patterns, the hkO plane of β glycine is the most frequent and most stable. Next in frequency

of appearance is the hkO plane of alpha glycine, while that of hOl of β glycine is relatively rare.

Spot patterns of other planes are not encountered, neither did we find any pattern of the gamma form. The frequent appearance of the hkO planes agree with the fact that the C axis is the axis of growth of crystals, and the crystal grows with its elongated axis perpendicular to the specimen support. The fact that spot patterns rather than rings are formed indicates that the crystals on the average are longer than the effective diameter of the electron beam.

The hkO plane spot pattern of alpha glycine is often incomplete and warped. This is probably due to a poor mosaic structure of these crystals.

The diffraction patterns of β glycine, on the other hand, are quite stable. Both the hkO and the hOl planes are clear and without distortion. They both have an estimated fading time of about three minutes at 80 kv, under the conditions of illumination used in this work.

The β glycine patterns, both hkO and hOl are shown in Figure 602 and 603 respectively.

IV. SELECTED AREA DIFFRACTION

Selected Area diffraction techniques [13] and [28] are specially suited for choosing single particles, single crystals, or small portions of a specimen for diffraction patterns. Normally the procedure is that an area is selected from the image on the fluorescent screen. The optical mode of the column is then changed to present the diffraction pattern, which corresponds to the area selected from the image in the magnification mode. A diffraction spot pattern is formed if the specimen is crystalline.

After an area has been selected, the column is switched to the Selected Area Diffraction (SAD) mode. The SAD mode leaves the illumination system and the objective lens unchanged, but the intermediate lens is changed in focal length so that it has a new object plane (Figure 401). This new object is the back focal plane of the unchanged objective lens, instead of the image plane of the objective lens as was the case with normal microscopy.

At the back focal plane of the objective lens, for parallel illumination entering the lens, there is by definition a focused image of the source. If a crystalline specimen is placed in the object plane of the lens (objective), a diffraction pattern will be formed at the back focal plane.

Figure 401

Ray diagram of the selected area diffraction mode of operation of the electron microscope.

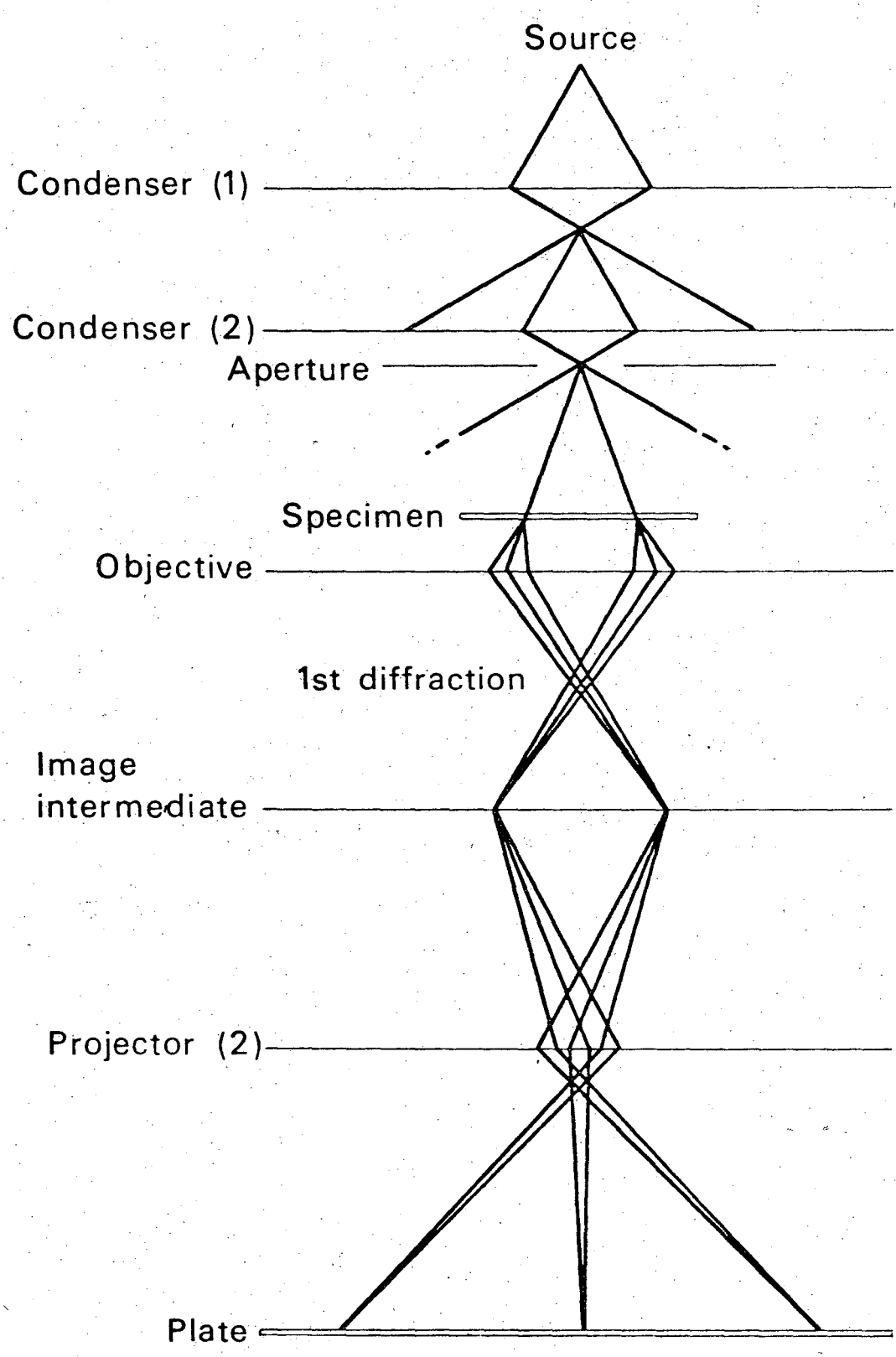
Source
Condenser (1)
Condenser (2)
Aperture
Specimen
Objective
1st diffraction
Image
intermediate
Projector (2)
Plate

Figure 401.

By using the back focal plane of the objective lens as the object plane for the intermediate lens, the remaining lenses of the column magnify and transfer the diffraction pattern to the fluorescent screen.

In the SAD mode, the primary diffraction camera length is the focal length of the objective lens which is about 3-4 mm. The magnification introduced by the post-objective lenses, i.e., the intermediate and projector, in transferring the pattern to the screen, makes an effective camera length of the order of 40-50 cm.

In doing SAD diffraction, a real image of the specimen is formed in a plane close to the intermediate lens. The diffraction aperture (of the field limited aperture, as it is also called) placed in this plane will define the area of the specimen contributing to the diffraction pattern. Since the magnification of the objective lens is about 40x, a 25μ diffraction aperture will define an area of 0.6μm at the specimen[13].

Agar [37] discussed some precautions which must be taken if the area selection must be extremely precise.

In actual experiments, it was found that the specimen is extremely sensitive to the electron beam. It was estimated that the glycine specimen has a fading time of about 3 minutes. Therefore, the following practices were used:

(1) Keeping the filament current and bias to the lowest minimum.

(2) Use the smallest condensor aperture.

(3) Do not go through the magnification mode, i.e., as soon as the sample is mounted, operate in the SAD mode immediately. This is possible because there are enough thin crystalline areas to give ample diffraction patterns in a single specimen grid preparation.

(4) Any one sample is never used twice.

After a sufficiently clear diffraction pattern is found, a photograph is immediately taken. The usual exposure time is 3 minutes.

V. DATA COLLECTION

The presently used data collection system is as outlined in Figure 501. The procedure is as follows:

(1) Electron diffraction patterns are recorded by photographic plates which are then developed.

(2) The plate is then scanned by the Joyce microdensitometer. A tracing of each row or column is produced.

(3) The response of the photographic plate to the electron beam and the output of the microdensitometer are calibrated. The systematic error due to non-linearity can be approximated empirically by assuming an overall exponential correction function.

(4) The background is subtracted by visually drawing onto the microdensitometer tracing a background line and reading off from it a net density.

(5) Data from the microdensitometer tracing are then corrected for non-linearity and crystal angular distribution by a PDP-81 computer.

(6) The corrected, indexed data are then punched into IBM cards, which serve as the input to the program INCOR. INCOR is the first of the structural determination programs. It is not difficult to see that the data collection system as it is set up now is ill-equipped to handle large amounts in a

Figure 501

Data collection and conversion system.

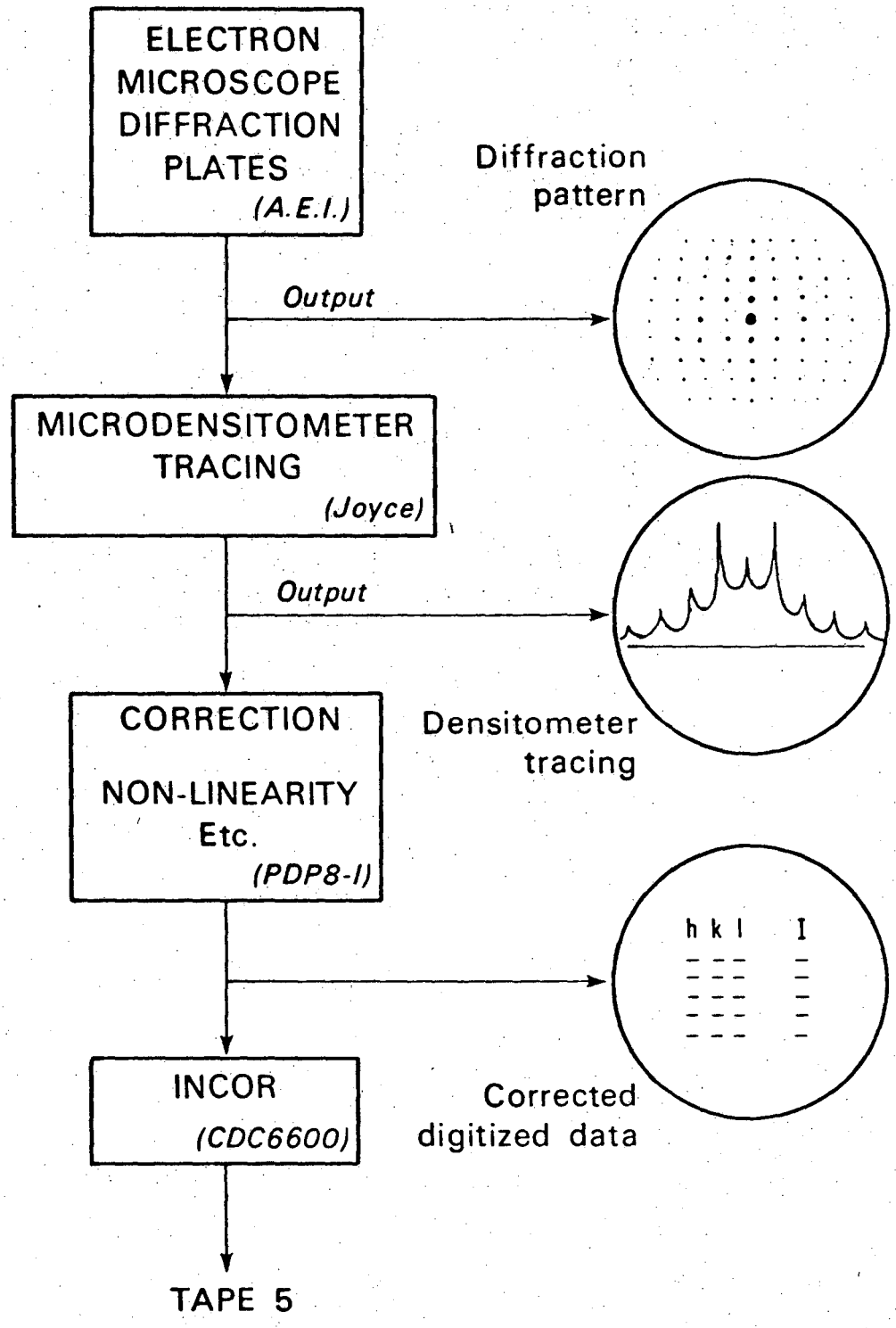
ELECTRON MICROSCOPE DIFFRACTION PLATES
(A.E.I.)
Diffraction pattern
Output
MICRODENSITOMETER TRACING
(Joyce)
Output
Densitometer tracing
CORRECTION
NON-LINEARITY
Etc.
(PDP8-I)
h k l
I
INCOR
(CDC6600)
Corrected digitized data
TAPE 5

Figure 501.

speedy manner, which is absolutely necessary if accurate determination of crystal structure is to be carried out. Compared with the levels of sophistication that x-ray crystalography has developed, this kind of experimental setup is still in its infancy.

Conceptually it is an easy extension to completely automate the process which was outlined in Figure 501. Such an attempt is now being developed in our laboratory. The automated system would involve a TV image intensifier and a video disc recorder to take the place of the camera plate. Signals from the video recorder will go through an analog to digital converter unit. The digitized data will be indexed and corrected for non-linearity of calibration, etc., with the help of a computer. The output from this should be repacked and written into magnetic tape to be used as the input tape of structure determination programs.

VI. DATA CONVERSION

A. Indexing

1. Calibration of the Camera Length

The effective camera length of the electron microscope is calibrated with a gold powder pattern. The d_{111} and d_{200} rings of the powder are used as standard, since they are known to have the distances 2.356 Å and 2.04 Å respectively. A selected area diffraction pattern superimposed on the selected area image is shown in Figure 601.

2. Indexing of the hk0 Pattern

The unit cell dimensions are measured with the equation

$$d = \frac{\lambda L}{r} \qquad 601$$

where λ is the wavelength, L the effective camera length and r the distance from the (000) central spot. The result is shown in Table 601. The estimated error of the measurement is less than 2%. In the diffraction pattern along the 0k0 row, the symmetry-forbidden reflections for k equals to odd integers do appear. If the space group and unit cell dimensions were not previously known, this would present difficulties in indexing. The significance of the appearing of these systematic absences are discussed in Ch. X. The angle between

Figure 601

Selected area diffraction pattern of gold powder. The diffraction pattern is superimposed on the selected area image.

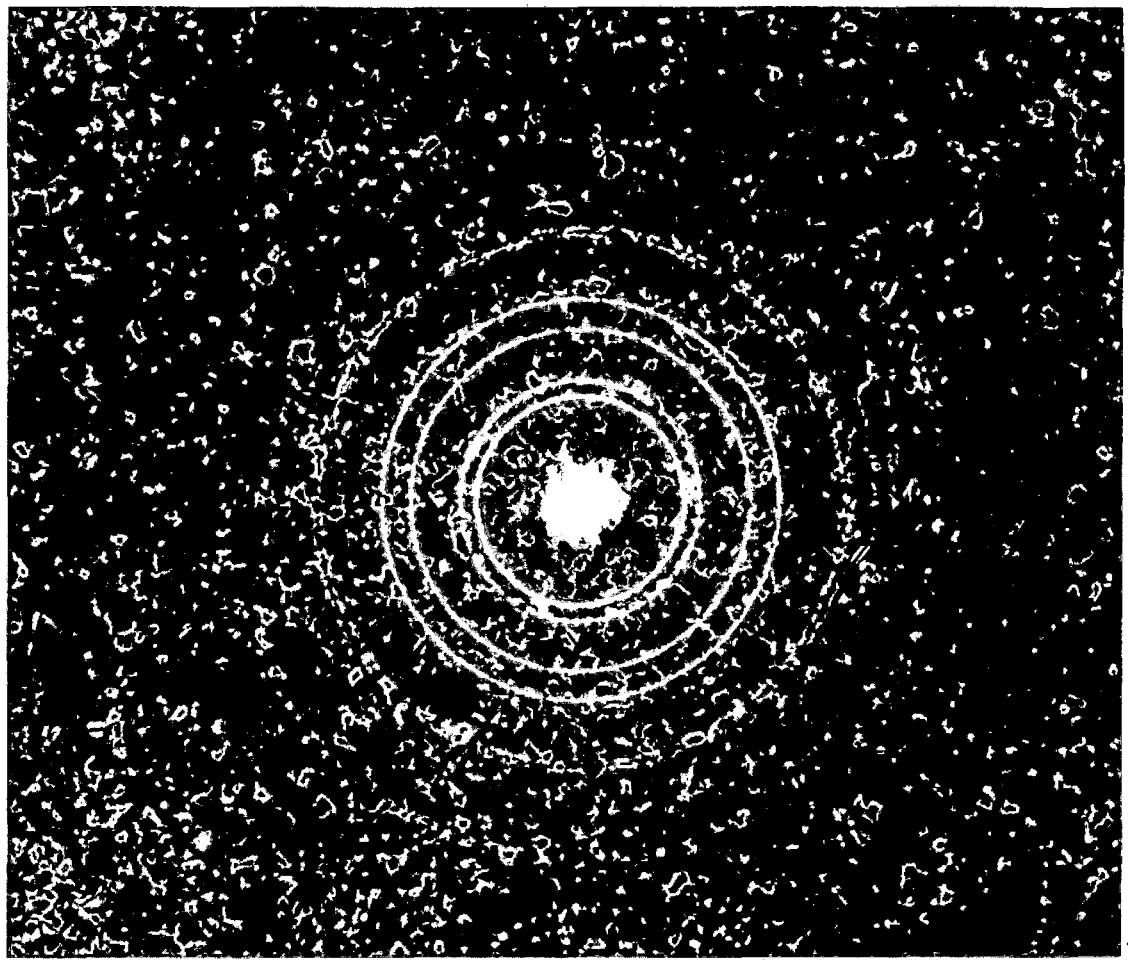

XBB 703-3750

Figure 601.

the 0k0 and h00 axes is 90°.

3. Indexing of the h01 Pattern

According to the known space group P_{21} [38] there are no systematic absences in this projection. The angle between the h00 and the 001 axes is measured to be 67.0° which is the angle β in the reciprocal space. Figure 603 shows the h01 projection.

The above measurements confirm the space group of P_{21} as given by Iitaka [24].

B. Calibration

The intensities of electron diffraction spots vary tremendously, sometimes differing by as much as several orders of magnitude. One way of calibrating the photographic response over this range of intensities is by internal calibration. This is done by doing multiple exposures of the same pattern and by noting the differences in exposure times and the changes in photographic blackening [39, 40]. In this way, a blackening curve is constructed every time. This is the best way of calibration if not the most convenient one.

It was mentioned before that glycine crystals have a fading time of about three minutes under the present experimental conditions. This creates a problem for internal calibration, because the structure becomes disordered after several exposures. If one does multiple exposure with

Table 601

Experimentally determined unit cell dimensions of β glycine.

Figure 602

Diffraction pattern of the hk0 plane of β glycine.

Figure 603

Diffraction pattern of the h0l plane of β glycine.

lattice distance from projection	d_{h00}	d_{0k0}	d_{001}
hk0	4.616A ± 0.06A	6.20A ± 0.06A	-
h01	4.60 ± 0.6	-	4.90A ± 0.06A

unit cell dimensions	experimental	known value
a	5.0A ± 0.1A	5.077A
b	6.2 ± o.1	6.267
c	5.33 ± 0.1	5.397
angle between a* and c*	67.0° ± 0.2°	66.8°

Table 601.

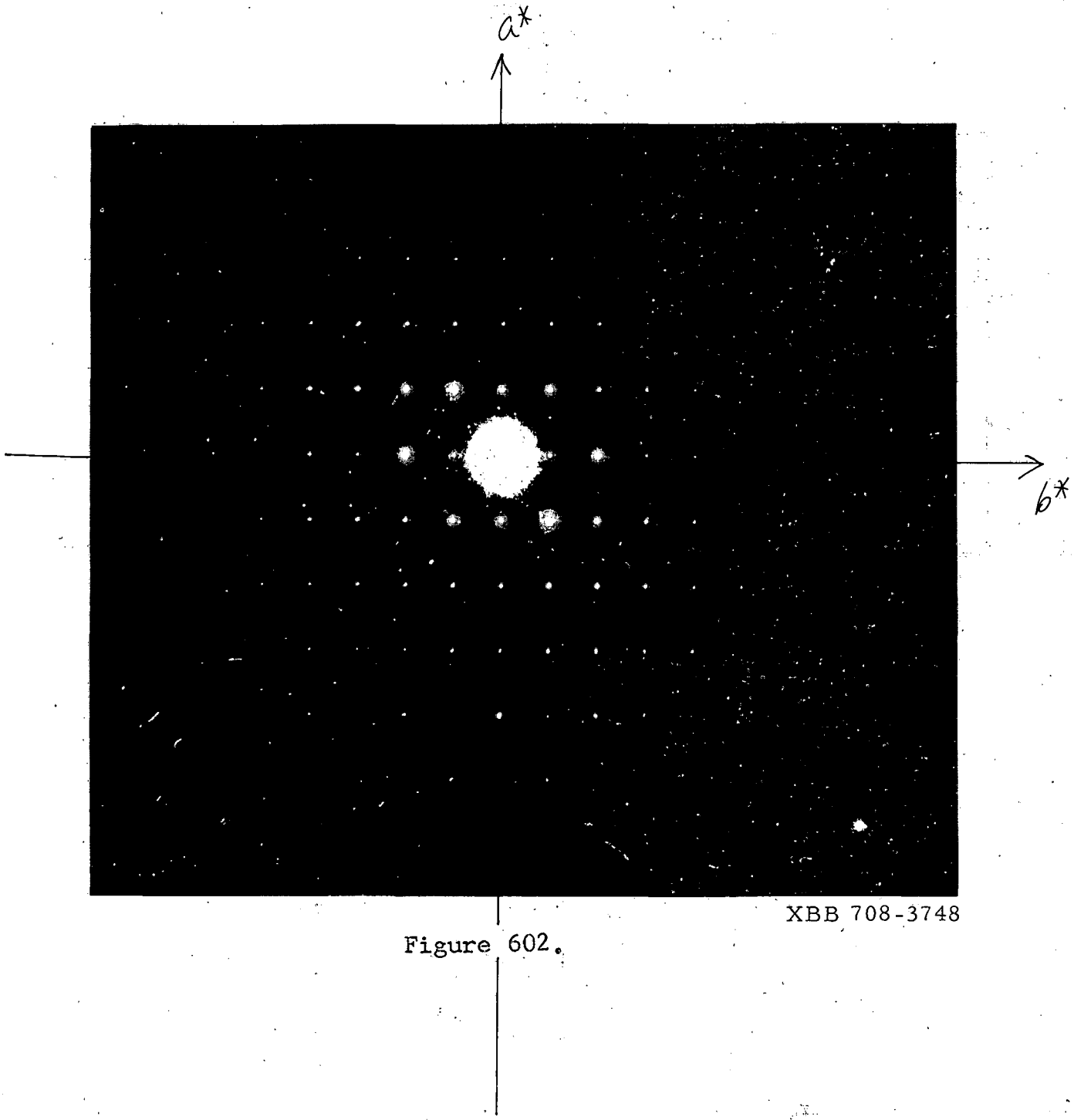

XBB 708-3748

Figure 602.

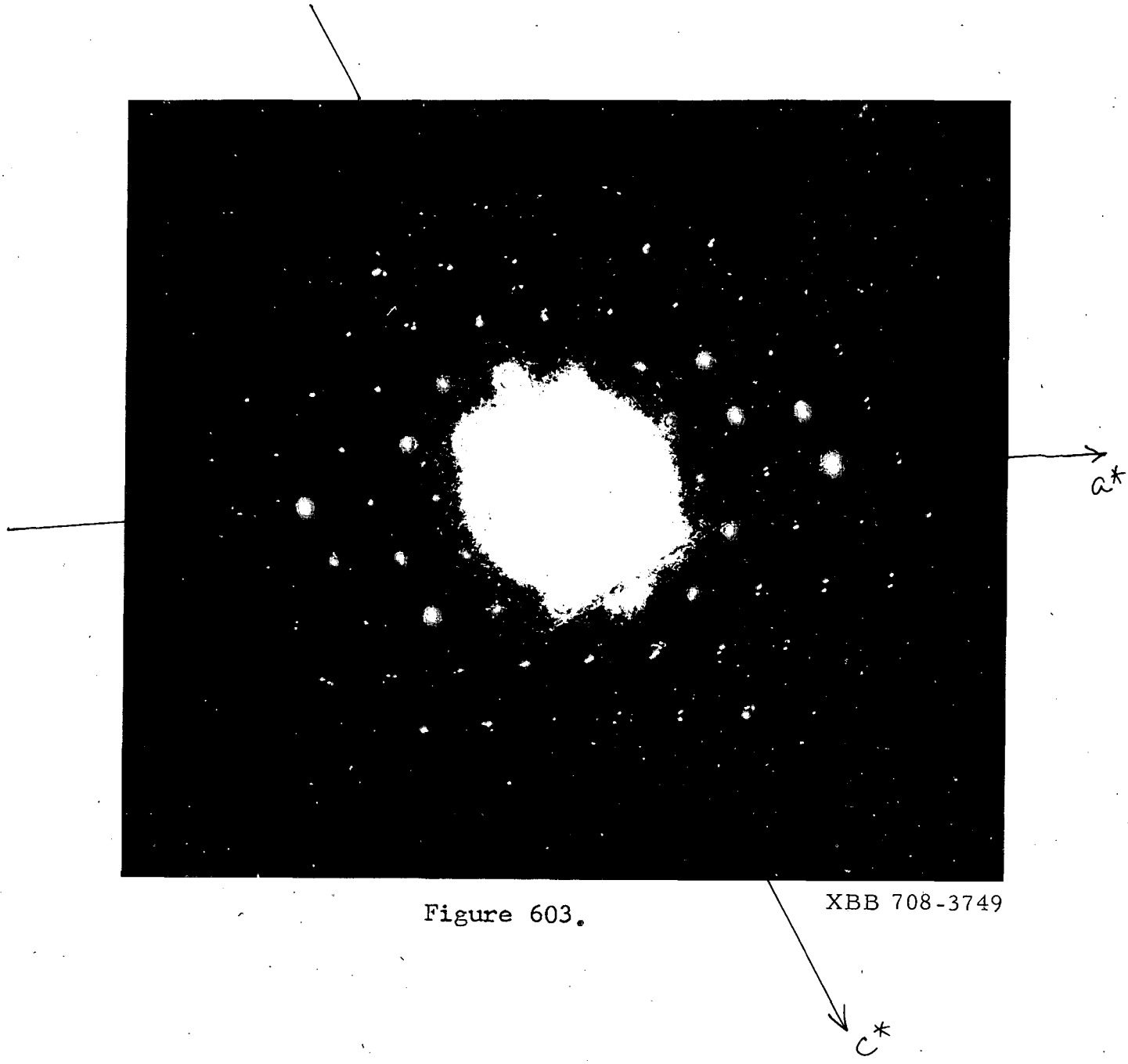

Figure 603.

XBB 708-3749

different crystals, the difficulty is the variation of thickness with different crystals.

Besides internal calibration, one can calibrate the general response behavior of the photographic emulsion to electron beams. Since it is very difficult to time the extremely short exposure-times that are needed at the low intensity end of the calibration curve, an electronic device has been constructed which sweeps the electron beam across the photographic plate with an exponential acceleration time. It is basically a RC circuit and its behavior is shown in Figure 601. The output is governed by the equation

$$V = V_o[1-\exp(-\frac{t}{RC})] \qquad 602$$

$$i = \frac{V}{R'} \qquad 602a$$

where V = voltage across the capacitor

V_o = maximum voltage

i = current

t = time

R = resistance

R' = load resistance at the output

C = capacitance

The equation 602a is a valid approximation within the range of time constants used. The current i, which the circuit sends out in the exponential manner as described by equation 602, is used to drive the scanning of the electron beam. The more current that is supplied to the deflection

coils, the greater will be the deflection of the beam. Therefore, the electron beam is deflected across the photoplate by the current i. The amount of deflection is proportional to i. Hence Eq. 602a can be written as

$$X = 1-\exp(-\frac{t}{RC}) \qquad 603$$

where $(X'/X_o)R'$

$X = X'/X_o$

X' = the distance deflected corresponding to the deflecting current i.

X_o = the maximum deflection which depends on the overall gain of the amplifier.

Eq. 603 can be re-arranged to give the amount of time that the electron beam spends within a small increment of distance

$$\Delta x = x_2 - x_1$$

$$\Delta t = RC\ \ln(1-x_1) - \ln(1-x_2)) \qquad 604$$

$$\Delta t = RC\ \ln((1-x_1)/(1-x_2))$$

Figure 602 is a plot of Δt against X; it shows how much time the beam spend with the position along the path. The RC value can be changed to cover a wide range of times.

A tracing of the deflected electron path is then done on the microdensitometer. The microdensitometer is a "double beam" instrument in which two beams of light are used, one passing through the film to be measured and one through a reference wedge, which is a continuous density wedge. The

instrument measures optical density and the reading of the tracings are linear, i.e., if one peak is twice as high as another, then the D of the former peak is twice that of the latter.

Since the tracing is along the path of the electron beam deflection, there is a one to one correspondence between the optical density measured at each position and the time interval Δt which corresponds to the position (X). The plot of the optical density or D, the photographic blackening, against it gives the desired calibration curve.

In general, D is defined as

$$D = f(It) \qquad 605a$$

where I is the intensity of the beam and t is the time of exposure. In this experiment, D is related to the optical density by a constant of proportionality

$$D = k[OD] \qquad 605b$$

where k is a constant dependent on the range of the optical wedge used in the microdensitometer and OD denotes optical density.

In the present experiment, only the lower ranges of D is plotted in the above mentioned manner. For longer exposure times a direct, timed-spot exposure is used. The total calibration curve is shown in Figure 606. Assuming that the electron current density is constant in time, the exposure is then proportional to t, so that

$$I = I_e \cdot \Delta t \qquad 606$$

Figure 604

Oscilloscope trace showing a typical curve of the current i used to deflect the electron beam. The upper and lower graphs are of different RC values.

Figure 605

Typical curve showing the time duration Δt which the beam spends at each interval $X+\Delta X$ along the path of the sweep.

Figure 606

Calibration curve of the photographic blackening and the time of exposure. It is used to correct for nonlinearity effects in the data collection and conversion systems.

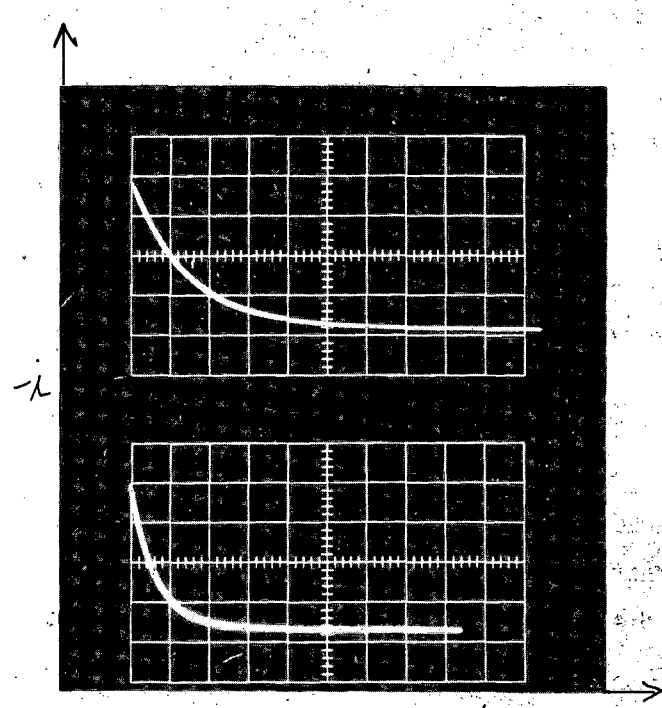

Figure 604.

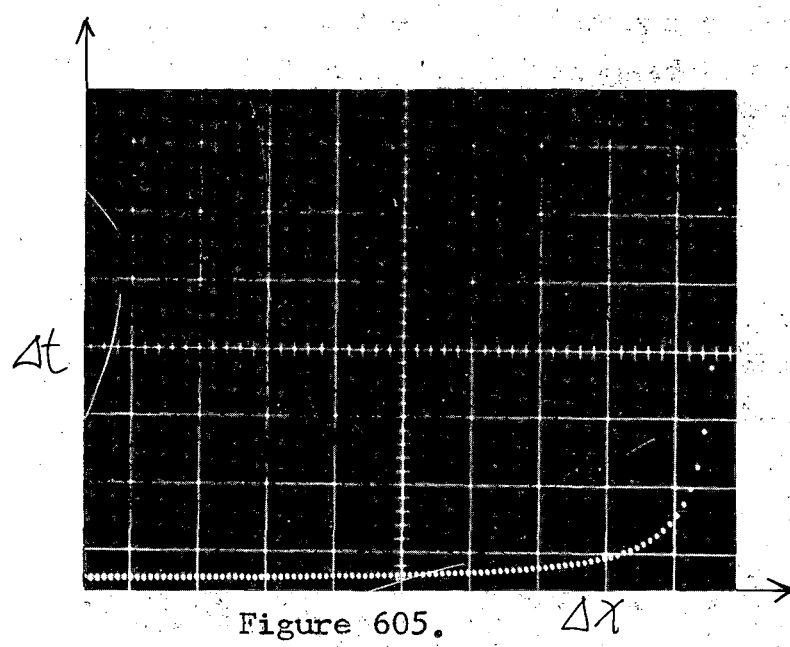

Figure 605.

XBB 708-3744

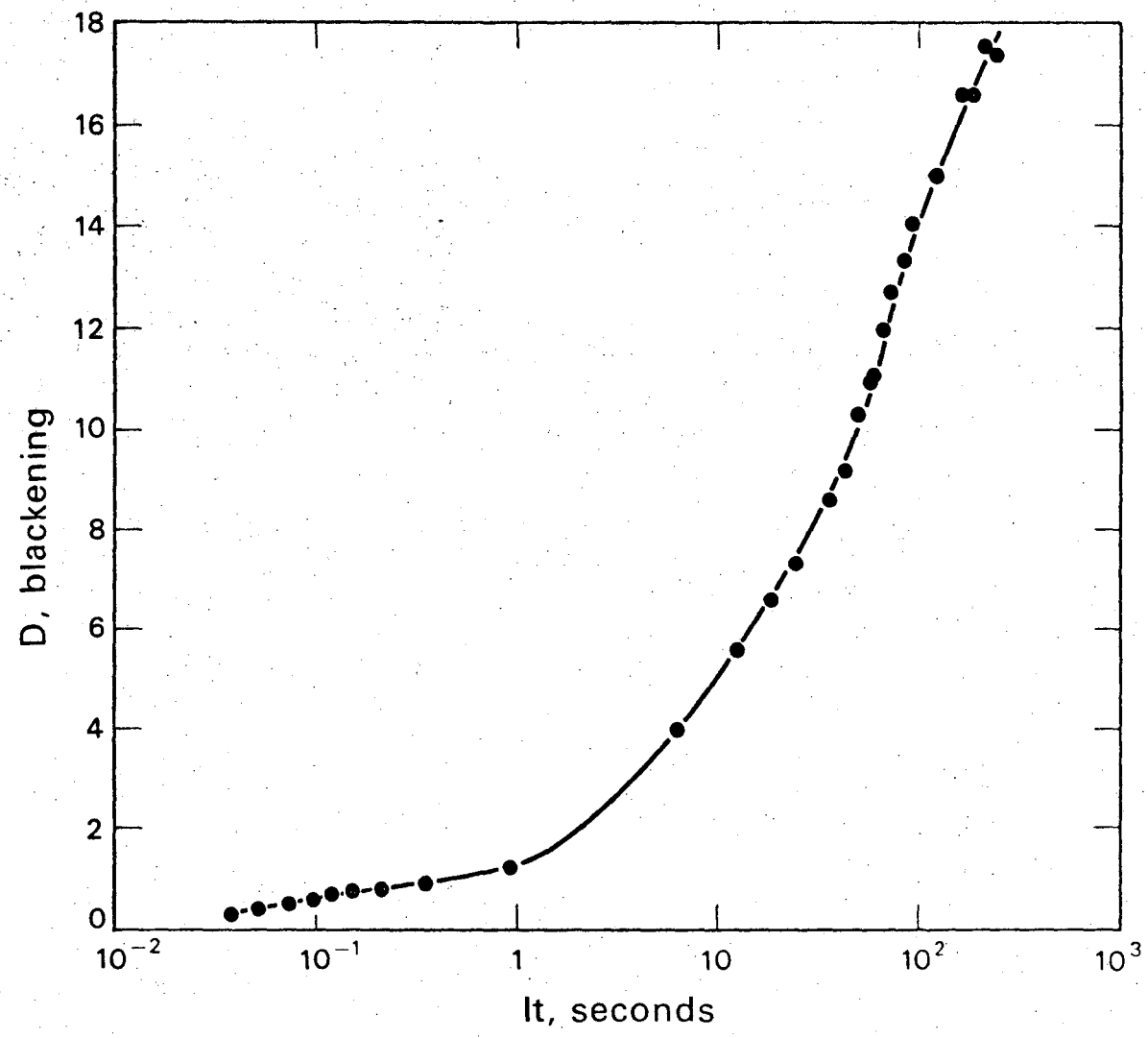
18
16
14
12
10
8
6
4
2
0
D, blackening
10^{-2}
10^{-1}
1
10
10^{2}
10^{3}
It, seconds

Figure 606.

where I is the integrated intensity of the diffraction spot and I_e is the electron density.

The shape of the curve in Figure 604 confirms the result of Vainshtein [39] in that in the low intensity region there is a "toe" which differs from the exponential behavior of the higher intensity regions. At very high intensity regions when saturation effects occur, the curve would plateau out. However, Valentine [41] reports that the initial slope of the response of photographic emulsion to electrons in the energy range 40 to 80 kv is linear. Our result appears superficially different from this. The explanation for this difference probably lies in the range of optical densities covered. Or as Valentine suggests, a deviation from non-linearity could be due to the fact that because of small penetration (about 15μ for 60KV electrons) only the surface layer is exposed and thus the saturation density is low.

1. Correction for Non-linearity

Most of the intensity data fall on the exponential region, some however, fall on the "toe" region. The curve was therefore assumed to consist of two exponential regions with two different slopes. The slopes of the "normal" exponential region and that of the "toe" region are taken separately with the joining point at D = 2.0. The correction is applied according to the formula

$$I = C \exp(kD) \qquad 607$$

where k is the slope of either the "normal" or of the "toe" region depending on whether D is larger or smaller than two. C is a scale factor determined by the boundary position of D = 2 where the two slope regions meet. Eq. 607 is applied to each diffraction spot, with C = 1 if D = 2.

2. Correction for Angular Distribution

Assuming that the specimen is a mosaic single crystal [42] with a uniform angular distribution, the diffraction spot intensity is divided by a factor, which in the case of uniform angular distribution has the form

$$L = d_{hkl}/\alpha \qquad 608$$

where d_{hkl} is the distance between crystal planes defined by the Miller indices hkl, and α is an angular measure defining the width of the angular spread of the mosaic crystal. Since α is a constant, it can be disregarded in the correction of relative intensities.

Hence, the intensity of the diffraction spot hkl is given by

$$I_{hkl} = (C/d_{hkl})\exp(kD) \qquad 609$$

where C is some constant which normalizes the two different slope regions and k can assume either one of the two values of the "normal" or "toe" region. The Bragg spacings are given by

$$d_{hkl} = (k^2a^{*2}+k^2b^{*2}+l^2c^{*2}+2hla^*\cos\beta^*)^{-\frac{1}{2}} \qquad 610$$

where a^*, b^*, and C^* are the reciprocal space unit cell dimensions and β^* is the angle between a^*b^* and the b^*c^* planes of the reciprocal lattice.

It must be noticed that I_{hkl} is only the relative intensity and not the absolute intensity. The structural amplitude is then given by

$$\Phi_{hkl} \sim \sqrt{I_{hkl}}$$

or

$$\Phi_{hkl} = \frac{S\Omega}{\lambda} \sqrt{I_{hkl}}$$

where S is a scale factor which brings the $\sqrt{I}$ into absolute units consistent with Φ. Ω is the unit cell volume in real space and $\lambda = 0.0418$ Å which is the wave length of the electron.

The square root of the diffraction intensities which are the experimental structure amplitudes are listed in Appendix B together with the calculated structure amplitudes of the reference structure. The values of the I_{hkl} are used as input for the program INCOR.

PART III:

RESULTS

VII. STRUCTURAL DETERMINATION PROGRAMS

It is beyond the scope of this dissertation to give a full or even a reasonable treatment of structural determination programs. All of the programs used in connection with this work are library programs developed and modified by many different researchers. They are all developed for x-ray diffraction work; however, they can easily be adapted to be used for electron diffraction. This chapter will only attempt to describe briefly the logic of the programs and the manner in which they are used in connection with our experiments.

There are three main programs used, all of which were kindly supplied by Dr. Zalkin of the Lawrence Radiation Laboratory at Berkeley. The programs are named INCOR, XRAY (LSLONG) and FORDAP respectively. The way in which they are used is outlined in Figure 701.

INCOR

The program INCOR is normally used to process raw x-ray data and repack them for input uses for either XRAY or FORDAP. It processes both goniostat or weissenberg data, which are not applicable in electron diffraction. Program INCOR also subtracts background and omits forbidden reflection if instructed besides calculating the structural amplitude Φ_{hkl} from input raw intensities.

Figure 701

Diagram showing how the different programs are linked together. See text (Chapter VII) for an explanation of the various programs.

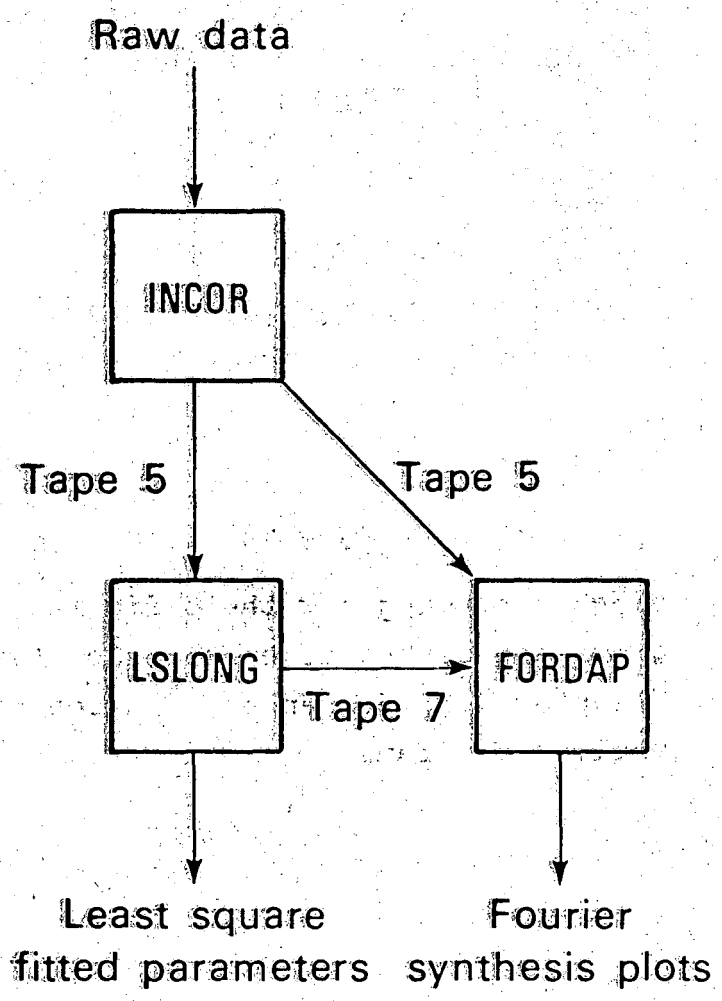
Raw data
INCOR
Tape 5
Tape 5
LSLONG
FORDAP
Tape 7
Least square
fitted parameters
Fourier
synthesis plots

Figure 701.

For the present work, this program is mainly used to calculate F_{obs}, which is the symbol designating the observed structural amplitude Φ_{hkl}, and to exclude unwanted intensities in the systematic absences. Its output is on magnetic tape called Tape 5.

LSLONG

Its original name is LS. Tape 5 from INCOR is the input to LSLONG. It basically is a Least Square Program which calculates the phase and the scattering amplitude Φ_{cal} from the input atom coordinates and atom scattering tables according to Eq. 218 and 220. Then it compares Φ_{cal} with Φ_{obs} which is inputted from INCOR for each hkl. It calculates a new scale factor, changes the atom coordinates and the temperature factor by a small increment and calculates a new set of Φ_{cal}. For each new attempt, it also calculates a R value which is a figure of merit for least square fitting known as the reliability factor (the reliability factor is further discussed in Ch. IX). The program does this reiteratively for as many cycles as instructed. The atom coordinates and the temperature factors of the last cycle define the best fitted structure according to the input data at that particular stage of refinement.

The program converges if the last shifts in the refining parameters are small and the R value no longer decreases appreciably.

The output is written on magnetic tape called tape 7.

FORDAP

FORDAP is essentially a Fourier syntheses program coupled with a plotting routine. As input, it can take either Tape 5 from INCOR or Tape 7 from LSLONG, or from similar data punched on IBM cards if instructed to do so. If the input is Tape 5, then this program sums Φ^2 in the Fourier synthesis, thereby calculating the Patterson Function. In the input is Tape 7, the program calculates the distribution of scattering potential according to Equation 213. In addition it can calculate the difference Fourier, or it can do the Fourier summation of the observed structure amplitudes with the phases of the calculated structure. FORDAP also plots, using the CAL-COMP plotter, either sections of projections of the Fourier synthesis, with either Φ or Φ^2 depending on instruction from the programmer. By putting in three dimensional data it can even calculate and plot sections through an oblique section.

For a more complete discussion of the general topic of computing methods used in crystallographic work, refer to standard texts such as Computing Methods in Crystallography, edited by J. S. Rollett.

VIII. THE PATTERSON PLOT

The raw data, after the background and the systematic corrections were made as mentioned in Chapter V, is then fed into the program INCOR. The output of INCOR, after rearranging the data and putting them on magnetic tape, serves as the input to the program FORDAP which plots the Patterson Function. The plots for the h0l, hk0, and 0hl are shown in Figures 801a, 801b, and 801c respectively. The peak positions calculated from the FORDAP plots are listed in Tables 801a, b, and c respectively.

The Patterson Plot, interpreted kinematically, is the auto-correlation function of the scattering potential Eq. 225. If the structure is known, a "point Patterson" can be calculated by plotting the differences of the known coordinates of the atoms (inter-atomic vectors). The plot of these inter-atomic vectors should be similar to the experimental Patterson Plot. In this case, the β glycine coordinates as determined by Iitaka by x-ray diffraction are used as a standard to plot a "point Patterson" map. The x,y,z, projections are shown in Figures 802a, 802b, and 802c respectively.

A visual comparison of the two plots shows that essentially they are similar with some systematic omissions.

Figure 801a

h01 projection of the Patterson Function of β glycine. The peaks are listed in Table 801a.

Table 801a

Peak positions of the Patterson Function, h01 projection. This is a printout from program INCOR. RHO is the value of the peak heights. A projection of these peaks is plotted in Figure 801a.

Figure 802a

"Point Patterson" map. h01 projection. This is calculated by plotting points of the interatomic vectors from the known atom positions of the molecules within one unit cell.

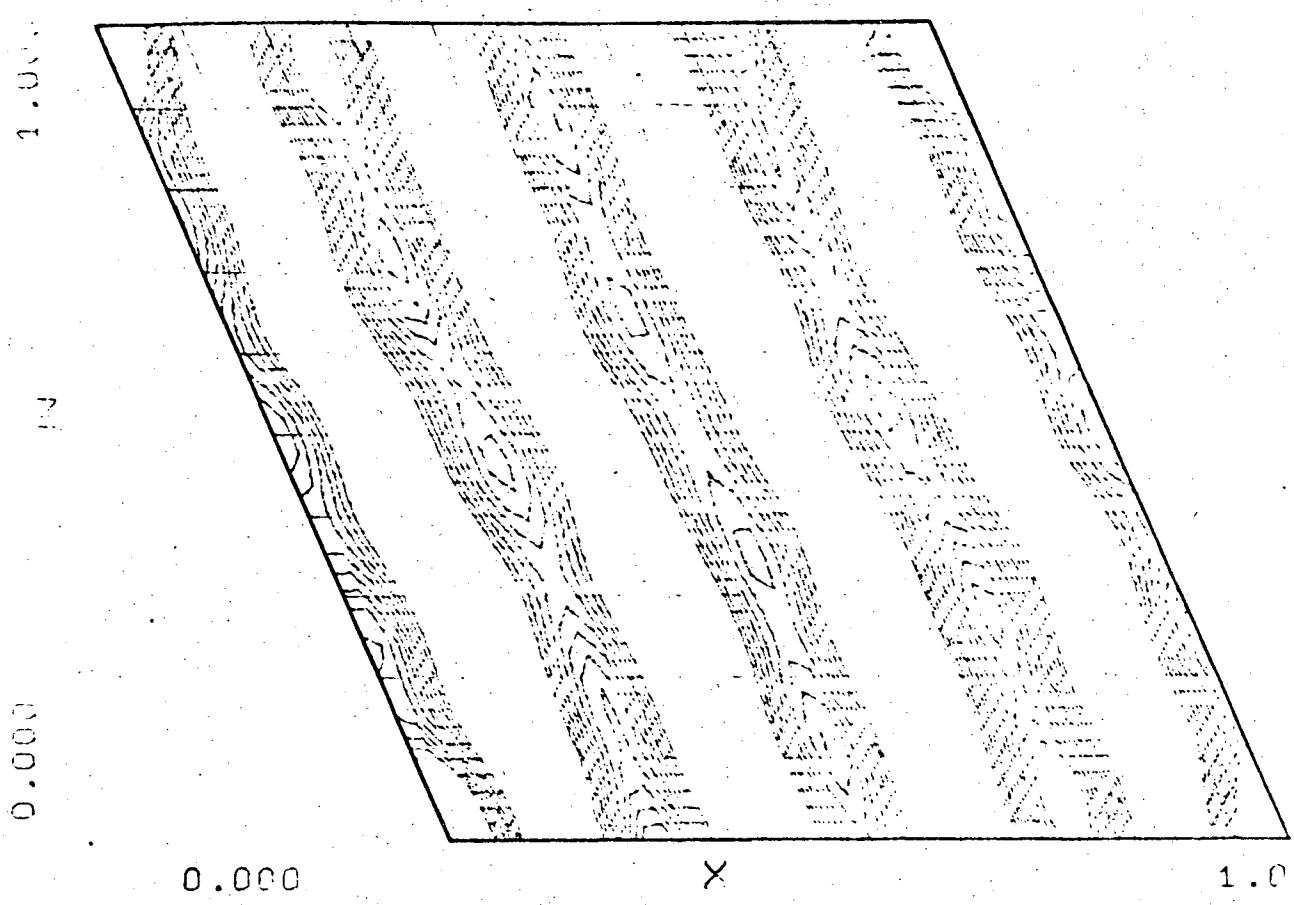

Figure 801. a

IST OF PEAK POSITIONS AND THEIR HEIGHTS. RHO=TRUE RHO X 999. / RHO MAX.

SYMETRICALLY DUPLICATED PEAKS ARE INDICATED IN PARENTHESES. (999) INDICATES A SHOULDER AND NOT A TRUE PEAK.

NO.	X	Y	Z	RHO	TRUE RHO	NO.	INTERPOLATED PEAKS					
1	0.000	0.000	0.000	999	(195.80)	1	0.000	0.000	0.000	999	(195.80)	
1)	1.000	0.000	0.000	999	(195.80)							
1)	0.000	0.000	1.000	999	(195.80)							
1)	1.000	0.000	1.000	999	(195.80)							
1)	0.000	1.000	0.000	999	(195.80)							
1)	1.000	1.000	0.000	999	(195.80)							
1)	0.000	1.000	1.000	999	(195.80)							
1)	1.000	1.000	1.000	999	(195.80)							
2	0.000	0.000	.780	864	(169.29)	2	0.000	0.000	.780	864	(169.29)	
2)	1.000	0.000	.780	864	(169.29)							
2)	0.000	1.000	.780	864	(169.29)							
2)	1.000	1.000	.780	864	(169.29)							
2)	0.000	0.000	.220	864	(169.29)							
2)	1.000	0.000	.220	864	(169.29)							
2)	0.000	1.000	.220	864	(169.29)							
2)	1.000	1.000	.220	864	(169.29)							
3	0.000	0.000	.500	839	(164.35)	3	0.000	0.000	.500	839	(164.35)	
3)	1.000	0.000	.500	839	(164.35)							
3)	0.000	1.000	.500	839	(164.35)							
3)	1.000	1.000	.500	839	(164.35)							
4	.500	.500	.120	533	(104.46)	4	.503	.500	.121	533	(104.54)	
4)	.500	.500	.880	533	(104.46)							
5	.500	.500	.640	511	(100.09)	5	.492	.500	.651	513	(100.59)	POOR PEAK
5)	.500	.500	.360	511	(100.09)							
6	.720	.500	.040	275	(53.83)	6	.728	.500	.036	277	(54.36)	
6)	.280	.500	.960	275	(53.83)							
7	.720	.500	1.000	270	(52.90)	7	.725	.500	1.000	271	(53.06)	
7)	.280	.500	0.000	270	(52.90)							
8	.720	.500	.840	241	(47.24)	8	.714	.500	.833	243	(47.55)	
8)	.280	.500	.160	241	(47.24)							
9	.700	.500	.540	239	(46.93)	9	.702	.500	.541	240	(46.95)	
9)	.300	.500	.460	239	(46.93)							
10	.720	.500	.260	231	(45.19)	10	.732	.500	.263	235	(46.07)	POOR PEAK
10)	.280	.500	.740	231	(45.19)							

```
  1    0   20    0   10
NO. OF PLOTS =   1
EVEL =  0.000
EVEL =   .100
EVEL =   .200
EVEL =   .300
EVEL =   .400
EVEL =   .500
EVEL =   .600
EVEL =   .700
EVEL =   .800
EVEL =   .900
EVEL =  1.000
NO. OF COMPLETED SECTIONS = 11.

EVEL OF THE LAST SECTION = 1.000.
```

Table 801.a

XBB 709-3855

Figure 802.a

Figure 801b

hk0 projection of the Patterson Function

Table 801b

Peak position of the Patterson Function, hk0 plane. This is a printout from program INCOR. RHO is the value of the peak heights. A projection of these peaks is plotted in Figure 801b.

Figure 802b

hk0 projection of the "Point Patterson." This is calculated by plotting points of the interatomic vectors from the known atom positions of the molecules within one unit cell.

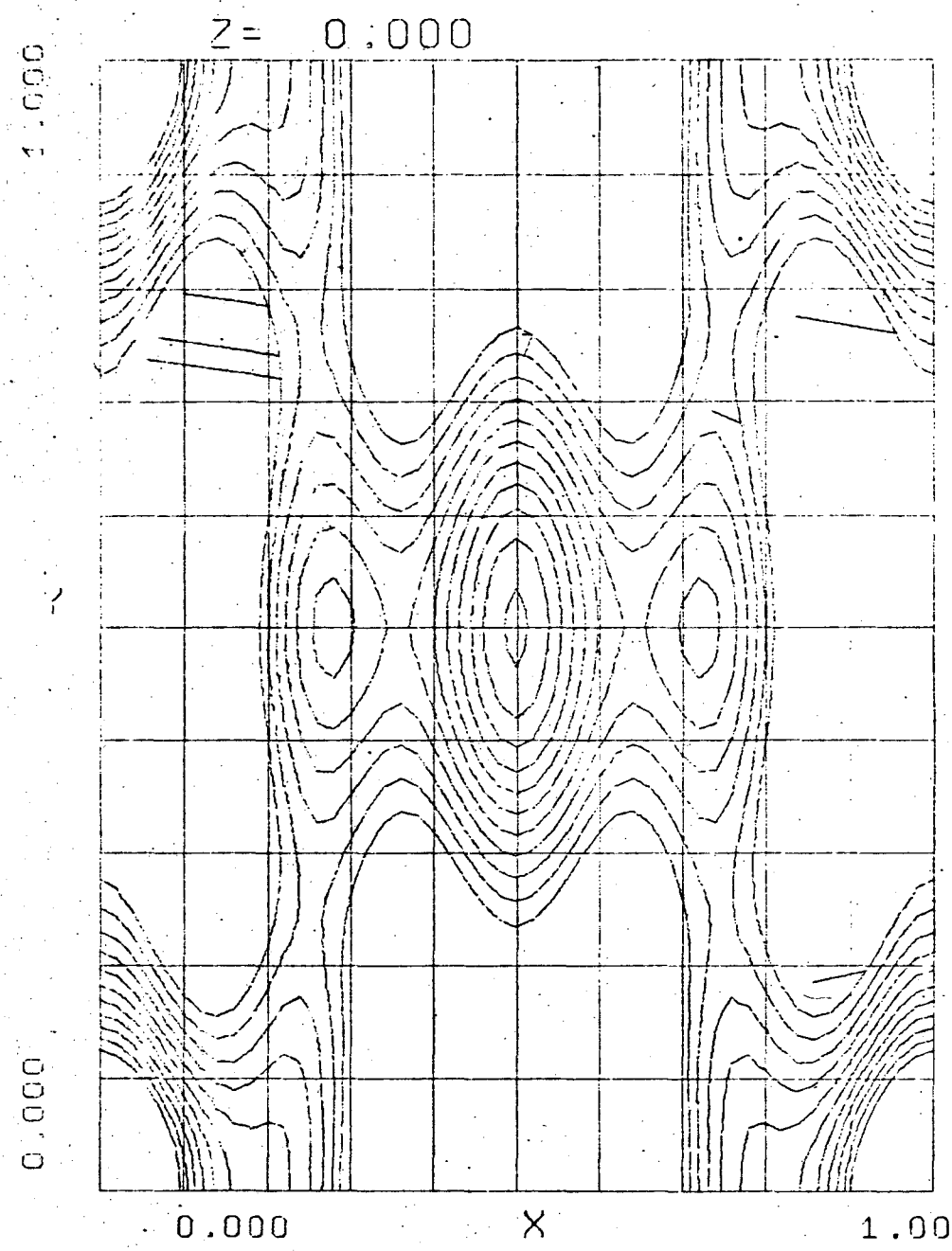

Figure 801.b

LIST OF PEAK POSITIONS AND THEIR HEIGHTS. RHO=TRUE RHO X 999. / RHO MAX.

SYMETRICALLY DUPLICATED PEAKS ARE INDICATED IN PARENTHESES. (999) INDICATES A SHOULDER AND NOT A TRUE PEAK.

NO.	X	Y	Z	RHO	TRUE RHO	NO.	INTERPOLATED PEAKS				
1	0.000	0.000	0.000	999	(195.80)	1	0.000	0.000	0.000	999	(195.80)
(1)	1.000	0.000	0.000	999	(195.80)						
(1)	0.000	1.000	0.000	999	(195.80)						
(1)	1.000	1.000	0.000	999	(195.80)						
(1)	0.000	0.000	1.000	999	(195.80)						
(1)	1.000	0.000	1.000	999	(195.80)						
(1)	0.000	1.000	1.000	999	(195.80)						
(1)	1.000	1.000	1.000	999	(195.80)						
2	0.000	0.000	.500	839	(164.35)	2	0.000	0.000	.500	839	(164.35)
(2)	1.000	0.000	.500	839	(164.35)						
(2)	0.000	1.000	.500	839	(164.35)						
(2)	1.000	1.000	.500	839	(164.35)						
3	.500	.500	.100	531	(104.16)	3	.503	.500	.106	532	(104.22)
(3)	.500	.500	.900	531	(104.16)						
4	.720	.500	0.000	270	(52.90)	4	.722	.500	0.000	270	(52.92)
(4)	.720	.500	1.000	270	(52.90)						
(4)	.280	.500	0.000	270	(52.90)						
(4)	.280	.500	1.000	270	(52.90)						
5	.700	.500	.500	235	(45.97)	5	.697	.500	.534	236	(46.32)
(5)	.300	.500	.500	235	(45.97)						

/ 1 0 20 0 10

*NO. OF PLOTS = 1

LEVEL = 0.000
LEVEL = .100
LEVEL = .200
LEVEL = .300
LEVEL = .400
LEVEL = .500
LEVEL = .600
LEVEL = .700
LEVEL = .800
LEVEL = .900
LEVEL = 1.000

NO. OF COMPLETED SECTIONS = 11.

LEVEL OF THE LAST SECTION = 1.000.

Table 801.b

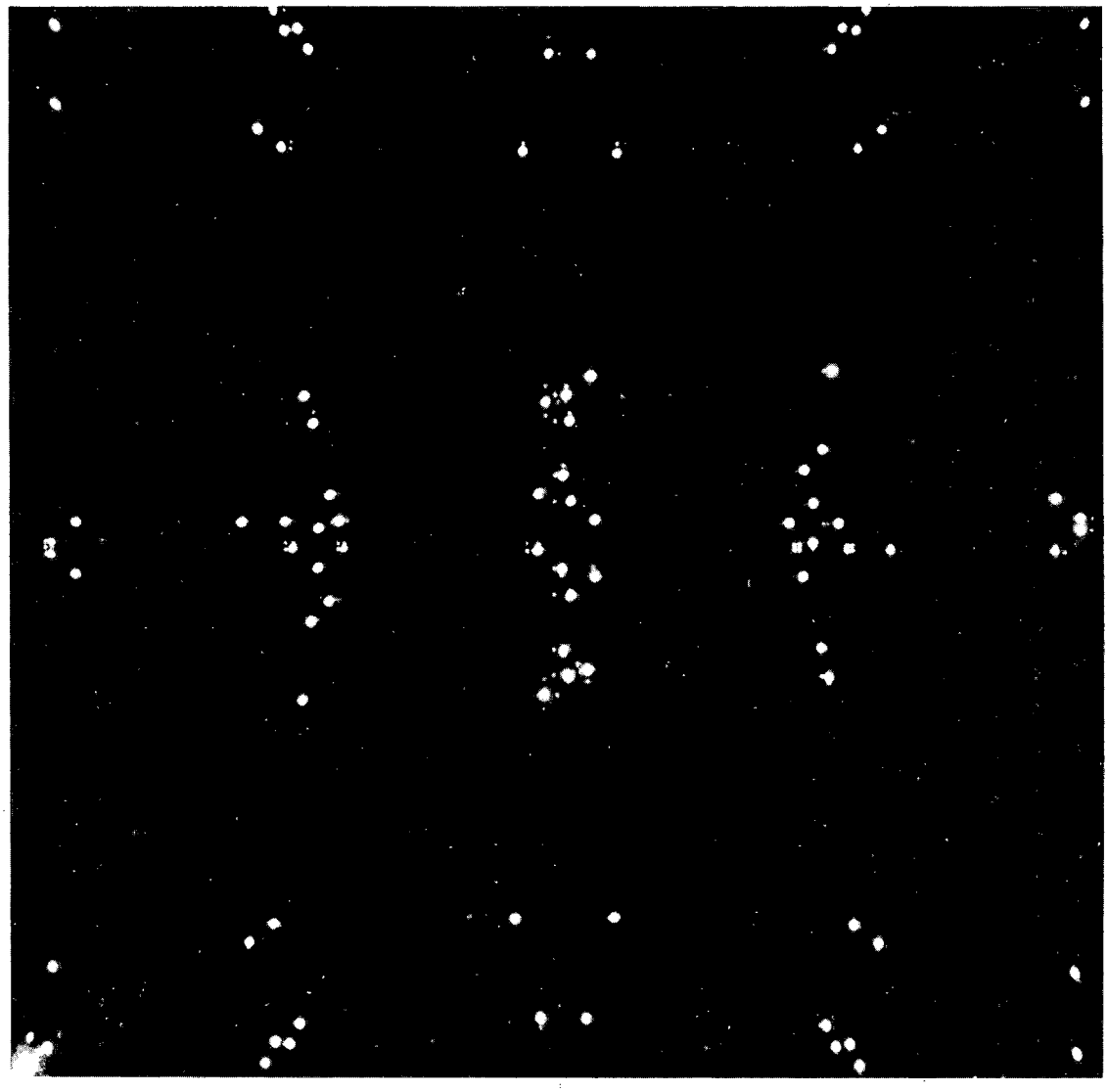

XBB 709-3853

Figure 802.b

Figure 801c

0hl projection of the Patterson Function. The peaks are listed in Table 801c.

Table 801c

Peak positions of the Patterson Function. 0kl projection. This is a printout from program INCOR. RHO is the value of the peak heights. A projection of these peaks is plotted in Figure 801c.

Figure 802c

0kl projection of the "Point Patterson." This is calculated by plotting the points of the interatomic vectors from the known atom positions of the molecules within one unit cell.

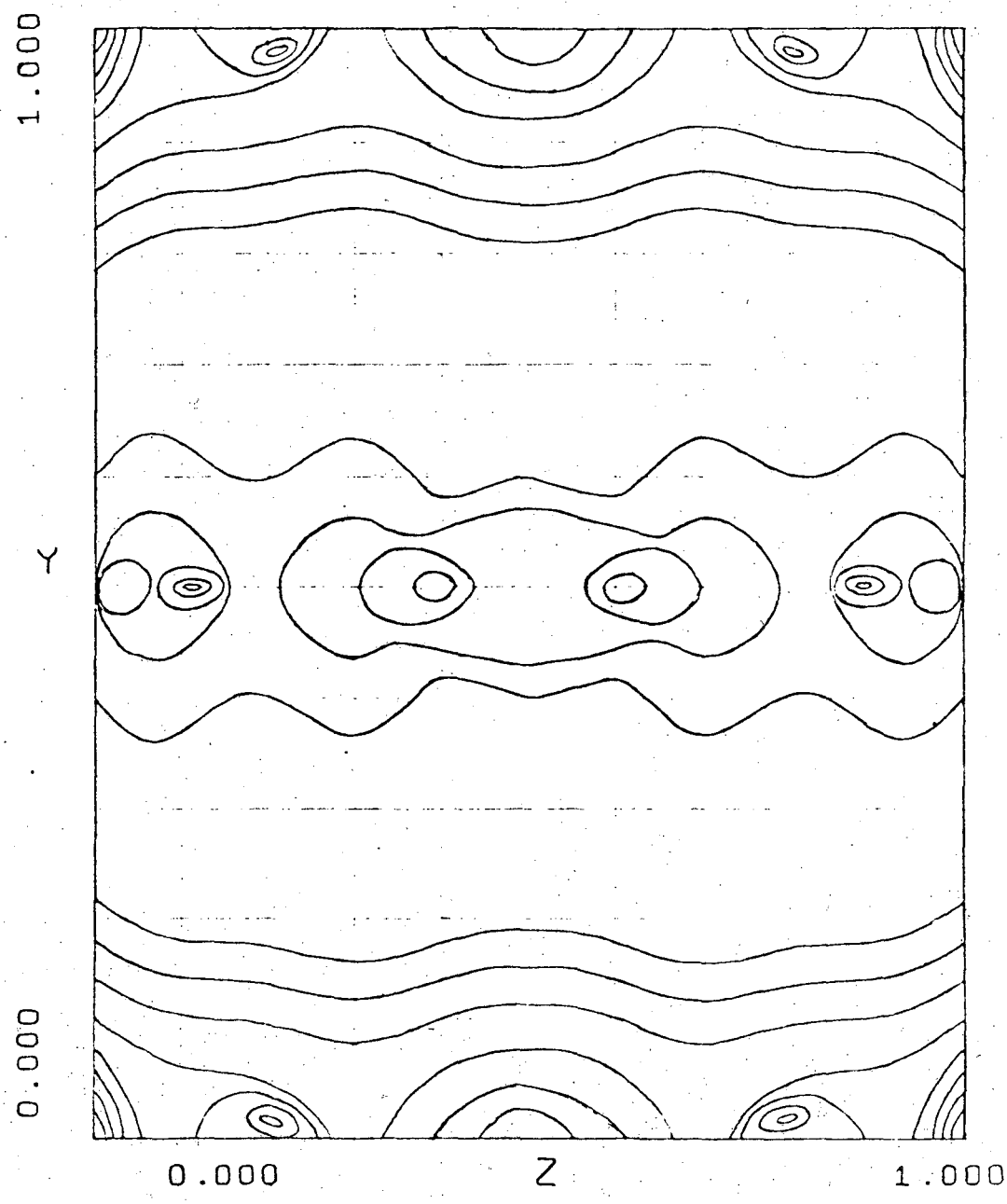

Figure 801.c

LIST OF PEAK POSITIONS AND THEIR HEIGHTS. PRINTED ONLY X 999. / SHC MAX.

SYMETRICALLY DUPLICATED PEAKS ARE INDICATED IN PARENTHESES. (999) INDICATES A SHOULDER AND NOT A TRUE PEAK.

NO.	X	Y	Z	PKH	THIS PKH	NO.	INTERPOLATED PEAKS				
1	0.000	0.000	0.000	999	(195.80)	1	0.000	0.000	0.000	999	(195.80)
(1)	0.000	0.000	1.000	999	(195.80)						
(1)	0.000	1.000	0.000	999	(195.80)						
(1)	0.000	1.000	1.000	999	(195.80)						
(1)	1.000	0.000	0.000	999	(195.80)						
(1)	1.000	0.000	1.000	999	(195.80)						
(1)	1.000	1.000	0.000	999	(195.80)						
(1)	1.000	1.000	1.000	999	(195.80)						
2	0.000	0.000	.220	864	(169.29)	2	0.000	0.000	.220	864	(169.29)
(2)	0.000	0.000	.220	864	(169.29)						
(2)	1.000	0.000	.220	864	(169.29)						
(2)	1.000	1.000	.220	864	(169.29)						
(2)	0.000	0.000	.780	864	(169.29)						
(2)	0.000	1.000	.780	864	(169.29)						
(2)	1.000	0.000	.780	864	(169.29)						
(2)	1.000	1.000	.780	864	(169.29)						
3	0.000	0.000	.500	839	(164.35)	3	0.000	0.000	.500	839	(164.35)
(3)	0.000	1.000	.500	839	(164.35)						
(3)	1.000	0.000	.500	839	(164.35)						
(3)	1.000	1.000	.500	839	(164.35)						
4	.500	.500	.125	533	(104.50)	4	.502	.500	.125	533.	(104.50)
(4)	.500	.500	.875	533	(104.50)						
5	.500	.500	.360	511	(100.09)	5	.500	.500	.360	511	(100.09) POOR PEAK
(5)	.500	.500	.640	511	(100.09)						
6	.300	.500	.960	258	(50.67)	6	.343	.500	.962	310	(60.70) POOR PEAK
(6)	.700	.500	.038	258	(50.67)						
(6)	.300	.500	0.038	255	(50.05)						
(6)	.700	.500	1.038	255	(50.05)						

1 0 20 0 10

NO. OF PLOTS = 1

LEVEL = 0.000
LEVEL = .100
LEVEL = .200
LEVEL = .300
LEVEL = .400
LEVEL = .500
LEVEL = .600
LEVEL = .700
LEVEL = .800
LEVEL = .900
LEVEL = 1.000

NO. OF COMPLETED SECTIONS = 11.

LEVEL OF THE LAST SECTION = 1.000.

Table 801.c

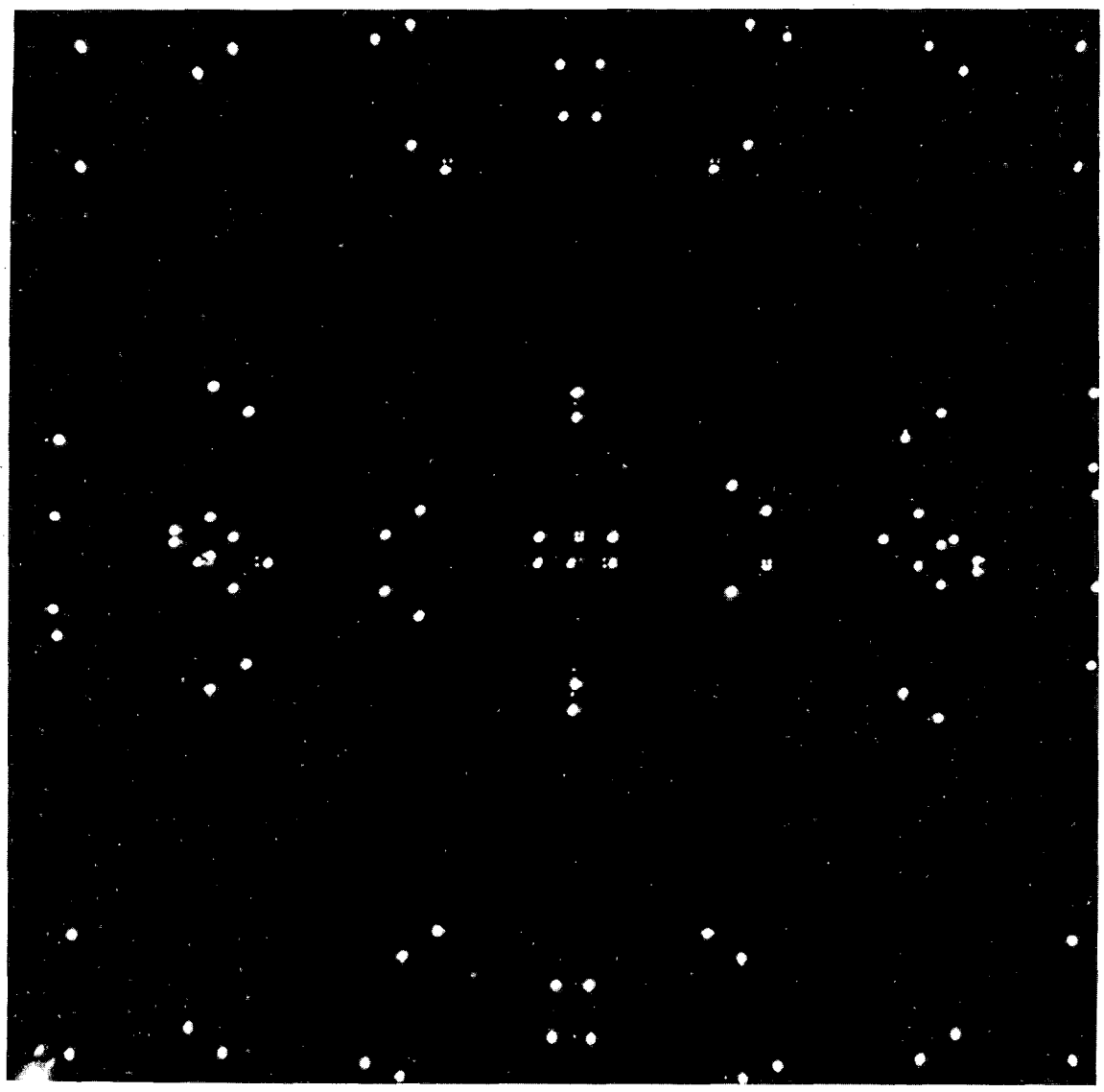

XBB 709-3854

Figure 802.c

Two conclusions are possible:

(1) The diffraction patterns have no significant dynamical effect and hence can be interpreted on purely kinematical grounds. Their Patterson plots are similar to what they should be theoretically; the omissions means that certain interatomic distances are not resolved well.

(2) The diffraction patterns have significant dynamical effect, but the Patterson function is not sensitive enough to show the difference. This is plausible because the Patterson is a convolution of two functions. Even if these functions are modified, as in the case of dynamical effect, so that the ψ is modified by a factor K, according to the two-beam approximation discussed below, and would appear differently from that of the Kinematic ψ, the convolution function would not change appreciably.

From the consideration of the two-beam dynamical approximation [43] in the case of a medium thickness block, the integrated intensity can be expressed as

$$I_{hkl} = C\lambda^2 |\Phi_{hkl}|^2 \cdot K(\bar{t}, \Phi_{hkl}) \cdot \Gamma \qquad 801$$

where C is some constant, λ is the wavelength, Φ_{hkl} is the structural amplitude. Γ is a factor which takes into account the mosaic nature of the sample and is proportional to d_{hkl}, the plane distance.

$$K(\bar{t}, \Phi_{hkl}) \approx \exp(-\tfrac{1}{3}\bar{t}^2\lambda^2 |\frac{\Phi_{hkl}}{\Omega}|^2) \qquad 802$$

and Ω = volume, $\bar{t}$ = the thickness of the crystal. Eq. 801

can be rewritten as

$$I_{hkl} \sim \Phi^2_{hkl} \cdot K \qquad 803$$

The Patterson function is defined as

$$P = F^{-1}(I) \qquad 804$$

where Γ is omitted for convenience and F^{-1} denotes the operation of a Fourier summation and the subscripts are dropped for convenience. Therefore

$$\begin{aligned} P &\sim F^{-1}(\Phi^2 \cdot K) \\ &\sim F^{-1}(\Phi^2) \cdot F^{-1}(K) \\ &\sim P_k \cdot F^{-1}(K) \end{aligned} \qquad 805$$

Where P_k denotes the Patterson in the kinematic case and $\frown$ denotes the convolution operator. This shows that the Patterson is further convoluted with the transform of the modification factor.

Alternately, if Φ' is the "true" kinematic structure amplitude, and Φ the dynamical or apparent structure amplitude and K the two-beam correction factor as defined in Eq. 802, then Φ' can be expressed as

$$\Phi' = \Phi \cdot K^{-1} \qquad 806$$

The Patterson in this case is then

$$P' = F(|\Phi'|^2) \qquad 807$$

The correction factor K is plotted in Figure 803.

As shown by Eq. 806, K modifies Φ; but according to

Figure 803, its effect is only considerable if $\bar{t}\Phi$ is large. It is readily seen that K^{-1} only increased the amplitude of Φ with no other effect. Eq. 807 indicates that the Patterson function is now calculated with each intensity increased by a factor K^{-1}. In the case of the modification being small, i.e., $K \approx 1$, it is seen that according to the two beams approximation, the Patterson map will not significantly differ from the kinematical Patterson and therefore does not show any definite effects in the locations of peaks because of dynamical scattering. For a multiple beam dynamical approximation such as that published by Schiff [44] the modified Patterson is more difficult to interpret. According to Schiff, the structural amplitude can be expressed as

$$\Phi \sim iF(1-e^{-i\psi}) \qquad 808$$

where ψ is the electric potential within the unit cell. The Patterson is then

$$\begin{aligned} P &= F^{-1}[\Phi\cdot\Phi^*] \sim F^{-1}(I) \\ &= F^{-1}\{F(1-e^{-i\psi(x,y)})\ F^{-1}(1-e^{i\psi(x,y)})\} \qquad 809 \\ &= \overline{(1-e^{-i\psi(x,y)})}(1-e^{i\psi(-x,-y)}) \end{aligned}$$

It is the convolution of a complex function of the electric potential instead of the autocorrelation of the electric potential. In the case that the dynamical scattering is not very strong, i.e., if ψ is small, the complex function goes over to the kinetic case readily. For small ψ if $\psi \ll 1$, then

Figure 803

Theoretical values of K (after Vainshtein, ref. [3]). This is the factor which corrects for dynamical effect according to the two-beam approximation. When $\bar{t}\cdot\lambda\cdot\left|\frac{\Phi}{r}\right|<2K$ can be approximated as $\exp\{-y_3\bar{t}^{-2}\lambda^2\left|\frac{\Phi}{r}\right|^2\}$.

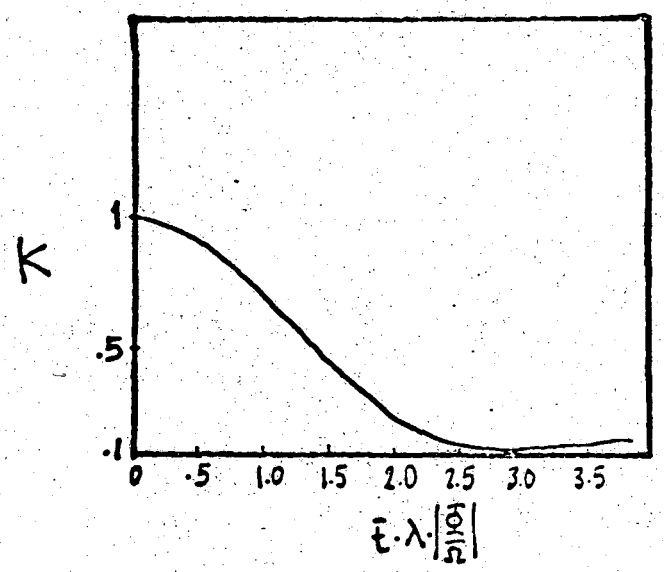

Figure 803.

$$i(i-e^{-i\psi}) \rightarrow i(1-1+i\psi\ldots) \rightarrow \psi \qquad 810$$

Therefore, in the case of not very strong scattering, the Schiff formula approaches the kinematic formulation and we would not expect the Patterson to differ appreciably from the kinematic case also.

According to the theory of Cowley and Moodie [45] for the case of a one dimensional centrosymmetric crystal with Gaussian atoms

$$\psi(x, y) = c \exp(-x^2) \qquad 811$$

the Patterson function can be expressed as (see Eq. 229)

$$P = \exp\{ic\overbrace{e^{-x^2}\}\ \exp\{ic}e^{-x^2}\} \qquad 812$$

where c is some number which represents variations in the atomic number of the atoms or the crystal thickness. For the cases of light atoms c is less than 2. The way in which the peak heights and the total areas of the peaks of Eq. 812 vary with c is given by Figure 804. It is seen that for light atoms (with c less than 2) the dynamical Patterson is not appreciably different from the kinematical Patterson.

The present experiment uses more accurate atomic scattering factors and three dimensional data. The crystal of β glycine is centrosymmetric. Therefore the analysis of Cowley and Moodie has relevance even though their calculation is one dimensional and is based on an assumed Gaussian scattering potential. The experimental observation reported here seem to confirm their result.

Figure 804

The variation with c of the peak height and peak area for Patterson Peaks [9]. c is some number which represents either the atomic number or the atoms or the crystal thickness. This graph shows the difference between the Patterson function calculated with the kinematic theory and that which was calculated by the dynamic approximation of Cowley and Moodie.

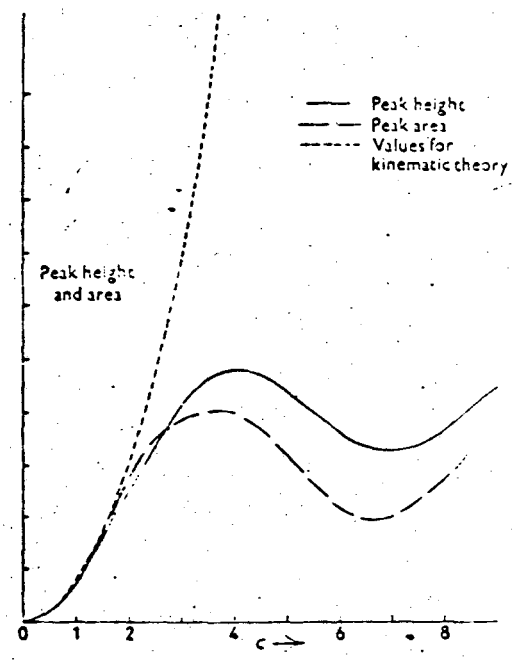
Peak height
Peak area
Values for
kinematic theory
Peak height
and area
0
1
2
4
c →
6
8

Figure 804.

IX. STRUCTURE OF β GLYCINE

The raw intensity data, after correcting for the non-linearity previous to the digitizing process (Chapter VI), and after being arranged by the program INCOR, are used as input to the Least Square Structural Factor Program XRAY (LSLONG). The logic and mechanics of the programs are discussed briefly in Chapter VII. For a more detailed discussion of structural programs of this type, we refer to Stout and Jensen [32] and other standard x-ray crystallography textbooks.

Procedure

(1) Use the atomic scattering factors for electrons f_{el} to calculate the structure amplitudes Φ_{hkl} of the "trial" structure. The "trial" structure in this case is our reference structure determined by Iitaka using x-ray methods. We have put in as input coordinates the atom coordinates as published by Iitaka in 1959 [24]. The Φ_{hkl} thus calculated serves as the basis for determining to what extent the diffraction data show dynamical effects. The result of this experiment is discussed in Chapter X.

(2) Using the Iterative Least Square Procedure, to see how well the diffraction data compare with the trial structure. This program calculates the atom coordinates of a new

structure whose electron scattering amplitudes Φ_{hkl} are the most consistent with the diffraction data as determined by the Least Square Method. The program also calculates a new temperature factor for each atom; in this case we have only attempted the isotropic case. The initial temperature factor should be determined by a Wilson plot, but for simplicity we have put in as input the temperature factor as given by Iitaka.

(3) By putting a small variation of the atomic coordinates in such a trial structure from the standard reference structure we can see whether the diffraction data converges to the same minimum or whether they converge to a different minimum. If they converge to a different minimum, this would indicate that the set of experimental data is not good enough to give a unique structure and hence, we would have less confidence in this experimental procedure.

(A) Reliability Factor: After a five cycle refinement, the program converges with a reliability factor R = 0.48, the R value for modern x-ray crystallography technique is for most cases less than 10% and for careful work can be refined to as low as 1-2%. A. J. C. Wilson showed that the theoretical value for R which would be obtained by using the proper kind and number of atoms placed randomly is R = 0.59 for acentric space groups and for centric space groups R = 0.83 [45][46]. Vainshtein [47] has pointed out

that for electron diffraction the reliability factor should be about 1.5 times higher in the absence of termination of series for a three dimensional series and 2 times higher for projections than x-ray diffraction.

However, in any experiment, a R value more than 20-30% is indicative of the fact that low levels of confidence should be given to the structure. The reliability is defined as

$$R = \frac{\Sigma|\Phi_o|-|\Phi_c|}{\Sigma|\Phi_o|} \qquad 901$$

where Φ_o and Φ_c denote the observed and calculated structural amplitudes respectively. This parameter shows the degree of agreement between the observed and calculated data. Even though the R value does not assure the correctness or incorrectness of a structure, at least a large R value shows poor agreement with the data.

(B) Bond Lengths and Bond Angles: The atom positions given by the program LSLONG are calculated with the coordinates of the atom N being instructed to be fixed in the program so that an origin of the coordinate system of the unit cell can be defined. The atom coordinates from the calculated structure are tabulated in Table 901, and that of the reference structure in Table 901b. The bond lengths and bond angles calculated respectively from these coordinates are listed in Table 902a, b. Table 902b also lists the differences in bond lengths and bond angles between the values

Figure 901

Molecule of β glycine

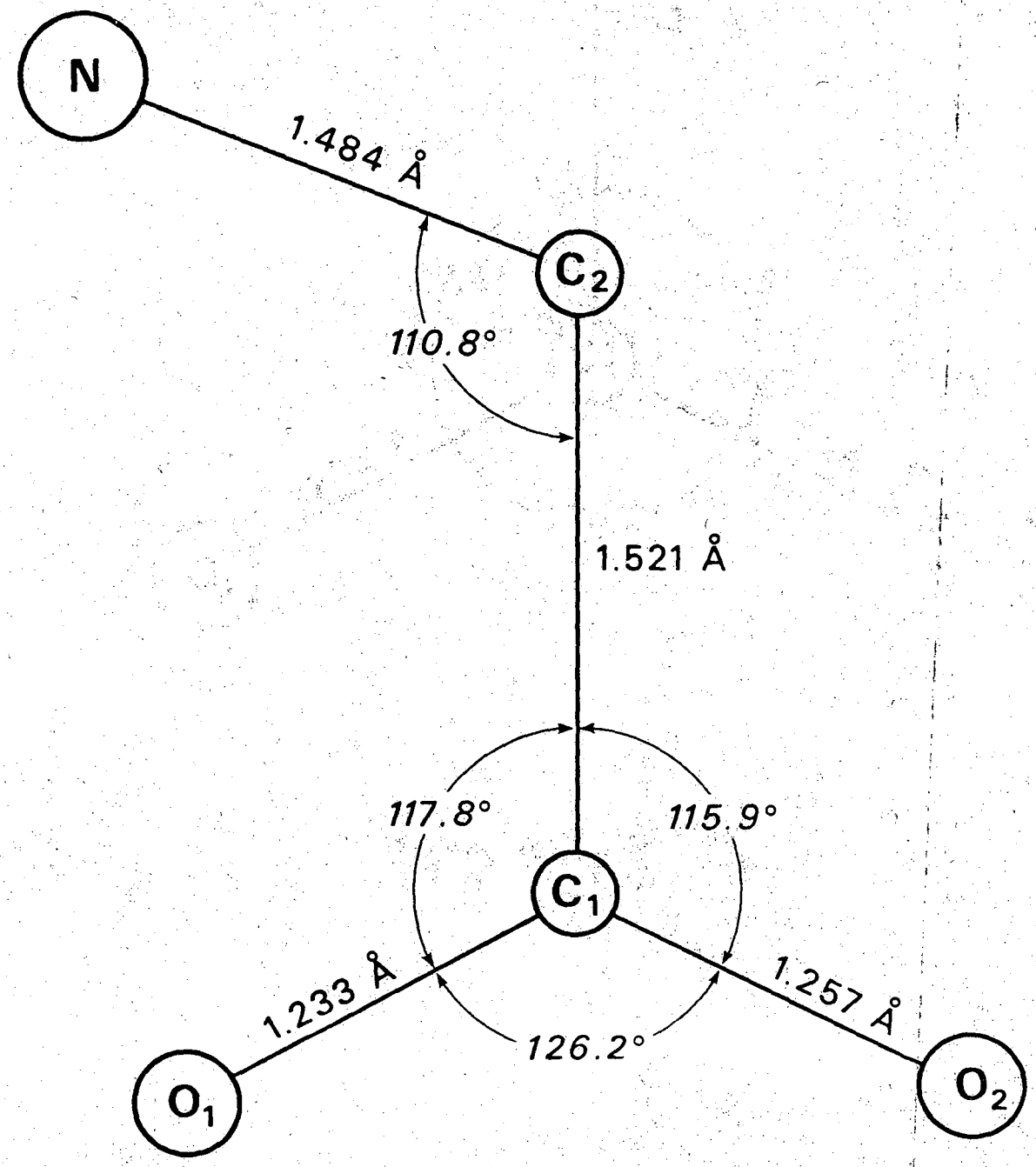

Figure 901.

Table 901a

Atom coordinates of β glycine in fractional units of the unit cell dimensions as given by Iitaka.

Table 901b

Atom coordinates in fractional coordinates as calculated by the present experiment. Hydrogen atoms not included in the structure factor program.

Table 901a

	x	y	z
N	0.3522	-0.0440	-0.2619
O1	0.3772	0.0270	0.2420
O2	-0.0896	0.0773	0.0970
C1	0.1378	0.0532	0.0633
C2	0.1145	0.0719	-0.2265

Table 901b

	x	y	z
N	0.3522	-0.0440	-0.2619
O1	0.3834	0.0402	0.2369
O2	-0.0901	0.0980	0.1248
C1	0.1319	0.0099	0.0756
C2	0.1095	0.1230	-0.2396

Table 902a

Bond lengths and bond angles, calculated by using the atom coordinates of Table 901a.

Table 902b

Bond lengths and bond angles, calculated by the atom coordinates of Table 901b. The differences are the differences calculated by subtracting this value from the standard value which is given in Table 902a.

BOND LENGTHS	calculated	difference
N-C2	1.4837 A	
C2-C1	1.5207	
C1-O1	1.2279	
C1-O2	1.2464	

BOND ANGLES	calculated	difference
C2-C1-O2	115.9320°	
C1-C2-N	110.8000	
C2-C1-O1	117.7790	
O1-C1-O2	126.1790	

Table 902a. Bond lengths and bond angles.

BOND LENGTHS	calculated	difference
N-C2	1.6409 A	-0.1572 A
C2-C1	1.7995	-0.2788
C1-O1	1.2435	-0.0156
C1-O2	1.3712	-0.1248

BOND ANGLES	calculated	difference
C2-C1-O2	105.7590°	10.1734°
C1-C2-N	93.0441	17.7559
C2-C1-O1	105.2870	12.4925
O1-C1-O2	120.0000	6.1792

Table 902b. Bond lengths and bond angles.

given by Iitaka and that which is given by the present experiment. The atoms of β glycine are labeled in Figure 901. It can be seen readily that the changes in bond lengths are relatively small compared with the changes in bond angles. The largest changes in bond length occurs with the C_1--C_2 bond which is 0.27 Å or about 20%. The largest change in bond angle is the angle at atom C_2. The change is 17° or almost 17%. Assuming the correctness of the reference structure, this degree of deviation is very significant.

(C) <u>The Question of Temperature Factor</u>: In the early stages of structure determination, we encountered negative temperature factors in the structural program refinement. Taking the thermal motion of the atoms into account, the structure amplitude can be expressed as

$$\Phi_{hkl} = \sum_i f_{el_{i,T}} \exp(2\vec{r}i(\vec{r}_i \cdot \vec{H})) \qquad 902$$

where r_i is the position vector of atom i, $\vec{H}$ is the vector of the reciprocal lattice and $f_{el_{i,T}}$ is the atomic scattering factor of the ith atom multiplied by the thermal function, i.e.,

$$f_{el,T} = f_{el} \cdot f_T$$

$$f_T = \exp(-B(\frac{\sin\theta}{\lambda})^2)$$

where B is defined as the temperature factor. Unreal or negative temperature factors can be due to the following situations.

(1) Uncorrected non-linear effects of the data processing procedure.

In Chapter VI, it has been shown that the response of the photographic plate is non-linear. For the most part, a correction of the form $I = e^{KD}$, where D is the blackening and K is some constant, is adequate. Suppose that the slope K is corrected, and K' is the true slope, then Eq. 904 can be written as

$$I = e^{KD} = e^{(K'-\Delta K)D} = e^{K'D} \cdot e^{-\Delta KD} \qquad 905$$

recalling that

$$\Phi \sim U^{I} = \sqrt{e^{KD} \cdot e^{-\Delta KD}} = \sqrt{I \cdot e^{-1/2\Delta KD}}$$

$$\therefore \sqrt{I} \simeq \Phi \cdot e^{1/2\Delta KD} \qquad 906$$

Equation 906 shows that in this case the effect is the introduction of a factor of the form $e^{1/2\Delta KD}$ into Eq. 902. This factor also varies although in some complicated manner, as $(\frac{\sin\theta}{\lambda})^2$ and it also counteracts the temperature factor.

(2) The atomic scattering factor f_{el} as a function of $(\frac{\sin\theta}{\lambda})^2$ falls off too slowly. This needs a re-calculation of the f_{el} tables.

The f_{el} as a function of angle is shown in Figure 902. It can be seen from Figure 902 that f_{el} approximates an $e^{-K(\frac{\sin\theta}{\lambda})^2}$ curve. If it is falling off less sharply than it should, the effect is as though f_{el} is modified by some factor of the form $e^{+K'(\frac{\sin\theta}{\lambda})^2}$ with some constant K'. This

factor has the same functional form as f_T and counteracts to it.

(3) Dynamical effects

For a single crystal of "medium" thickness, the integrated intensity according to the two beam dynamical approximation can be expressed as

$$I = c\lambda^2 |\frac{\Phi}{\Omega}|^2 \cdot t \cdot K \qquad 907$$

where c is some constant, t is the thickness of the crystal, and

$$K \simeq \exp\{-\frac{1}{3}(t)^2 \cdot \lambda^2 |\frac{\Phi}{\Omega}|^2\} \qquad 908$$

with Ω denoting the unit cell volume.

If I' is the correct intensity $\qquad I' \sim \Phi^2$

and $\qquad \Phi \sim \sqrt{I'} = \sqrt{I} \cdot \frac{1}{K} \qquad 908a$

It is obvious from Eq. 908 that the dynamical correction factor 1/K introduces into Eq. 902 a factor of the form $e^{+k\Phi^2}$ which also is dependent on $(\frac{\sin\theta}{\lambda})^2$ and counteracts the temperature function f_T.

From the experimental results Case (2) clearly does not apply. If Case (2) were true, then the temperature factor of the same kind of atom, for example carbon, will be negative. The results of three types of experiments directed to this question are tabulated in Tables 904, 905, and 906. The experimental results as listed: Tables 904 and 905 are calculated from the same raw intensity data but their

intensities are corrected for non-linearity by different values of slope K.

From Tables 904 and 905, it is shown that the temperature factor of C1 and C2 are of different signs. Therefore, case (2) is ruled out.

Case (1) seems probable because, as shown in Table 906, after correction of non-linearity effect by assuming a two slope correction curve (Chapter VI) all the temperature factors become positive. While the correction of non-linearity as described in Chapter VI yields positive temperature factors, it does not improve the R value. This means that the reliability for the calculated structure is lower than before.

The increase in R value with positive temperature factors may mean that the correction method for the non-linearity of the calibration curve is not adequate and introduces systematic errors which cause the increase in R. This explanation seems acceptable because, as was pointed out in Chapter VI, a point by point correction according to the calibration curve should give much more reliable results than the two slope systematic correction method we have used.

Another explanation for the negative temperature factor is Case (3). The evaluation of the extent to which the diffraction data are dynamical will be discussed in Chapter X.

A combination of the effects of Case (1) and Case (3) is possible.

Figure 902

The atomic scattering factor f_{el} as a function of $\sin\theta/\lambda$ (after Vainshtein, ref. [3]).

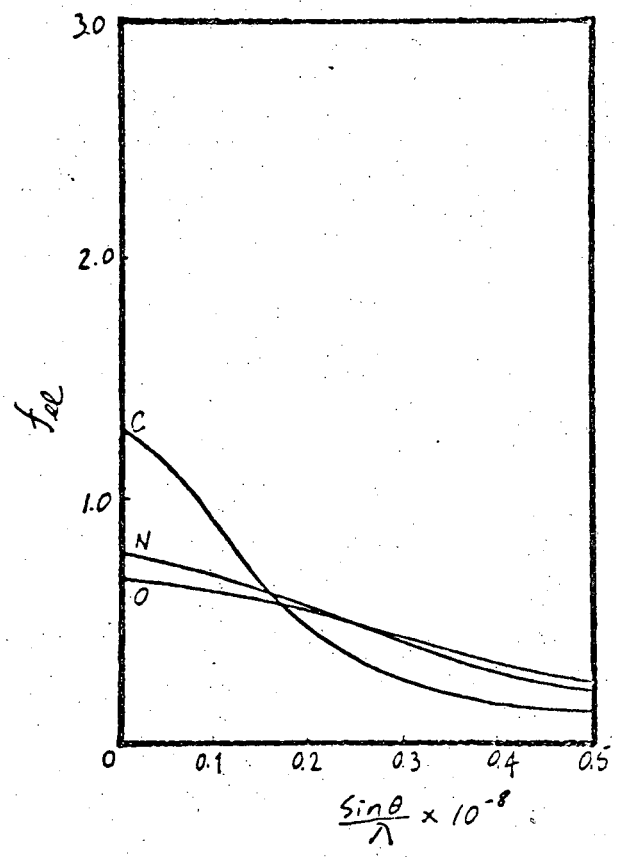

Figure 902.

Output of the Least Square program XRAY (LSLONG). Listed are: The reliability factor R, the scale factor, the new atom coordinates x, y, z, the new temperature factor B, and the atom types. This is the result after 5 cycles of refinement.

Table 904

Calculated with a one slope non-linearity correction for the raw intensities.

Table 905

Calculated with a one slope non-linearity correction for the raw intensities. Slope different from Figure 904.

Table 906

Calculated with a two-slope non-linearity correction for the raw intensity data.

Table 904

R (INCLUDING ZERO WEIGHT DATA) = .48732 FOR 235 DATA.
NEW SCALE FACTOR FOR FOBS = .18774

ATOM	NEW X	NEW Y	NEW Z	NEW B11 OR B	
1	.352200	-.040000	-.261900	.420	N
2	.384036	.047212	.237306	.694	O1
3	-.089686	.109566	.124899	2.164	O2
4	.131694	.032853	.075080	-.377	C1
5	.103824	.128619	-.239098	.856	C2

Table 905

R (INCLUDING ZERO WEIGHT DATA) = .35765 FOR 199 DATA.
NEW SCALE FACTOR FOR FOBS = .48993

ATOM	NEW X	NEW Y	NEW Z	NEW B11 OR B	
1	.352200	-.040000	-.261900	.252	N
2	.379734	.032229	.222471	.968	O1
3	-.091263	.077586	.112815	1.374	O2
4	.115799	.038816	.075358	-1.296	C1
5	.102688	.111666	-.237292	1.677	C2

Table 906

R (INCLUDING ZERO WEIGHT DATA) = .48925 FOR 235 DATA.
NEW SCALE FACTOR FOR FOBS = .18657

ATOM	NEWX	NEW Y	NEW Z	NEW B11 OR B	
1	.352200	-.040000	-.261900	.532	N
2	.383419	.040202	.236902	.510	O1
3	-.090100	.098018	.124817	2.122	O2
4	.131947	.009902	.075626	.053	C1
5	.109545	.123050	-.239618	.703	C2

(D) Convergence and the Number of Minima: To get some idea about the convergence behavior of the data, as determined by the least square program, three experiments are performed under the following conditions:

1. A small random variation of magnitude 0.02 fractional units is introduced into the input coordinates of the trial structure,

2. All other parameters are kept unchanged.

The results of such experiments are tabulated in Tables 907 and 908. It is clearly seen that they all converge to different minima with high R values.

These experiments add another testimony to the unreliability of the result.

It is not unusual that least square programs do sometimes converge to different minima, for variation in input coordinates of ± 0.02 fractional units, or about 0.1 Å. This kind of variation is not too unreasonable if the atom positions are not accurately known beforehand. If there were enough data to completely overdetermine the parameters, the programs should converge to the same minimum. In the present investigation, the three dimensional data together have about 235 different spots. This is equivalent to having about half that amount of unique data points because of symmetry. When this number is compared with the situation in x-ray diffraction, where data usually run into thousands, our technique at this stage of development seems crude indeed.

Output of the Least Square Program XRAY (LSLONG). Listed are: The reliability factor R, the scale factor, the new atom coordinates x,y,z, the new temperature factor B, and the atom types. This is the result after 5 cycles of refinement.

Table 907a

Result of a slight variation in input trial structure. Experiment I.

Table 907b

Result of a slight variation in input trial structure. Note the unphysical 7 coordinate. Experiment II.

Table 907c

Result of a slight variation in input trial structure. Note the unphysical 7 coordinates. Experiment III.

FIG. 907a

R (INCLUDING ZERO WEIGHT DATA) = .53306 FOR 235 DATA.
NEW SCALE FACTOR FOR FOBS = .16976

ATOM	NEW X	NEW Y	NEW Z	NEW B11 OR B	
1	.352200	-.040000	-.261900	1.538	N
2	.385092	.055257	.263301	1.006	O1
3	-.107160	.111679	.155236	.692	O2
4	.143601	.018659	.073841	1.606	C1
5	.131034	.131650	-.391769	4.859	C2

FIG. 907b

R (INCLUDING ZERO WEIGHT DATA) = .49739 FOR 235 DATA.
NEW SCALE FACTOR FOR FOBS = .19677

ATOM	NEW X	NEW Y	NEW Z	NEW B11 OR B	
1	.352200	-.040000	-.261900	.817	N
2	.365630	.030775	.248559	1.299	O1
3	-.091743	.109148	.091064	2.655	O2
4	.121159	.033912	.027822	-.577	C1
5	.103518	.117382	-33.275909	-.534	C2

FIG. 907c

R (INCLUDING ZERO WEIGHT DATA) = .48482 FOR 235 DATA.
NEW SCALE FACTOR FOR FOBS = .18574

ATOM	NEW X	NEW Y	NEW Z	NEW B11 OR B	
1	.352200	-.040000	-.261900	.560	N
2	.386393	.048405	.246947	1.065	O1
3	-.090810	.114103	.138166	2.092	C2
4	.132133	.043887	.072743	-.681	C1
5	.103031	.127044	-38.264245	1.419	C2

Table 908a

Bond lengths and bond angles. Result of variation of input Experiment I. Calculated with the atom coordinates given in Table 907a. The difference is that between this result and the known values.

Table 908b

Bond lengths and bond angles. Result of variation of input Experiment II. Calculated with the atom coordinates given in Table 907b. The difference is that between this result and the known values. Unphysical values in the bond lengths are due to flaws in the least square program which allow the atom coordinates to exceed the unit cell dimension.

Table 908c

Bond lengths and bond angles. Result of variation of input Experiment III. Calculated with the atom coordinates given in Table 907c. The difference is that which is between this result and known values. Unphysical values in bond lengths are due to flaws in the least square program which allow the atom coordinates to exceed the unit cell dimension.

BOND LENGTHS	calculated	difference
N-C2	1.5124 A	-0.0287 A
C2-C1	1.5786	-0.1579
C1-O1	1.2686	-0.0407
C1-O2	1.6095	-0.3631

BOND ANGLES	calculated	difference
C2-C1-O2	116.4200°	-0.4879°
C1-C2-N	68.0730	41.127
C2-C1-O1	112.1560	-5.6234
O1-C1-O2	109.4600	-16.7192

Table 908a. Bond lengths and bond angles.

BOND LENGTHS	calculated	difference
N-C2	*	
C2-C1	*	
C1-O1	1.3378	-0.1099
C1-O2	1.3395	-0.0931

BOND ANGLES	calculated	difference
C2-C1-O2	124.7770°	-8.8447°
C1-C2-N	*	
C2-C1-O1	121.4860	-3.7066
O1-C1-O2	109.8330	16.3457

*Unphysical values (please see legend)

Table 908b. Bond lengths and bond angles.

BOND LENGTHS	calculated	difference
N-C2	*	
C2-C1	*	
C1-O1	1.2616	-0.0337
C1-O2	1.3828	-0.1364

BOND ANGLES	calculated	difference
C2-C1-O2	125.1380°	-9.2057°
C1-C2-N	*	
C2-C1-O1	109.8960	-7.8828
O1-C1-O2	120.2668	-5.9132

*Unphysical values (please see legend)

Table 908c. Bond lengths and bond angles.

The number of unique data points used in Iitaka's work was only about one hundred, however. His data were from the h01 and 0kl projections. This number should be looked upon as the barest minimum that can be used, as present day x-ray crystallography usually works with data points numbering one or two orders of magnitude higher.

(E) Hydrogen Atoms: A Fourier synthesis using the phases and scattering amplitudes of the calculated structure is shown in Figure 902. A ΔF synthesis using the same conditions is shown in Figure 903.

The difference Fourier synthesis is a powerful tool in the refinement of the atom parameters. It is a Fourier synthesis using the difference between the magnitudes of the observed and calculated structure amplitudes $|\Phi_o|-|\Phi_c|$ as coefficients. It can be expressed in the form

$$\Delta F = \sum_{hkl} (|\Phi_o|-|\Phi_c|) e^{i\alpha_c} e^{-2\pi(\vec{H}\cdot\vec{r})} \qquad 909$$

where α_c is the phase of Φ_c. If the phases are correct, Eq. 909 provides a direct measure of the errors between the model used and the "true" structure implied by the Φ_o's.

The difference map has a peak everywhere that the Φ_c model fails to provide the electron density implied by the $|\Phi_o|$ (the phases of the Φ_c are used). It shows a hole where it provides too much. As a first approximation, correctly placed atoms will not appear in the synthesis, incorrectly placed ones will be in holes and missing ones will appear as

Figure 902

Fourier synthesis map of the scattering potential of β glycine at a section along the b-axis where b = 0.8 fractional units.

Figure 903

The ΔF synthesis of β glycine along the b axis. It is a section at b = 0.8 fractional units. The solid dots are the atom centers of the β glycine molecule minus hydrogens. The open circles denote hydrogen atoms. See text for further discussion.

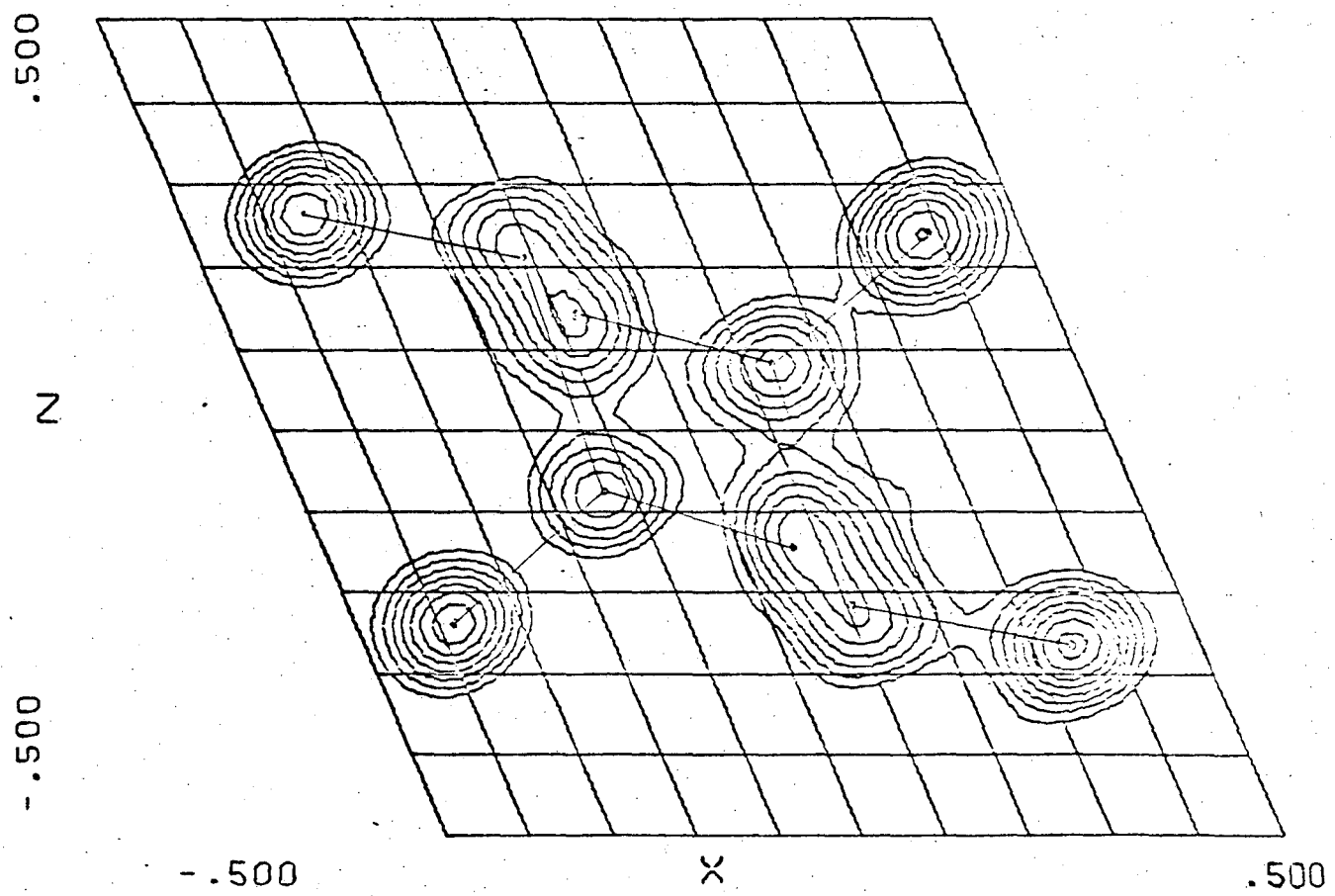

Figure 902.

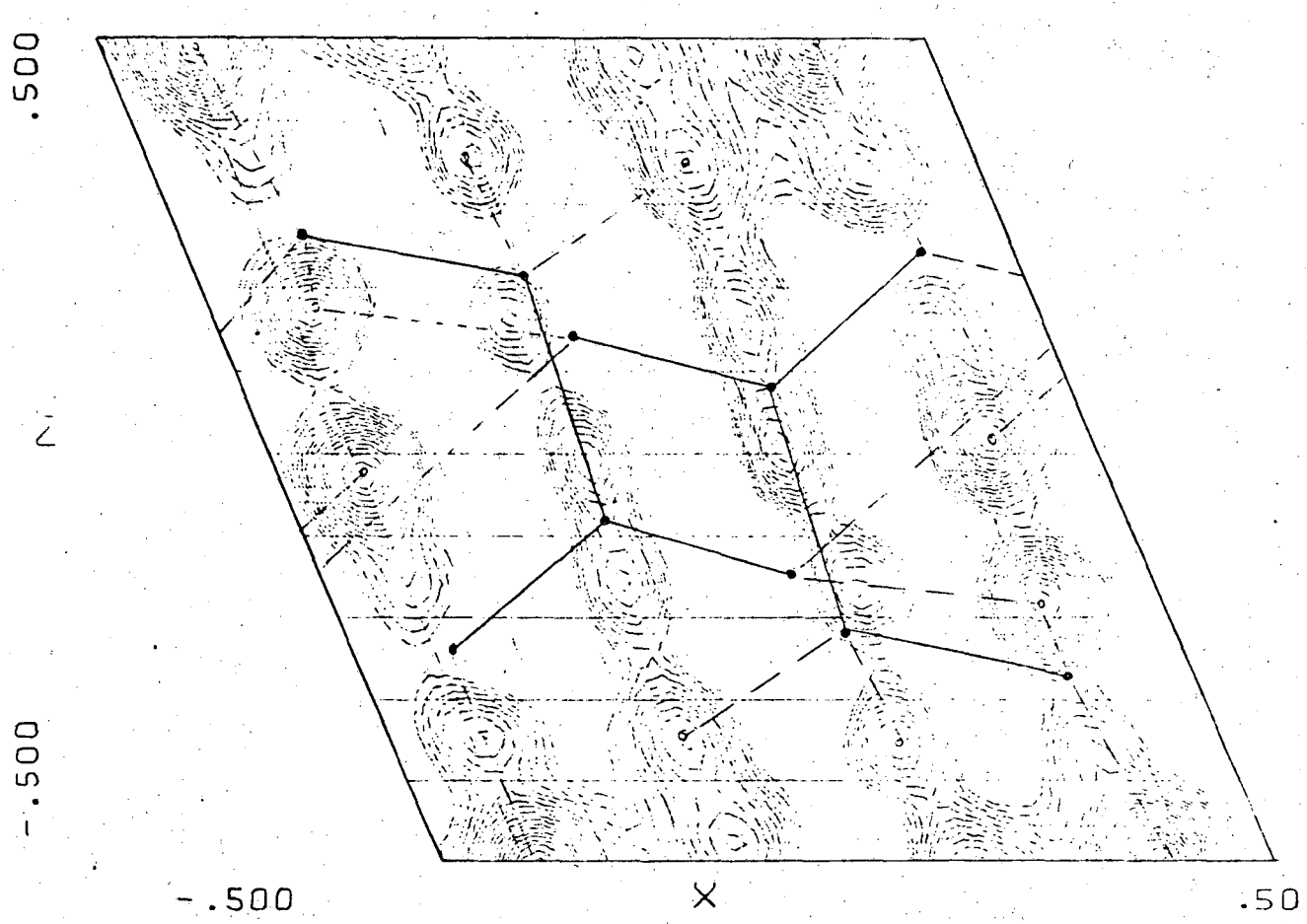

Figure 903.

Output of the Least Square Program XRAY (LSLONG). Listed are: The reliability factor R, the scale factor, the new atom coordinates x,y,z, the new temperature factor B, and the atom types. This is the result after 5 cycles of refinement.

Table 909

Hydrogen positions as given by Iitaka are included in the calculation, but they are not refined.

Table 910

Bond lengths and bond angles. Calculated from Table 909. The difference shows the discrepancy between this result and that of the known values.

FIG. 909

R (INCLUDING ZERO WEIGHT DATA) = .47185 FOR 235 DATA.
NEW SCALE FACTOR FOR FOBS = .19515

ATOM	NEW X	NEW Y	NEW Z	NEW B11 OR B	
1	.352200	-.040000	-.261900	.590	N
2	.383831	.039544	.241836	.591	O1
3	-.085458	.120674	.105738	2.989	O2
4	.131949	.027645	.077351	-.796	C1
5	.109340	.114648	-.213692	-.061	C2

ATOMS NOT REFINED.

6	.540000	.012000	-.135000	2.000	H1
7	.340000	-.031000	-.449000	2.000	H2
8	.337000	-.203000	-.216000	2.000	H3
9	.125000	.241000	-.274000	2.000	H4
10	-.091000	.008000	-.362000	2.000	H5

BOND LENGTHS	calculated	difference
N-C2	1.6669 A	-0.1832 A
C2-C1	1.6189	-0.0982
C1-O1	1.2378	-0.0099
C1-O2	1.3093	-0.0629

BOND ANGLES	calculated	difference
C2-C1-O2	102.7440°	13.1883°
C1-C2-N	100.3580	10.4422
C2-C1-O1	109.2890	8.4904
O1-C1-O2	124.8320	1.3475

Table 910. Bond lengths and bond angles.

peaks.

It also shows where an anisotropic temperature factor is needed. For further discussion on the role of the ΔF synthesis in the refinement of structures, the reader is referred to standard texts such as Stout and Jensen [48].

From the difference Fourier map of Figure 903 it is readily seen that

1. Atom O1 has too large an isotropic temperature factor (TF) and anisotropic TF correction is necessary,

2. Atom C1 has too small an isotropic TF and also anisotropic TF correction is needed,

3. Atom O2 needs a larger shift in coordinates, and/or probably has too large a temperature factor,

4. Hydrogen atoms are easily located and occur at peaks labeled with open circles and connected by dotted lines as shown in Figure 903.

These observations indicate that further refinements in the direction of

a. Putting in anisotropic temperature factors for at least atoms O1 and C1.

b. Including hydrogen atom positions are in order. But as mentioned above, because of the high reliability factor value, further refinement was not attempted.

The above observations testify to the fact that the scattering cross-sections of hydrogen with electron diffraction is considerably higher than that of x-ray diffraction,

hence detection is much easier.

Except for the fact that a couple of the smaller peaks in the difference map (Figure 903) cannot be accounted for, Figure 903 is an excellent example of the detection of hydrogen atom locations by the difference Fourier synthesis of electron diffraction methods.

Figure 903 further suggests that including the hydrogen atoms into the calculation of structural amplitudes can reduce the error. The result is shown in Table 908, in which a 5 cycle refinement of the least square program with the hydrogen atoms included but not refined is tried.

As shown in Table 909 and 910, this experiment produces a slightly better result, as the calculated bond lengths and bond angles are concerned, but it neither reduces the R factor nor gives a reasonable temperature factor. The conclusions drawn previously in this chapter therefore still hold.

(F) Refinement of Calculated Structure: In view of the preceding results, refinement of the calculated structure seems out of the question. Therefore, we have decided not to further refine by the normal techniques such as using anisotropic temperature factors, doing difference Fourier synthesis and refining the positions of the hydrogen atoms, etc.

X. EXTENT OF DYNAMICAL SCATTERING

The first sign indicating possible effects of dynamical scattering is the presence of forbidden reflections. Since we are working with a structure that has been accurately determined by x-ray diffraction, these forbidden reflections do not present serious problems in space group determination. If the structure is unknown and if there were no accurate x-ray diffraction data to act as a standard reference, the presence of forbidden reflections would pose serious problems in the determination of space groups.

The space group of glycine as by Iitaka is P_{2_1} [24]. This is confirmed by the indexing of our electron diffraction patterns except for the forbidden reflections along the k axis. The extinction rule is k = odd, for the oko reciprocal lattice row of the hko projection, and none for the h0l projection. As can be readily seen from Figure 1001, the 010, 030, 050, $0\bar{1}0$, $0\bar{3}0$, $0\bar{5}0$ reflections do appear with appreciable intensities. In Chapter VI it was pointed out that since we have the x-ray diffraction data as standard, the INCOR program was instructed to ignore these forbidden reflections. However, the appearance of these systematic reflections may be interpreted either as a sign of dynamical effect or as a result of incoherent secondary scattering [9,

Figure 1001

Microdensitometer tracing of the 0h0 reflections. These are values of the diffraction spots before non-linearity connections are made.

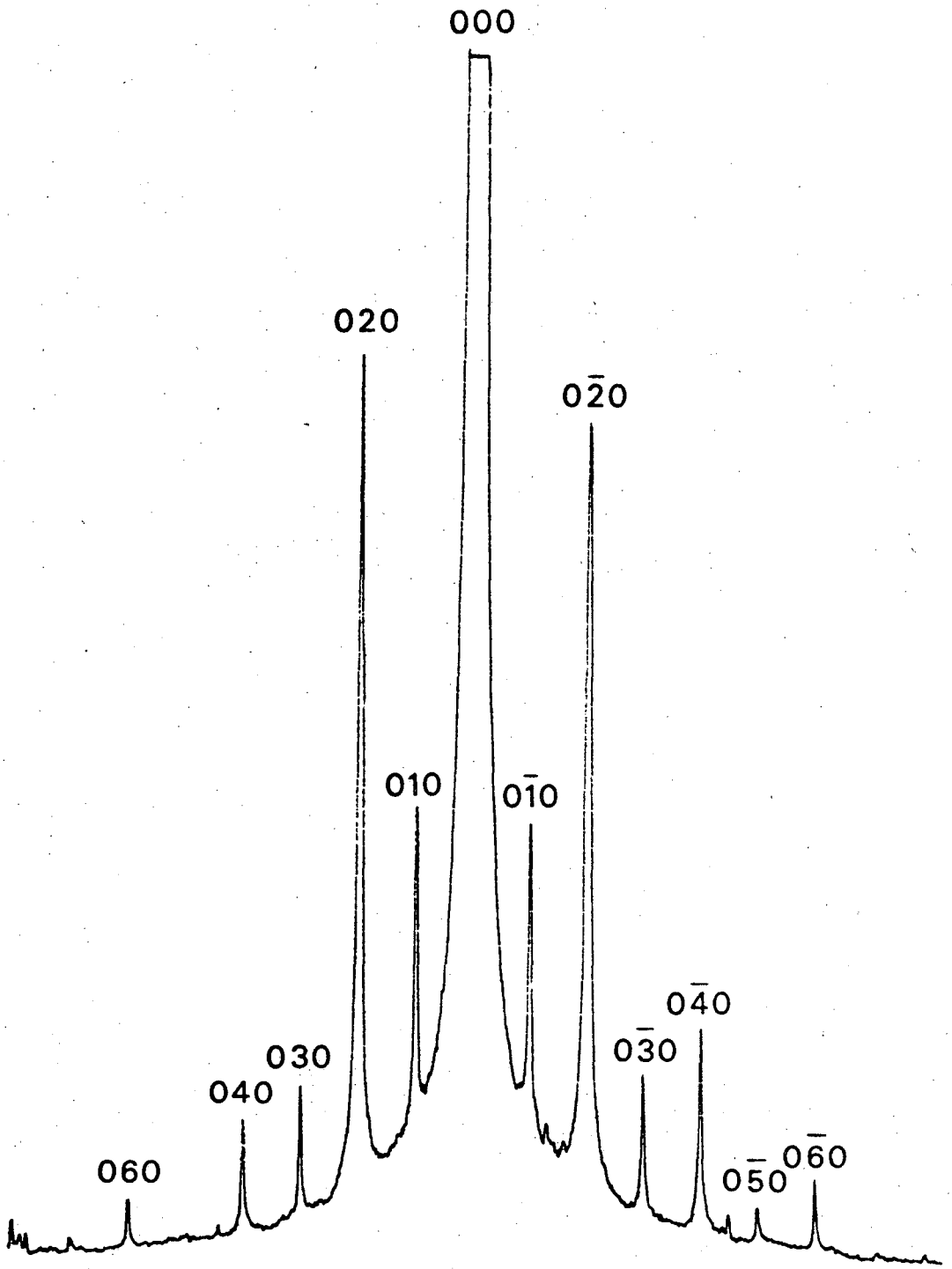
000
020
0$\bar{2}$0
010
0$\bar{1}$0
0$\bar{4}$0
0$\bar{3}$0
030
040
060
0$\bar{5}$0
0$\bar{6}$0

Figure 1001.

27,44]. If the forbidden reflections are due to secondary scattering rather than multiple scattering, it is possible to correct for it if its influence is not very strong [49, 50]. This represents yet another stage of refinement which we shall not attempt to do.

There are methods for correcting the effect of dynamical scattering such as that proposed by Honjo and Kitamura [51] and by Nagakura [52]. Honjo and Kitamura made their dynamical correction based on the two beam approximation of Blackman. They proposed a method of recording data at several wavelengths and extrapolating the observed intensities to zero wavelength. Nagakura proposed another method utilizing Wilson's intensity statistics combined with the theory of primary extinction.

Any effort compensating the effects of dynamic scattering would undoubtedly improve both the resolution and the reliability of structural determination. The correction represents yet another stage in the refinement of the calculated structure.

If a standard reference structure is known and its structure amplitude Φ is calculated, Vainshtein [53,54] suggests a method which allows the comparison of the two beam correction factor K_{exp} with the theoretical value of that quantity. The K_{exp}, which is arrived at experimentally, also allows a crude calculation of $\bar{t}$, the mean thickness of the crystal. The method is valid for crystals of "medium"

thickness and for the region $\bar{t}\cdot\bar{\lambda}\left|\frac{\Phi_{hkl}}{\Omega}\right|<2$.

According to the two beam approximation, the integrated intensity for a "medium" thickness crystal can be expressed as

$$I_{hkl} = \lambda^2\left|\frac{\Phi_{hkl}}{\Omega}\right|^2\bar{t}\cdot K(\bar{t},\Phi) \qquad 1001$$

with

$$K(\bar{t},\Phi) \simeq \exp\{-\frac{1}{3}(\bar{t}\cdot\lambda\left|\frac{\Phi_{hkl}}{\Omega}\right|)^2\} \qquad 1002$$

These equations are the same as Eq. 907 and 908 respectively and the symbols are as defined in those two equations.

Equation 1001 can be written as

$$\frac{k\cdot I^{rel}_{exp}}{\Phi^2_{cal}} = c\cdot K_{exp} \qquad 1003$$

where c is equal to $\frac{\Omega^2}{\lambda^2\cdot\bar{t}}$, I^{rel}_{exp} is the experimental relative intensity, and k is the scale factor which brings I^{rel}_{cal} into the same unit as Φ^2_{cal}. Equation 1003 is valid for each hkl reflection in the two beam case. Since Eq. 1002 defines the functional form of K, it follows that K_{exp}, defined by Eq. 1003, would also have the same functional form if the two beam dynamical approximation for the medium thickness case were applicable. Equation 1002 can be re-written as

$$\sqrt{-\ln K} = \frac{1}{\sqrt{3}}\frac{\bar{t}\cdot\lambda}{\Omega}\Phi = m\Phi \qquad 1004$$

Equation 1004 defines m. If we put into Equation 1004 K_{exp} instead of K, then the slope of the plot of K_{exp} against Φ_{cal} is m. With the value of m thus determined, the average

thickness $\bar{t}$ can readily be obtained from Equation 1004.

The average thickness $\bar{t}$ could also be measured by using the intercept of Equation 1003,

$$k \left[\frac{I^{rel}_{exp}}{\Phi^2_{cal}}\right]_{\Phi=0} = \frac{\Omega^2}{\lambda^2 \bar{t}} \qquad 1004a$$

However, in this case k which is the scale factor, would have to be determined independently such as by varying λ.

The plot of K_{exp} against Φ_{cal} is shown in Figure 1002. The slope determined from it is m = 0.2 ± 0.1. The average thickness of the crystal is then

$$\bar{t} = \frac{m\sqrt{3}\Omega}{\lambda} \qquad 1005$$

Substituting into Equation 1005, λ = 0.0418Å, Ω = 157.835Å^3, we obtain $\bar{t}$ = 1310Å, within a factor of two.

This value of the average thickness is of the same order of magnitude as that which was estimated theoretically by Vainshtein for organic crystals with Z = 6-8, and having 20-25 atoms in the unit cell. For such a case Vainshtein gives a thickness of about 1200A as the thickness of crystallites at which kinematic scattering changes to dynamic scattering. From this, we can infer that the sample we have used had a thickness which is beginning to or is showing effects of dynamical scattering.

From Eq. 1002, it is obvious that the purely kinematical case would mean a zero slope, i.e., m = 0. The more dynamical the situation is, the larger is the value of m. The conclusion

that our sample is on the border line of showing dynamical effect is evident from Figure 1002 and 1003. A "best fit" straight line through the points, as judged by eye, has almost a zero but slightly positive slope. The scatter of the points makes an accurate determination of m almost impossible.

This way of calculating the mean thickness and interpreting the extent of dynamical scattering has validity only if the following set of conditions apply:

1. The two beam dynamical approximation is valid. However, the large intensities in the forbidden reflections may indicate the presence of multiple beam effects.

2. The crystal is of "medium" or intermediate thickness so that absolute dynamical effect is not taking place.

3. The standard structure or reference from which the Φ_{cal} is calculated, is correct with a high degree of confidence.

4. $\bar{t} \cdot \left|\frac{\Phi}{\Omega}\right| < 2$.

5. The thickness of each mosaic element must be the same, and there must not be large statistical variations in volume between the individual mosaic elements that give rise to the individual reflections.

The above conditions seem to apply in this case.

The inclusion of hydrogen atoms into the calculation of structural amplitudes produces slightly different values for

Figure 1002

Curve to show dynamical effects. Φ_{cal} is calculated without H atoms. The ordinate is the ratio I_{exp}/Φ^2_{cal} which is assumed to be equal to $\sqrt{-\log(K_{exp})}$ according to the two beam dynamical theory. A best-fit straight line is drawn through these points by eye. Because of the functional form of K (see text), the points corresponding to large Φ values are given more weight than those corresponding to small Φ, in drawing the line. The slope of the line determines the extent of dynamical scattering.

Figure 1003

Curve to show dynamical effect, Φ_{cal} is calculated with hydrogen atoms.

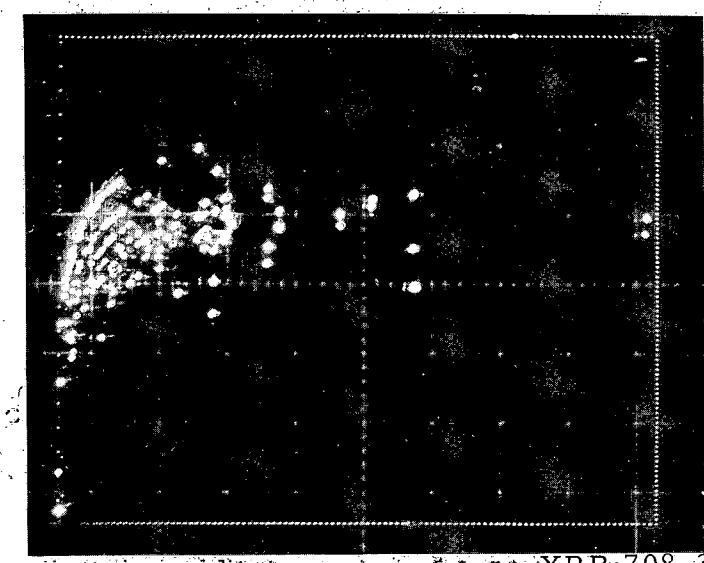

XBB 708-3743

Figure 1002.

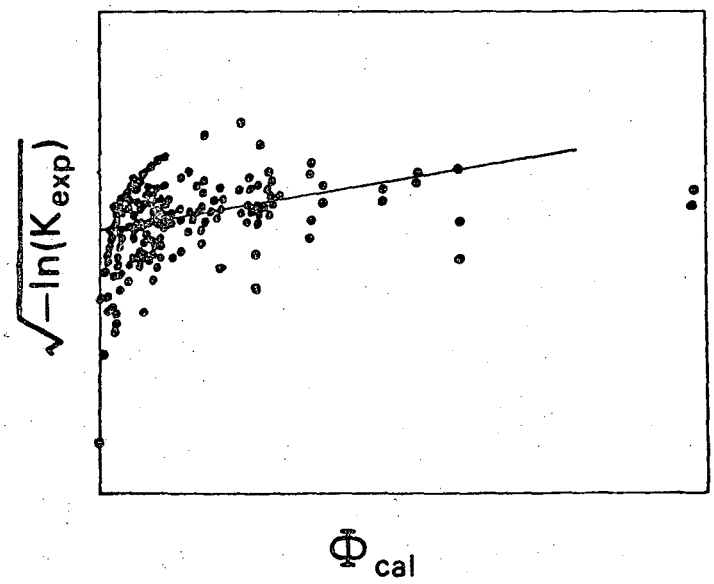

Graphic representation of Figure 1002.

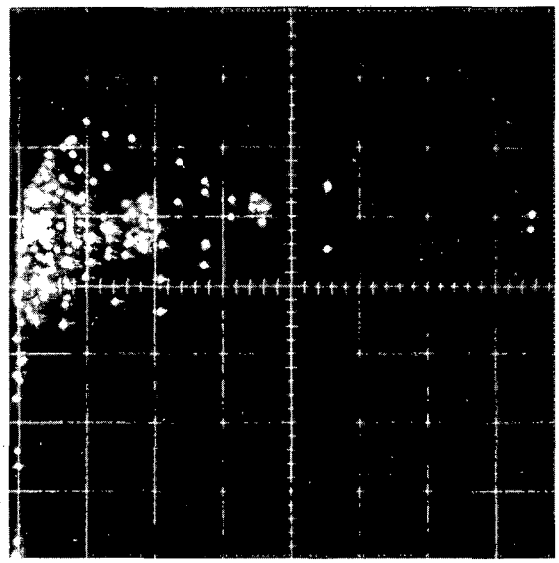

XBB 709-3852

Figure 1003.

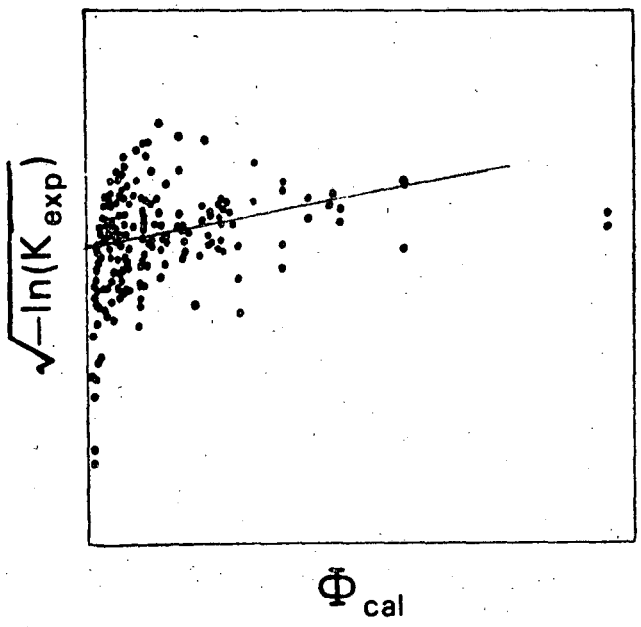

Graphic representation of Figure 1003.

the calculated structure amplitudes (Appendix B-2). Figure 1003 is the same as Figure 1002 but calculated with the structure amplitudes which includes hydrogen. It is not appreciably changed, hence the mean crystal thickness can be taken as being the same order of magnitude as that which was estimated from the previous plot, particularly since the whole method is extremely crude to begin with.

XI. CONCLUSIONS AND SUMMARY

(1) Patterson Function

All three projections of the Patterson function (h0l, hk0, and 0kl) are qualitatively similar to the "point" Patterson maps calculated from the atom coordinates determined by x-ray diffraction methods. This can be taken to mean that either the Patterson function is not sensitive enough to show the difference between kinematic scattering and dynamical scattering behavior, or that the specimen under investigation is thin enough so that the mode of scattering is totally within the kinematic domain. It has been shown theoretically by Cowley and Moodie [45] that the Patterson function is indeed not sensitive enough to reflect the difference between kinematic scattering and moderate dynamical scattering for light atoms.

(2) Dynamical Scattering

Assuming the validity of the atom coordinates as determined by x-ray diffraction, and assuming the validity of the two beam dynamical scattering theory, a test was applied to the electron diffraction data for the two cases of including and excluding the hydrogen atoms, in order to further assess the extent of the dynamical effect. The results for both cases indicate that the specimen is weakly dynamical with a

roughly measured mean thickness of approximately 1300A. This mean thickness is of the same order of magnitude which Vainshtein calculated, for an organic crystal of 20-30 atoms in the unit cell, at which kinematic scattering changes into dynamical scattering effects. To correct the effect of dynamical scattering, experiments of the type performed by Honjo, et al., should be attempted in future work.

(3) Hydrogen Atoms

The difference Fourier synthesis shows distinct peaks located at approximately where the hydrogen atoms should be. This fact shows that hydrogen atoms have a much more pronounced effect in electron scattering than in x-ray scattering. Therefore, in future work, the positions of the hydrogen atoms should be included into the structural amplitude calculation at an earlier stage than it would be for x-ray work. This confirms the work of Vainshtein that H atoms can be located accurately even if the data are not good enough to do the entire structure.

The difference Fourier map also suggested refinement by putting in anisotropic temperature factor for the atoms O1 and C1.

(4) Least Square Method

The structural determination program using the Least Square approximation method is very sensitive in the present work to the initial trial structure. With slight variations

in input, it can converge to different minima. This reduces the level of confidence which can be placed on a calculated structure. Again, better statistics in the overdetermination of the parameters may be able to reduce the number of minima.

(5) Reliability Factor

The reliability factor R of the calculated structure is too high. Therefore, further refinement at this stage is not warranted. A high R value can in the general case be due to a multitude of reasons, such as

a. An incorrect trial structure;

b. Inadequate non-linearity correction;

c. Insufficient overdetermination of the parameters because of the small amount of data available;

d. Dynamical scattering.

It is assumed in this case that the trial structure as determined by x-ray diffraction is correct except for possible dynamical effects which are not significant in x-ray diffraction. Non-linearity correction was discussed extensively in Chapter VI. It is assumed that in the present experiment the necessary correction has been made. The result from Iitaka's work seems to indicate that about 100 unique data points is sufficient to determine the structure even though using a tilting stage to collect reflections from other planes will yield many more data points for a better determination of the parameters.

Hence it may be concluded that the high R value is due primarily to the effect of dynamical scattering that is discussed in point (2) above.

(6) Data Handling

The data collection and conversion system is too limited to process the large amounts of data which any attempt of accuracy in structural determination must require. An automated and integrated system such as the one being developed now (Chapter V) is very much needed.

It has not been the goal of this research to solve completely the crystallographic structure of glycine by the electron diffraction method. This is not yet possible because of theoretical limitations and because the present level of instrumentation is still too crude to yield the large quantity of data that is necessary for very reliable results. Throughout the research, the structure of β glycine as determined by x-ray diffraction has served both as a guide as well as a standard. It is assumed that the structure as "seen" by x-rays is the same as that which is "seen" by electrons. With these assumptions and within the limitations of instrumentation, the above conclusions are drawn from the present investigation.

REFERENCES

1. Thomson, G. P., and Cochrane, W. (1939) Theory and Practice of Electron Diffraction. Macmillan, London.

2. Beeching, R. (1936) Electron Diffraction. Methuen & Co., Ltd.

3. Vainshtein, B. K. (1964) Structural Analysis by Electron Diffraction. Macmillan, New York.

4. Pinsker, Z. G. (1953) Electron Diffraction. Butterworths Scientific Publications, London.

5. Vainshtein, ref. 3, p. 4.

6. Glaecer, R. M. (1970) 7th Int. Congr. of Elec. Micr. in press.

7. Hirsch, P. B., Howie, A., Nicholson, R.B., Pashley, D. W., and Whelan, M.J. (1965) Electron Microscopy of Thin Films. p. 384. Butterworth, London.

8. Vainshtein, B. K. (1960) Quarterly Reviews, XIV, The Chemical Society, London.

9. Cowley, J. M. (1959) Acta Cryst. 12, 367.

10. Vainshtein, B. K., Lobachou, A. N. and Stasova, M. M. (1958) Kristallografiya 3, 374, 452; (1958) Dokl. Akad. Nauk SSSR 120, 523.

11. Hoffman, C. W. (1957) An electron Diffraction Investigation of the molecular structure of cis-dichloroethylene, Ann Arbor, University Microfilms, Doctoral dissertation Series #24, 161, 1967.

12. Vaughn, G. (1954) Ann Arbor, University Microfilms, Doctoral dissertation Series #9900.

13. Ferrier, R. P. (1969) Adv. in Opt. & Electron Microscopy. 3, 155.

14. Parsons, D. F. (1968) Int. Rev. of Expt. Path., G. W. Richter and M. A. Epstein, edition, Academic Press, New York.

15. Glaeser, R. and Thomas G. (1969) Biophysical Journal 9 1073.

16. Klug, A. and Berger, J. E. (1964) J. Mol. Bio., 10, 565.

17. De Rosier, D. J. and Klug, A. (1968) Nature, 217, 130.

18. Moore, P. B., Huxley, H. H., and De Rosier, D. J. (in press) J. Mol. Biol.

19. Finch, J. T., and Gibbs, A. J. (1970) J. Gep. Virol. 6, 141.

20. Crowther, R. A. Amos, L. A., Finch, J. T., De Rosier, D. J. and Klug, A (1970) Nature, 226, 421.

21. Vainshtein, ref. 3., p. 365.

22. Marsh, R. E., and Donohue, J. (1967) Adv. in Protein Chem. 22, 2:35. Academic Press, New York.

23. Marsh, R. E. (1958) Acta Cryst. 11, 654.

24. Iitaka, Y. (1960) Acta Cryst. 13, 35.

25. Iitaka, Y. (1961) Acta Cryst. 14, 1.

26. Scott, W. T. (1963) Rev. Mod. Phys. 35, 231.

27. Mott, N. F., and Massey, H. S. W. (1949) The Theory of atomic Collisions. Clarendon Press.

28. Raether, H. (1965) Spring Tracts in Mod. Phys. 38, 84. Spring-Verlag, Berlin.

29. Born, M. (1926) Z. Physik. 37, 863; 38, 803.

30. Ivanenko, D., and Sokolov, A. (1951) Classical Field Theory. G.I.T.T.L.

31. Sands, D. E. (1969) Introduction to Crystallography. p. 117, W. A. Benjamin, Inc., New York.

32. Stout, G. H., and Jensen, L. H. (1968) X-ray structure Determination. p. 270, Macmillan, New York.

33. Blackman, M. (1939) Proc. Roy. Soc. A, 173, 68.

34. Cowley, J. M., and Moodie, A. F. (1957) Acta Cryst. 10, 609.

35. Albrecht, G., and Corey, R. B. (1939) J. Am. Chem. Soc. 61, 1087.

36. Fischer, E. (1905) Ber. Dtsch. Chem. Ges. 28, 2917.

37. Agar, A. W. (1960) Br. J. Appl. Phys. 11, 185.

38. International Tables for X-ray Crystallography, 1, (1966).

39. Vainshtein, ref. 3, p. 197.

40. Kimura, K., and Bauer, S. H. (1963) J. Chem. Phys. 39 (12) 3171.

41. Valentine, R. C. (1966) Adv. in Opt. & Electron Microscopy. 1, 180.

42. Vainshtein, ref. 3, p. 162.

43. Vainshtein, ref. 3, p. 172.

44. Schiff, L. I. (1956) Physical Review. 103, #2, 443.

45. Wilson, A. J. C. (1950) Acta Cryst. 3, 397.

46. Douglas, A. S., and Woolfson, M. M. (1954) Acta Cryst. 7, 517.

47. Vainshtein, ref. 3, p. 278.

48. Stout and Jensen, ref. 22, p. 356.

49. Vainshtein, B. K. (1956) Trud. Inst. Krist. Akad. Nauk. SSSR. 12, 25.

50. Cowley, J. M., and Rees, A. L. G. and Spink, J. A. (1951) Proc. Phys. Soc. A, 64, 609.

51. Honjo, G., and Kitamura, N. (1957) Acta Cryst. 10, 533.

52. Nagakura, S. (1957) Acta Cryst. 10, 601.

53. Vainshtein, ref. 3, p. 175.

54. Pinsker, Z. G., and Dvoryankina, G. G. (1958) Kristallografiya. 3, 438.

APPENDIX A

Table of the atomic scattering factor f_{el} in p units, i.e., scattering factor relationship to scattering factor or proton for the atoms H, C, N, and O.* Values have been converted into p units from the table given by the International Tables of x-ray Crystallography, Vol. 3, 1966.

$\frac{\sin\theta}{\lambda} \times 10^{-8}$	H	C	N	O
0.00	.221	1.024	.919	.840
0.05	.212	.944	.877	.815
0.10	.189	.861	.798	.752
0.15	.160	.727	.702	.677
0.20	.130	.597	.601	.593
0.25	.104	.480	.500	.510
0.30	.083	.384	.418	.434
0.35	.067	.310	.347	.368
0.40	.055	.250	.288	.313
0.50	.037	.170	.200	.225
0.60	.027	.125	.146	.167
0.70	.020	.092	.113	.130
0.80	.015	.075	.0877	.100
0.90	.012	.058	.071	.079
1.00	.010	.050	.0585	.0668

*The p unit is defined as the ratio of f_{el} of an atom to the scattering power of a proton scattering at a $\frac{\sin\theta}{\lambda} = 0.1 \times 10^{-8}$.

APPENDIX B-1

These are the listings of the computer printouts of the first cycle and fifth cycle of the program LSLONG. Here the F's are the same as the notation Φ that was used throughout, which denotes the structural amplitude. The scaling factor k of the F_{obs} is arbitrary in the first cycle, and the reflection F_{obs} (0,0,0) is not an experimental point but a value put in by the program. In the listing, the H, K, L are the Miller indices, the sinA and CosA are the imaginary and real parts of the phase of the calculated structure. The other listings are only meaningful to the mechanics of the program and not to the physics of the problem.

5	-4	0	.624	.01	.21	.5859	.8104	-.20	.02	-.20	.21	.5859	.8104
5	-3	0	.587	.01	.31	-.4543	-.8909	-.30	.02	-.30	.31	-.4543	-.8909
5	-2	0	.559	.01	.23	-.3155	.9489	-.22	.03	-.22	.23	-.3155	.9489
5	-1	0	.542	.04	.57	-.1396	-.9902	-.53	.08	-.53	.57	-.1396	-.9902
5	0	0	.536	.00	.21	-1.0000	0.	-.21	.02	-.21	.21	-1.0000	0.
5	1	0	.542	.02	.57	.1396	-.9902	-.55	.03	-.55	.57	.1396	-.9902
5	2	0	.559	.01	.23	-.3155	-.9489	-.22	.03	-.22	.23	-.3155	-.9489
5	3	0	.587	.01	.31	.4543	-.8909	-.30	.03	-.30	.31	.4543	-.8909
5	4	0	.624	.01	.21	.5859	-.8104	-.20	.04	-.20	.21	.5859	-.8104
5	5	0	.668	.01	.07	.9544	-.2985	-.07	.07	-.07	.07	.9544	-.2985
5	6	0	.718	.01	.14	.9902	-.1398	-.13	.04	-.13	.14	.9902	-.1398
4	-8	0	.769	.00	.21	.7833	-.6216	-.21	.02	-.21	.21	.7833	-.6216
4	-7	0	.704	.01	.06	-.8865	.4628	-.06	.09	-.06	.06	-.8865	.4628
4	-6	0	.643	.01	.17	.6550	.7556	-.16	.04	-.16	.17	.6550	.7556
4	-5	0	.586	.01	.18	-.9095	.4156	-.17	.03	-.17	.18	-.9095	.4156
4	-4	0	.534	.01	.45	-.4538	.8911	-.44	.03	-.44	.45	-.4538	.8911
4	-3	0	.491	.01	.28	-.9875	.1575	-.27	.03	-.27	.28	-.9875	.1575
4	-2	0	.457	.07	1.07	-.8971	.4419	-.99	.07	-.99	1.07	-.8971	.4419
4	-1	0	.436	.03	.17	-.9145	-.4046	-.15	.15	-.15	.17	-.9145	-.4046
4	0	0	.429	.11	1.45	-1.0000	0.	-1.34	.07	-1.34	1.45	-1.0000	0.
4	1	0	.436	.01	.17	.9145	-.4046	-.17	.04	-.17	.17	.9145	-.4046
4	2	0	.457	.05	1.07	-.8971	-.4419	-1.02	.05	-1.02	1.07	-.8971	-.4419
4	3	0	.491	.01	.28	.9875	.1575	-.27	.03	-.27	.28	.9875	.1575
4	4	0	.534	.02	.45	-.4538	-.8911	-.43	.05	-.43	.45	-.4538	-.8911
4	5	0	.586	.01	.18	.9095	.4156	-.17	.03	-.17	.18	.9095	.4156
4	6	0	.643	.01	.17	.6550	-.7556	-.16	.05	-.16	.17	.6550	-.7556
4	7	0	.704	.00	.06	.8865	.4628	-.06	.07	-.06	.06	.8865	.4628
3	-8	0	.715	.01	.07	.8120	.5837	-.06	.10	-.06	.07	.8120	.5837
3	-7	0	.644	.01	.09	.9910	-.1340	-.08	.11	-.08	.09	.9910	-.1340
3	-6	0	.577	.02	.28	.7024	.7117	-.26	.07	-.26	.28	.7024	.7117
3	-5	0	.512	.01	.22	.6675	.7446	-.21	.05	-.21	.22	.6675	.7446
3	-4	0	.453	.05	.60	.5244	.8515	-.55	.08	-.55	.60	.5244	.8515
3	-3	0	.401	.05	.51	.2502	.9682	-.47	.09	-.47	.51	.2502	.9682
3	-2	0	.359	.09	.66	.3876	.9218	-.57	.13	-.57	.66	.3876	.9218
3	-1	0	.331	.09	.74	.0284	.9996	-.65	.12	-.65	.74	.0284	.9996
3	0	0	.321	.04	.26	1.0000	0.	-.22	.17	-.22	.26	1.0000	0.
3	1	0	.331	.05	.74	-.0284	.9996	-.69	.07	-.69	.74	-.0284	.9996
3	2	0	.359	.03	.66	.3876	-.9218	-.63	.04	-.63	.66	.3876	-.9218
3	3	0	.401	.03	.51	-.2502	.9682	-.48	.06	-.48	.51	-.2502	.9682
3	4	0	.453	.03	.60	.5244	-.8515	-.57	.06	-.57	.60	.5244	-.8515
3	5	0	.512	.01	.22	-.6675	.7446	-.21	.04	-.21	.22	-.6675	.7446
3	6	0	.577	.01	.28	.7024	-.7117	-.27	.03	-.27	.28	.7024	-.7117
3	7	0	.644	.01	.09	-.9910	-.1340	-.08	.06	-.08	.09	-.9910	-.1340
2	-9	0	.749	.00	.06	.9483	.3174	-.05	.08	-.05	.06	.9483	.3174
2	-8	0	.673	.01	.01	-.9030	.4297	-.00	.94	-.00	.01	-.9030	.4297
2	-7	0	.598	.01	.18	.6513	-.7588	-.17	.06	-.17	.18	.6513	-.7588
2	-6	0	.524	.02	.11	-.7927	-.6097	-.09	.16	-.09	.11	-.7927	-.6097
2	-5	0	.453	.03	.47	.7568	-.6537	-.44	.06	-.44	.47	.7568	-.6537
2	-4	0	.384	.04	.31	-.4850	-.8745	-.27	.12	-.27	.31	-.4850	-.8745
2	-3	0	.321	.07	.82	.5423	-.8402	-.74	.09	-.74	.82	.5423	-.8402
2	-2	0	.267	.12	.40	-.0568	-.9984	-.28	.30	-.28	.40	-.0568	-.9984
2	-1	0	.229	.10	.94	.4225	-.9064	-.84	.11	-.84	.94	.4225	-.9064
2	0	0	.214	.05	.13	1.0000	0.	-.08	.35	-.08	.13	1.0000	0.
2	1	0	.229	.07	.94	-.4225	-.9064	-.87	.07	-.87	.94	-.4225	-.9064
2	2	0	.267	.05	.40	-.0568	.9984	-.35	.12	-.35	.40	-.0568	.9984
2	3	0	.321	.05	.82	-.5423	-.8402	-.77	.06	-.77	.82	-.5423	-.8402
2	4	0	.384	.03	.31	-.4850	.8745	-.28	.10	-.28	.31	-.4850	.8745
2	5	0	.453	.03	.47	-.7568	-.6537	-.44	.07	-.44	.47	-.7568	-.6537
2	6	0	.524	.00	.11	-.7927	.6097	-.10	.05	-.10	.11	-.7927	.6097
2	7	0	.598	.00	.18	-.6513	-.7588	-.17	.03	-.17	.18	-.6513	-.7588
-5	0	1	.505	.03	.19	-1.0000	0.	-.16	.17	-.16	.19	-1.0000	0.
-4	0	1	.400	.18	1.12	-1.0000	0.	-.94	.16	-.94	1.12	-1.0000	0.

-3	0	1	.297	.08	.93	-1.0000	0.	-.85	.09	-.85	.93	-1.0000	0.
-2	0	1	.198	.03	.97	-1.0000	0.	-.94	.03	-.94	.97	-1.0000	0.
-1	0	1	.115	.03	.91	1.0000	0.	-.87	.04	-.87	.91	1.0000	0.
0	0	1	.101	.08	2.95	1.0000	0.	-2.87	.03	-2.87	2.95	1.0000	0.
1	0	1	.174	.10	2.65	1.0000	0.	-2.56	.04	-2.56	2.65	1.0000	0.
2	0	1	.270	.06	1.02	1.0000	0.	-.96	.05	-.96	1.02	1.0000	0.
3	0	1	.373	.03	.10	-1.0000	0.	-.07	.28	-.07	.10	-1.0000	0.
4	0	1	.477	.01	.00	-1.0000	0.	.01	9.99	.01	.00	-1.0000	0.
5	0	1	.583	.01	.20	-1.0000	0.	-.18	.06	-.18	.20	-1.0000	0.
-7	0	3	.689	.01	.06	1.0000	0.	-.05	.22	-.05	.06	1.0000	0.
-6	0	3	.593	.02	.13	-1.0000	0.	-.11	.17	-.11	.13	-1.0000	0.
-5	0	3	.501	.02	.32	-1.0000	0.	-.30	.07	-.30	.32	-1.0000	0.
-4	0	3	.416	.02	.01	1.0000	0.	.02	3.41	.02	.01	1.0000	0.
-3	0	3	.344	.02	.08	-1.0000	0.	-.06	.26	-.06	.08	-1.0000	0.
-2	0	3	.294	.02	.18	1.0000	0.	-.16	.14	-.16	.18	1.0000	0.
-1	0	3	.278	.05	.25	1.0000	0.	-.20	.19	-.20	.25	1.0000	0.
0	0	3	.302	.05	.14	-1.0000	0.	-.09	.36	-.09	.14	-1.0000	0.
1	0	3	.358	.06	.56	-1.0000	0.	-.50	.10	-.50	.56	-1.0000	0.
2	0	3	.434	.03	.38	-1.0000	0.	-.35	.09	-.35	.38	-1.0000	0.
3	0	3	.521	.01	.04	1.0000	0.	-.04	.13	-.04	.04	1.0000	0.
4	0	3	.614	.01	.02	1.0000	0.	-.02	.23	-.02	.02	1.0000	0.
5	0	3	.711	.01	.17	1.0000	0.	-.16	.03	-.16	.17	1.0000	0.
-1	0	-6	.654	.01	.10	-1.0000	0.	-.09	.06	-.09	.10	-1.0000	0.
0	0	-6	.605	.01	.50	-1.0000	0.	-.49	.02	-.49	.50	-1.0000	0.
1	0	-6	.571	.00	.09	1.0000	0.	-.09	.05	-.09	.09	1.0000	0.
2	0	-6	.556	.01	.08	-1.0000	0.	-.07	.11	-.07	.08	-1.0000	0.
3	0	-6	.562	.01	.01	-1.0000	0.	.00	1.17	.00	.01	-1.0000	0.
4	0	-6	.588	.00	.51	1.0000	0.	-.51	.01	-.51	.51	1.0000	0.
5	0	-6	.630	.01	.02	-1.0000	0.	-.01	.27	-.01	.02	-1.0000	0.
6	0	-6	.688	.01	.04	1.0000	0.	-.04	.12	-.04	.04	1.0000	0.
7	0	-6	.756	.00	.18	1.0000	0.	-.18	.02	-.18	.18	1.0000	0.
-4	0	4	.458	.05	.84	-1.0000	0.	-.79	.06	-.79	.86	-1.0000	0.
-3	0	4	.405	.06	.52	1.0000	0.	-.46	.11	-.46	.52	1.0000	0.
-2	0	4	.375	.01	.41	1.0000	0.	-.40	.02	-.40	.41	1.0000	0.
-1	0	4	.374	.03	.49	-1.0000	0.	-.46	.06	-.46	.49	-1.0000	0.
0	0	4	.403	.05	.80	1.0000	0.	-.75	.06	-.75	.80	1.0000	0.
1	0	4	.456	.07	.49	-1.0000	0.	-.43	.13	-.43	.49	-1.0000	0.
2	0	4	.526	.02	.36	-1.0000	0.	-.35	.04	-.35	.36	-1.0000	0.
-7	0	2	.696	.01	.19	1.0000	0.	-.18	.05	-.18	.19	1.0000	0.
-6	0	2	.593	.02	.04	-1.0000	0.	-.02	.51	-.02	.04	-1.0000	0.
-5	0	2	.493	.04	.38	-1.0000	0.	-.34	.11	-.34	.38	-1.0000	0.
-4	0	2	.395	.04	.43	1.0000	0.	-.39	.08	-.39	.43	1.0000	0.
-3	0	2	.305	.07	1.60	-1.0000	0.	-1.52	.05	-1.52	1.60	-1.0000	0.
-2	0	2	.229	.02	.47	-1.0000	0.	-.45	.04	-.45	.47	-1.0000	0.
-1	0	2	.187	.04	1.58	1.0000	0.	-1.53	.03	-1.53	1.58	1.0000	0.
0	0	2	.202	.07	2.07	-1.0000	0.	-2.00	.03	-2.00	2.07	-1.0000	0.
1	0	2	.263	.05	1.10	1.0000	0.	-1.05	.04	-1.05	1.10	1.0000	0.
2	0	2	.347	.03	.46	1.0000	0.	-.43	.07	-.43	.46	1.0000	0.
3	0	2	.442	.03	.36	-1.0000	0.	-.34	.07	-.34	.36	-1.0000	0.
4	0	2	.541	.03	.51	1.0000	0.	-.49	.05	-.49	.51	1.0000	0.
5	0	2	.642	.00	.04	1.0000	0.	-.04	.10	-.04	.04	1.0000	0.
-3	0	5	.479	.02	.02	1.0000	0.	-.00	.83	-.00	.02	1.0000	0.
-2	0	5	.463	.01	.04	-1.0000	0.	-.03	.27	-.03	.04	-1.0000	0.
-1	0	5	.472	.01	.12	-1.0000	0.	-.11	.10	-.11	.12	-1.0000	0.
0	0	5	.504	.01	.18	-1.0000	0.	-.17	.05	-.17	.18	-1.0000	0.
-6	0	6	.688	.01	.04	1.0000	0.	-.03	.19	-.03	.04	1.0000	0.
-5	0	6	.630	.01	.02	-1.0000	0.	-.01	.33	-.01	.02	-1.0000	0.
-4	0	6	.588	.02	.51	1.0000	0.	-.49	.04	-.49	.51	1.0000	0.
-3	0	6	.562	.01	.01	-1.0000	0.	.00	1.60	.00	.01	-1.0000	0.
-2	0	6	.556	.02	.08	-1.0000	0.	-.06	.24	-.06	.08	-1.0000	0.
-1	0	6	.571	.00	.09	1.0000	0.	-.09	.05	-.09	.09	1.0000	0.
0	0	6	.605	.01	.50	-1.0000	0.	-.50	.01	-.50	.50	-1.0000	0.

1	0	0	.654	.01	.10	-1.0000	0.	-.08	.15	-.08	.10	-1.0000	0.
-3	0	-4	.607	.00	.15	1.0000	0.	-.15	.03	-.15	.15	1.0000	0.
-2	0	-4	.526	.01	.36	-1.0000	0.	-.35	.03	-.35	.36	-1.0000	0.
-1	0	-4	.456	.09	.49	-1.0000	0.	-.40	.19	-.40	.49	-1.0000	0.
0	0	-4	.403	.05	.80	1.0000	0.	-.75	.06	-.75	.80	1.0000	0.
1	0	-4	.374	.05	.49	-1.0000	0.	-.45	.09	-.45	.49	-1.0000	0.
2	0	-4	.375	.03	.41	1.0000	0.	-.37	.08	-.37	.41	1.0000	0.
3	0	-4	.405	.08	.52	1.0000	0.	-.44	.15	-.44	.52	1.0000	0.
4	0	-4	.458	.06	.84	-1.0000	0.	-.78	.07	-.78	.84	-1.0000	0.
5	0	-4	.529	.01	.00	1.0000	0.	.00	2.10	.00	.00	1.0000	0.
0	0	-5	.504	.00	.18	-1.0000	0.	-.17	.03	-.17	.18	-1.0000	0.
1	0	-5	.472	.01	.12	-1.0000	0.	-.11	.04	-.11	.12	-1.0000	0.
2	0	-5	.463	.01	.04	-1.0000	0.	-.04	.16	-.04	.04	-1.0000	0.
3	0	-5	.479	.05	.02	1.0000	0.	.02	1.97	.02	.02	1.0000	0.
4	0	-5	.517	.02	.15	-1.0000	0.	-.13	.10	-.13	.15	-1.0000	0.
5	0	-5	.573	.01	.06	1.0000	0.	-.05	.12	-.05	.06	1.0000	0.
-5	0	-1	.583	.02	.20	-1.0000	0.	-.18	.10	-.18	.20	-1.0000	0.
-4	0	-1	.477	.01	.00	-1.0000	0.	.01	9.99	.01	.00	-1.0000	0.
-3	0	-1	.373	.01	.10	-1.0000	0.	-.09	.10	-.09	.10	-1.0000	0.
-2	0	-1	.270	.06	1.02	1.0000	0.	-.96	.06	-.96	1.02	1.0000	0.
-1	0	-1	.174	.12	2.65	1.0000	0.	-2.53	.05	-2.53	2.65	1.0000	0.
0	0	-1	.101	.09	2.95	1.0000	0.	-2.86	.03	-2.86	2.95	1.0000	0.
1	0	-1	.115	.03	.91	1.0000	0.	-.88	.03	-.88	.91	1.0000	0.
2	0	-1	.198	.01	.97	-1.0000	0.	-.96	.01	-.96	.97	-1.0000	0.
3	0	-1	.297	.05	.93	-1.0000	0.	-.88	.06	-.88	.93	-1.0000	0.
4	0	-1	.400	.06	1.12	-1.0000	0.	-1.06	.05	-1.06	1.12	-1.0000	0.
5	0	-1	.505	.01	.19	-1.0000	0.	-.18	.04	-.18	.19	-1.0000	0.
-5	0	0	.536	.03	.21	-1.0000	0.	-.18	.16	-.18	.21	-1.0000	0.
-4	0	0	.429	.31	1.45	-1.0000	0.	-1.14	.21	-1.14	1.45	-1.0000	0.
-3	0	0	.321	.02	.26	1.0000	0.	-.25	.06	-.25	.26	1.0000	0.
-2	0	0	.214	.01	.13	1.0000	0.	-.12	.10	-.12	.13	1.0000	0.
-1	0	0	.107	.09	1.56	1.0000	0.	-1.47	.05	-1.47	1.56	1.0000	0.
1	0	0	.107	.10	1.56	1.0000	0.	-1.46	.06	-1.46	1.56	1.0000	0.
2	0	0	.214	.01	.13	1.0000	0.	-.12	.10	-.12	.13	1.0000	0.
3	0	0	.321	.02	.26	1.0000	0.	-.24	.07	-.24	.26	1.0000	0.
4	0	0	.429	.19	1.45	-1.0000	0.	-1.26	.13	-1.26	1.45	-1.0000	0.
5	0	0	.536	.02	.21	-1.0000	0.	-.20	.08	-.20	.21	-1.0000	0.
-2	0	-3	.434	.01	.38	-1.0000	0.	-.37	.03	-.37	.38	-1.0000	0.
-1	0	-3	.358	.04	.56	-1.0000	0.	-.51	.07	-.51	.56	-1.0000	0.
0	0	-3	.302	.04	.14	-1.0000	0.	-.10	.27	-.10	.14	-1.0000	0.
1	0	-3	.278	.05	.25	1.0000	0.	-.20	.19	-.20	.25	1.0000	0.
2	0	-3	.294	.04	.18	1.0000	0.	-.14	.20	-.14	.18	1.0000	0.
3	0	-3	.344	.01	.08	-1.0000	0.	-.07	.14	-.07	.08	-1.0000	0.
4	0	-3	.416	.04	.01	1.0000	0.	.03	6.36	.03	.01	1.0000	0.
5	0	-3	.501	.05	.32	-1.0000	0.	-.27	.16	-.27	.32	-1.0000	0.
-4	0	-2	.541	.03	.51	1.0000	0.	-.48	.06	-.48	.51	1.0000	0.
-3	0	-2	.442	.05	.36	-1.0000	0.	-.31	.14	-.31	.36	-1.0000	0.
-2	0	-2	.347	.02	.46	1.0000	0.	-.45	.03	-.45	.46	1.0000	0.
-1	0	-2	.263	.04	1.10	1.0000	0.	-1.06	.04	-1.06	1.10	1.0000	0.
0	0	-2	.202	.10	2.07	-1.0000	0.	-1.97	.05	-1.97	2.07	-1.0000	0.
1	0	-2	.187	.05	1.58	1.0000	0.	-1.53	.03	-1.53	1.58	1.0000	0.
2	0	-2	.229	.02	.47	-1.0000	0.	-.44	.05	-.44	.47	-1.0000	0.
3	0	-2	.305	.06	1.60	-1.0000	0.	-1.54	.04	-1.54	1.60	-1.0000	0.
4	0	-2	.395	.02	.43	1.0000	0.	-.41	.04	-.41	.43	1.0000	0.
5	0	-2	.493	.01	.38	-1.0000	0.	-.37	.03	-.37	.38	-1.0000	0.
6	0	-2	.593	.01	.04	-1.0000	0.	-.03	.16	-.03	.04	-1.0000	0.
0	0	0	0.	9.29	9.29	1.0000	0.	0.	*0.	0.	9.29	1.0000	0.
999	999	999	999.000	999.00	999.00	999.0000	999.0000	999.00	.16	999.00			

* ZERO WEIGHTED DATA.

A= 5 077000

PARAMETER	E.S.D.	LAST SHIFT	SCALE
1	.064370	.004762	N
2	0.	0.	N
3	0.	0.	N
4	0.	0.	N
5	.903604	.032000	N
6	.008422	.001229	O1
7	.013094	.005053	O1
8	.009179	.000593	O1
9	.910766	.136036	O1
10	.011286	-.001000	O2
11	.015311	.002760	O2
12	.013372	.000931	O2
13	1.392353	-.013230	O2
14	.009650	-.000785	C1
15	.019018	.012304	C1
16	.011407	-.000732	C1
17	1.004081	-.126540	C1
18	.010867	-.000386	C2
19	.018042	.005147	C2
20	.013689	-.001387	C2
21	1.299961	-.091516	C2

1	-9	0	.726	.10	.03	.4565	-.8897	.07	3.76	.07	.03	.4565	-.8897
1	-8	0	.647	.13	.41	.8302	.5575	-.28	.31	-.28	.41	.8302	.5575
1	-7	0	.569	.16	.27	-.1948	.9808	-.11	.58	-.11	.27	-.1948	.9808
1	-6	0	.491	.73	.44	-.3045	.9525	.29	1.64	.29	.44	-.3045	.9525
1	-5	0	.413	.27	.67	-.3613	.9324	-.40	.40	-.40	.67	-.3613	.9324
1	-4	0	.337	.96	1.02	-.9469	-.3215	-.06	.94	-.06	1.02	-.9469	-.3215
1	-3	0	.262	1.52	1.46	-.1204	.9927	.06	1.04	.06	1.46	-.1204	.9927
1	-2	0	.192	2.62	1.76	-.1038	-.9946	.87	1.49	.87	1.76	-.1038	-.9946
1	-1	0	.134	9.18	3.30	.0445	.9990	5.88	2.78	5.88	3.30	.0445	.9990
1	0	0	.107	1.13	1.61	1.0000	0.	-.48	.70	-.48	1.61	1.0000	0.
1	1	0	.134	1.51	3.30	-.0445	.9990	-1.79	.46	-1.79	3.30	-.0445	.9990
1	2	0	.192	.99	1.76	-.1038	.9946	-.77	.56	-.77	1.76	-.1038	.9946
1	3	0	.262	.96	1.46	.1204	.9927	-.50	.66	-.50	1.46	.1204	.9927
1	4	0	.337	.87	1.02	-.9469	.3215	-.14	.86	-.14	1.02	-.9469	.3215
1	5	0	.413	.27	.67	.3613	.9324	-.40	.40	-.40	.67	.3613	.9324
-3	-2	0	.359	.08	.55	.6810	.7323	-.47	.15	-.47	.55	.6810	.7323
-3	-1	0	.331	.37	1.02	-.0426	-.9991	-.65	.36	-.65	1.02	-.0426	-.9991
-3	0	0	.321	.32	.36	1.0000	0.	-.04	.88	-.04	.36	1.0000	0.
-3	1	0	.331	.79	1.02	.0426	-.9991	-.23	.77	-.23	1.02	.0426	-.9991
-3	2	0	.359	.67	.55	.6810	-.7323	.12	1.21	.12	.55	.6810	-.7323
-3	3	0	.401	.53	.66	.0381	-.9993	-.12	.81	-.12	.66	.0381	-.9993
-3	4	0	.453	.43	.31	.8849	-.4659	.12	1.38	.12	.31	.8849	-.4659
-3	5	0	.512	.11	.41	-.0170	-.9999	-.30	.26	-.30	.41	-.0170	-.9999
-3	6	0	.577	.17	.11	-.8534	.5212	-.04	.65	-.04	.11	-.8534	.5212
-3	7	0	.644	.10	.26	.3994	-.9168	-.16	.37	-.16	.26	.3994	-.9168
-3	8	0	.715	.10	.29	-.9989	-.0466	-.19	.34	-.19	.29	-.9989	-.0466
-2	-3	0	.321	.31	.76	.2190	.9757	-.44	.41	-.44	.76	.2190	.9757
-2	-2	0	.267	.86	.64	-.1232	-.9924	.21	1.33	.21	.64	-.1232	-.9924
-2	-1	0	.229	.84	.98	-.1810	.9835	-.14	.86	-.14	.98	-.1810	.9835
-2	0	0	.214	.68	.33	1.0000	0.	.35	2.07	.35	.33	1.0000	0.
-2	1	0	.229	.96	.98	.1810	.9835	-.03	.97	-.03	.98	.1810	.9835
-2	2	0	.267	.93	.64	-.1232	.9924	.29	1.45	.29	.64	-.1232	.9924
-2	3	0	.321	.90	.76	-.2190	.9757	.14	1.18	.14	.76	-.2190	.9757
-2	4	0	.384	.81	.48	-.7093	.7049	.33	1.69	.33	.48	-.7093	.7049
-2	5	0	.453	.32	.30	-.9811	-.1937	.02	1.07	.02	.30	-.9811	-.1937
-2	6	0	.524	.08	.13	-.9628	.2703	-.05	.60	-.05	.13	-.9628	.2703
-1	-6	0	.491	.10	.44	-.3045	.9525	-.35	.22	-.35	.44	-.3045	.9525
-1	-5	0	.413	.09	.67	.3613	-.9324	-.59	.13	-.59	.67	.3613	-.9324
-1	-4	0	.337	.18	1.02	-.9469	-.3215	-.83	.18	-.83	1.02	-.9469	-.3215
-1	-3	0	.262	.72	1.46	.1204	-.9927	-.75	.49	-.75	1.46	.1204	-.9927

-1	-2	0	.192	.79	1.76	-.1038	-.9946	-.97	.45	-.97	1.76	-.1038	-.9946
-1	-1	0	.134	1.42	3.30	-.0445	-.9990	-1.88	.43	-1.88	3.30	-.0445	-.9990
-1	0	0	.107	.76	1.61	1.0000	0.	-.85	.47	-.85	1.61	1.0000	0.
-1	1	0	.134	4.65	3.30	.0445	-.9990	1.35	1.41	1.35	3.30	.0445	-.9990
-1	2	0	.192	3.65	1.76	-.1038	.9946	1.89	2.08	1.89	1.76	-.1038	.9946
-1	3	0	.262	1.82	1.46	-.1204	-.9927	.36	1.25	.36	1.46	-.1204	-.9927
-1	4	0	.337	1.53	1.02	-.0469	.3215	.52	1.51	.52	1.02	-.0469	.3215
-1	5	0	.413	.90	.67	-.3613	-.9324	.22	1.33	.22	.67	-.3613	-.9324
-1	6	0	.491	.13	.44	-.3045	-.9525	-.32	.29	-.32	.44	-.3045	-.9525
0	-6	0	.479	.17	.43	.3146	.9492	-.27	.38	-.27	.43	.3146	.9492
0	-4	0	.319	.45	.67	.6818	-.7315	-.22	.67	-.22	.67	.6818	-.7315
0	-2	0	.160	4.11	4.95	.8748	-.4844	-.84	.83	-.84	4.95	.8748	-.4844
0	2	0	.160	5.53	4.95	.8748	.4844	.59	1.12	.59	4.95	.8748	.4844
0	4	0	.319	1.03	.67	.6818	.7315	.36	1.54	.36	.67	.6818	.7315
0	6	0	.479	.41	.43	.3146	-.9492	-.02	.95	-.02	.43	.3146	-.9492
5	-4	0	.624	.09	.30	.9833	-.1822	-.21	.31	-.21	.30	.9833	-.1822
5	-3	0	.587	.12	.47	-.0383	-.9993	-.35	.25	-.35	.47	-.0383	-.9993
5	-2	0	.559	.14	.27	.1895	.9819	-.13	.51	-.13	.27	.1895	.9819
5	-1	0	.542	.82	.83	-.0622	-.9981	-.01	.99	-.01	.83	-.0622	-.9981
5	0	0	.536	.09	.26	-1.0000	0.	-.17	.34	-.17	.26	-1.0000	0.
5	1	0	.542	.36	.83	-.0622	-.9981	-.47	.43	-.47	.83	-.0622	-.9981
5	2	0	.559	.14	.27	.1895	-.9819	-.13	.51	-.13	.27	.1895	-.9819
5	3	0	.587	.16	.47	-.0383	-.9993	-.31	.34	-.31	.47	-.0383	-.9993
5	4	0	.624	.14	.30	.9833	.1822	-.16	.47	-.16	.30	.9833	.1822
5	5	0	.668	.10	.23	-.4508	-.8926	-.13	.43	-.13	.23	-.4508	-.8926
5	6	0	.718	.10	.31	.1932	.9812	-.21	.33	-.21	.31	.1932	.9812
4	-8	0	.769	.09	.33	-.0110	-.9999	-.24	.28	-.24	.33	-.0110	-.9999
4	-7	0	.704	.10	.11	-.9994	.0336	-.01	.88	-.01	.11	-.9994	.0336
4	-6	0	.643	.14	.21	-.7917	-.6110	-.07	.66	-.07	.21	-.7917	-.6110
4	-5	0	.586	.10	.24	-.9868	.1619	-.13	.44	-.13	.24	-.9868	.1619
4	-4	0	.534	.23	.37	-.8853	.4650	-.14	.63	-.14	.37	-.8853	.4650
4	-3	0	.491	.16	.31	-.9999	.0101	-.15	.51	-.15	.31	-.9999	.0101
4	-2	0	.457	1.40	1.32	-.9182	.3961	.08	1.06	.08	1.32	-.9182	.3961
4	-1	0	.436	.48	.17	-.9097	-.4153	.32	2.93	.32	.17	-.9097	-.4153
4	0	0	.429	2.03	1.93	-1.0000	0.	.10	1.05	.10	1.93	-1.0000	0.
4	1	0	.436	.13	.17	.9097	-.4153	-.04	.77	-.04	.17	.9097	-.4153
4	2	0	.457	.90	1.32	-.9182	-.3961	-.41	.69	-.41	1.32	-.9182	-.3961
4	3	0	.491	.14	.31	.9999	.0101	-.17	.44	-.17	.31	.9999	.0101
4	4	0	.534	.44	.37	-.8853	-.4650	.07	1.18	.07	.37	-.8853	-.4650
4	5	0	.586	.11	.24	.9868	.1619	-.13	.47	-.13	.24	.9868	.1619
4	6	0	.643	.15	.21	-.7917	.6110	-.06	.71	-.06	.21	-.7917	.6110
4	7	0	.704	.09	.11	.9994	.0336	-.03	.76	-.03	.11	.9994	.0336
3	-8	0	.715	.13	.29	-.9989	.0466	-.16	.45	-.16	.29	-.9989	.0466
3	-7	0	.644	.19	.26	.3994	.9168	-.06	.75	-.06	.26	.3994	.9168
3	-6	0	.577	.37	.11	-.8534	-.5212	.25	3.25	.25	.11	-.8534	-.5212
3	-5	0	.512	.20	.41	-.0170	.9999	-.21	.48	-.21	.41	-.0170	.9999
3	-4	0	.453	.94	.31	.8849	.4659	.63	3.01	.63	.31	.8849	.4659
3	-3	0	.401	.86	.66	.0381	.9993	.20	1.30	.20	.66	.0381	.9993
3	-2	0	.359	1.62	.55	.6810	.7323	1.06	2.91	1.06	.55	.6810	.7323
3	-1	0	.331	1.65	1.02	.0426	.9991	.63	1.62	.63	1.02	.0426	.9991
3	0	0	.321	.84	.36	1.0000	0.	.48	2.33	.48	.36	1.0000	0.
3	1	0	.331	.97	1.02	-.0426	.9991	-.05	.95	-.05	1.02	-.0426	.9991
3	2	0	.359	.51	.55	.6810	-.7323	-.05	.91	-.05	.55	.6810	-.7323
3	3	0	.401	.53	.66	-.0381	.9993	-.12	.81	-.12	.66	-.0381	.9993
3	4	0	.453	.65	.31	.8849	-.4659	.34	2.09	.34	.31	.8849	-.4659
3	5	0	.512	.17	.41	.0170	.9999	-.24	.42	-.24	.41	.0170	.9999
3	6	0	.577	.16	.11	-.8534	.5212	.05	1.40	.05	.11	-.8534	.5212
3	7	0	.644	.10	.26	-.3994	.9168	-.16	.38	-.16	.26	-.3994	.9168
2	-9	0	.749	.09	.53	.3182	.9480	-.44	.17	-.44	.53	.3182	.9480
2	-8	0	.673	.15	.03	.8635	-.5043	.11	4.38	.11	.03	.8635	-.5043
2	-7	0	.598	.21	.44	-.2909	.9568	-.23	.48	-.23	.44	-.2909	.9568
2	-6	0	.524	.33	.13	-.9628	-.2703	.19	2.42	.19	.13	-.9628	-.2703

2	-5	0	.453	.49	.30	-.9811	.1937	.19	1.64	.19	.30	-.9811	.1937
2	-4	0	.384	.69	.48	-.7093	-.7049	.21	1.44	.21	.48	-.7093	-.7049
2	-3	0	.321	1.40	.76	-.2190	-.9757	.65	1.85	.65	.76	-.2190	-.9757
2	-2	0	.267	2.22	.64	-.1232	-.9924	1.58	3.46	1.58	.64	-.1232	-.9924
2	-1	0	.229	1.93	.98	.1810	-.9835	.95	1.96	.95	.98	.1810	-.9835
2	0	0	.214	.85	.33	1.0000	0.	.52	2.58	.52	.33	1.0000	0.
2	1	0	.229	1.25	.98	-.1810	-.9835	.26	1.27	.26	.98	-.1810	-.9835
2	2	0	.267	.89	.64	-.1232	.9924	.25	1.39	.25	.64	-.1232	.9924
2	3	0	.321	.96	.76	.2190	-.9757	.20	1.26	.20	.76	.2190	-.9757
2	4	0	.384	.60	.48	-.7093	.7049	.12	1.25	.12	.48	-.7093	.7049
2	5	0	.453	.61	.30	.9811	.1937	.31	2.02	.31	.30	.9811	.1937
2	6	0	.524	.09	.13	-.9628	.2703	-.04	.69	-.04	.13	-.9628	.2703
2	7	0	.598	.09	.44	.2909	.9568	-.36	.19	-.36	.44	.2909	.9568
-5	0	1	.505	.60	.28	-1.0000	0.	.32	2.14	.32	.28	-1.0000	0.
-4	0	1	.400	3.40	1.51	-1.0000	0.	1.88	2.25	1.88	1.51	-1.0000	0.
-3	0	1	.297	1.56	.93	-1.0000	0.	.62	1.67	.62	.93	-1.0000	0.
-2	0	1	.198	.60	1.03	-1.0000	0.	-.43	.58	-.43	1.03	-1.0000	0.
-1	0	1	.115	.63	.65	1.0000	0.	-.02	.97	-.02	.65	1.0000	0.
0	0	1	.101	1.41	2.70	1.0000	0.	-1.29	.52	-1.29	2.70	1.0000	0.
1	0	1	.174	1.80	2.55	1.0000	0.	-.75	.70	-.75	2.55	1.0000	0.
2	0	1	.270	1.04	1.16	1.0000	0.	-.13	.89	-.13	1.16	1.0000	0.
3	0	1	.373	.52	.12	-1.0000	0.	.40	4.34	.40	.12	-1.0000	0.
4	0	1	.477	.15	.12	1.0000	0.	.03	1.24	.03	.12	1.0000	0.
5	0	1	.583	.23	.24	-1.0000	0.	-.01	.96	-.01	.24	-1.0000	0.
-7	0	3	.689	.25	.13	1.0000	0.	.12	1.92	.12	.13	1.0000	0.
-6	0	3	.593	.43	.28	-1.0000	0.	.15	1.56	.15	.28	-1.0000	0.
-5	0	3	.501	.44	.43	-1.0000	0.	.01	1.02	.01	.43	-1.0000	0.
-4	0	3	.416	.40	.43	1.0000	0.	-.03	.92	-.03	.43	1.0000	0.
-3	0	3	.344	.40	.16	1.0000	0.	.25	2.58	.25	.16	1.0000	0.
-2	0	3	.294	.46	.38	1.0000	0.	.08	1.21	.08	.38	1.0000	0.
-1	0	3	.278	.91	.25	1.0000	0.	.67	3.70	.67	.25	1.0000	0.
0	0	3	.302	.98	.57	-1.0000	0.	.41	1.72	.41	.57	-1.0000	0.
1	0	3	.358	1.07	.92	-1.0000	0.	.15	1.17	.15	.92	-1.0000	0.
2	0	3	.434	.62	.77	-1.0000	0.	-.15	.80	-.15	.77	-1.0000	0.
3	0	3	.521	.11	.02	-1.0000	0.	.08	4.36	.08	.02	-1.0000	0.
4	0	3	.614	.10	.02	-1.0000	0.	.09	6.67	.09	.02	-1.0000	0.
5	0	3	.711	.10	.32	1.0000	0.	-.22	.32	-.22	.32	1.0000	0.
-1	0	-6	.654	.11	.18	-1.0000	0.	-.07	.60	-.07	.18	-1.0000	0.
0	0	-6	.605	.19	.86	-1.0000	0.	-.67	.22	-.67	.86	-1.0000	0.
1	0	-6	.571	.09	.32	1.0000	0.	-.23	.28	-.23	.32	1.0000	0.
2	0	-6	.556	.18	.10	-1.0000	0.	.08	1.78	.08	.10	-1.0000	0.
3	0	-6	.562	.17	.21	1.0000	0.	-.04	.79	-.04	.21	1.0000	0.
4	0	-6	.588	.09	.97	1.0000	0.	-.88	.09	-.88	.97	1.0000	0.
5	0	-6	.630	.09	.10	-1.0000	0.	-.01	.91	-.01	.10	-1.0000	0.
6	0	-6	.688	.10	.09	1.0000	0.	.01	1.12	.01	.09	1.0000	0.
7	0	-6	.756	.08	.23	1.0000	0.	-.15	.36	-.15	.23	1.0000	0.
-4	0	4	.458	.94	.82	-1.0000	0.	.12	1.15	.12	.82	-1.0000	0.
-3	0	4	.405	1.07	.93	1.0000	0.	.13	1.14	.13	.93	1.0000	0.
-2	0	4	.375	.17	.80	1.0000	0.	-.64	.21	-.64	.80	1.0000	0.
-1	0	4	.374	.58	.79	-1.0000	0.	-.22	.73	-.22	.79	-1.0000	0.
0	0	4	.403	.88	.86	1.0000	0.	.02	1.02	.02	.86	1.0000	0.
1	0	4	.456	1.24	.81	-1.0000	0.	.43	1.54	.43	.81	-1.0000	0.
2	0	4	.526	.30	.66	-1.0000	0.	-.36	.45	-.36	.66	-1.0000	0.
-7	0	2	.696	.17	.34	1.0000	0.	-.17	.49	-.17	.34	1.0000	0.
-6	0	2	.593	.39	.02	-1.0000	0.	.37	9.99	.37	.02	-1.0000	0.
-5	0	2	.493	.81	.61	-1.0000	0.	.20	1.33	.20	.61	-1.0000	0.
-4	0	2	.395	.66	.73	1.0000	0.	-.07	.90	-.07	.73	1.0000	0.
-3	0	2	.305	1.35	1.56	-1.0000	0.	-.21	.86	-.21	1.56	-1.0000	0.
-2	0	2	.229	.37	.54	-1.0000	0.	-.18	.67	-.18	.54	-1.0000	0.
-1	0	2	.187	.77	1.49	1.0000	0.	-.72	.52	-.72	1.49	1.0000	0.
0	0	2	.202	1.31	2.75	-1.0000	0.	-1.44	.48	-1.44	2.75	-1.0000	0.
1	0	2	.263	.90	.77	1.0000	0.	.13	1.17	.13	.77	1.0000	0.

2	0	2	.347	.62	.31	1.0000	0.	.31	2.00	.31	.31	1.0000	0.
3	0	2	.442	.51	.62	-1.0000	0.	-.11	.82	-.11	.62	-1.0000	0.
4	0	2	.541	.51	.86	1.0000	0.	-.35	.59	-.35	.86	1.0000	0.
5	0	2	.642	.08	.09	1.0000	0.	-.01	.86	-.01	.09	1.0000	0.
-3	0	5	.479	.39	.44	1.0000	0.	-.06	.87	-.06	.44	1.0000	0.
-2	0	5	.463	.23	.10	1.0000	0.	.13	2.36	.13	.10	1.0000	0.
-1	0	5	.472	.23	.25	-1.0000	0.	-.02	.94	-.02	.25	-1.0000	0.
0	0	5	.504	.16	.28	-1.0000	0.	-.13	.55	-.13	.28	-1.0000	0.
-6	0	6	.688	.15	.09	1.0000	0.	.06	1.70	.06	.09	1.0000	0.
-5	0	6	.630	.12	.10	-1.0000	0.	.01	1.12	.01	.10	-1.0000	0.
-4	0	6	.588	.39	.97	1.0000	0.	-.59	.40	-.59	.97	1.0000	0.
-3	0	6	.562	.23	.21	1.0000	0.	.02	1.08	.02	.21	1.0000	0.
-2	0	6	.556	.38	.10	-1.0000	0.	.27	3.67	.27	.10	-1.0000	0.
-1	0	6	.571	.08	.32	1.0000	0.	-.24	.26	-.24	.32	1.0000	0.
0	0	6	.605	.10	.86	-1.0000	0.	-.76	.11	-.76	.86	-1.0000	0.
1	0	6	.654	.27	.18	-1.0000	0.	.09	1.52	.09	.18	-1.0000	0.
-3	0	-4	.607	.09	.30	1.0000	0.	-.21	.31	-.21	.30	1.0000	0.
-2	0	-4	.526	.20	.66	-1.0000	0.	-.46	.30	-.46	.66	-1.0000	0.
-1	0	-4	.456	1.76	.81	-1.0000	0.	.95	2.17	.95	.81	-1.0000	0.
0	0	-4	.403	.87	.86	1.0000	0.	.00	1.00	.00	.86	1.0000	0.
1	0	-4	.374	.85	.79	-1.0000	0.	.06	1.07	.06	.79	-1.0000	0.
2	0	-4	.375	.64	.80	1.0000	0.	-.16	.80	-.16	.80	1.0000	0.
3	0	-4	.405	1.44	.93	1.0000	0.	.51	1.54	.51	.93	1.0000	0.
4	0	-4	.458	1.08	.82	-1.0000	0.	.26	1.32	.26	.82	-1.0000	0.
5	0	-4	.529	.11	.25	1.0000	0.	-.15	.42	-.15	.25	1.0000	0.
0	0	-5	.504	.09	.28	-1.0000	0.	-.19	.33	-.19	.28	-1.0000	0.
1	0	-5	.472	.10	.25	-1.0000	0.	-.15	.41	-.15	.25	-1.0000	0.
2	0	-5	.463	.14	.10	1.0000	0.	.04	1.40	.04	.10	1.0000	0.
3	0	-5	.479	.92	.44	1.0000	0.	.47	2.06	.47	.44	1.0000	0.
4	0	-5	.517	.28	.04	-1.0000	0.	.24	6.39	.24	.04	-1.0000	0.
5	0	-5	.573	.14	.30	1.0000	0.	-.17	.45	-.17	.30	1.0000	0.
-5	0	-1	.583	.39	.24	-1.0000	0.	.15	1.62	.15	.24	-1.0000	0.
-4	0	-1	.477	.21	.12	1.0000	0.	.09	1.69	.09	.12	1.0000	0.
-3	0	-1	.373	.18	.12	-1.0000	0.	.06	1.54	.06	.12	-1.0000	0.
-2	0	-1	.270	1.17	1.16	1.0000	0.	.01	1.01	.01	1.16	1.0000	0.
-1	0	-1	.174	2.31	2.55	1.0000	0.	-.24	.91	-.24	2.55	1.0000	0.
0	0	-1	.101	1.68	2.70	1.0000	0.	-1.02	.62	-1.02	2.70	1.0000	0.
1	0	-1	.115	.58	.65	1.0000	0.	-.08	.88	-.08	.65	1.0000	0.
2	0	-1	.198	.20	1.03	-1.0000	0.	-.83	.20	-.83	1.03	-1.0000	0.
3	0	-1	.297	.97	.93	-1.0000	0.	.04	1.04	.04	.93	-1.0000	0.
4	0	-1	.400	1.04	1.51	-1.0000	0.	-.47	.69	-.47	1.51	-1.0000	0.
5	0	-1	.505	.16	.28	-1.0000	0.	-.13	.55	-.13	.28	-1.0000	0.
-5	0	0	.536	.62	.26	-1.0000	0.	.37	2.43	.37	.26	-1.0000	0.
-4	0	0	.429	5.73	1.93	-1.0000	0.	3.80	2.97	3.80	1.93	-1.0000	0.
-3	0	0	.321	.29	.36	1.0000	0.	-.07	.80	-.07	.36	1.0000	0.
-2	0	0	.214	.23	.33	1.0000	0.	-.10	.71	-.10	.33	1.0000	0.
-1	0	0	.107	1.60	1.61	1.0000	0.	-.01	.99	-.01	1.61	1.0000	0.
1	0	0	.107	1.81	1.61	1.0000	0.	.20	1.13	.20	1.61	1.0000	0.
2	0	0	.214	.23	.33	1.0000	0.	-.10	.71	-.10	.33	1.0000	0.
3	0	0	.321	.35	.36	1.0000	0.	-.01	.98	-.01	.36	1.0000	0.
4	0	0	.429	3.52	1.93	-1.0000	0.	1.58	1.82	1.58	1.93	-1.0000	0.
5	0	0	.536	.30	.26	-1.0000	0.	.04	1.18	.04	.26	-1.0000	0.
-2	0	-3	.434	.24	.77	-1.0000	0.	-.53	.31	-.53	.77	-1.0000	0.
-1	0	-3	.358	.78	.92	-1.0000	0.	-.14	.85	-.14	.92	-1.0000	0.
0	0	-3	.302	.74	.57	-1.0000	0.	.17	1.30	.17	.57	-1.0000	0.
1	0	-3	.278	.88	.25	1.0000	0.	.64	3.58	.64	.25	1.0000	0.
2	0	-3	.294	.70	.38	1.0000	0.	.32	1.83	.32	.38	1.0000	0.
3	0	-3	.344	.22	.16	1.0000	0.	.06	1.39	.06	.16	1.0000	0.
4	0	-3	.416	.75	.43	1.0000	0.	.31	1.72	.31	.43	1.0000	0.
5	0	-3	.501	.95	.43	-1.0000	0.	.52	2.21	.52	.43	-1.0000	0.
-4	0	-2	.541	.56	.86	1.0000	0.	-.30	.65	-.30	.86	1.0000	0.
-3	0	-2	.442	.94	.62	-1.0000	0.	.32	1.51	.32	.62	-1.0000	0.

-2	0	-2	.347	.30	.31	1.0000	0.	-.01	.97	-.01	.31	1.0000	0.
-1	0	-2	.263	.76	.77	1.0000	0.	-.01	.98	-.01	.77	1.0000	0.
0	0	-2	.202	1.82	2.75	-1.0000	0.	-.93	.66	-.93	2.75	-1.0000	0.
1	0	-2	.187	.92	1.49	1.0000	0.	-.58	.61	-.58	1.49	1.0000	0.
2	0	-2	.229	.41	.54	-1.0000	0.	-.13	.75	-.13	.54	-1.0000	0.
3	0	-2	.305	1.05	1.56	-1.0000	0.	-.51	.67	-.51	1.56	-1.0000	0.
4	0	-2	.395	.29	.73	1.0000	0.	-.44	.39	-.44	.73	1.0000	0.
5	0	-2	.493	.23	.61	-1.0000	0.	-.38	.38	-.38	.61	-1.0000	0.
6	0	-2	.593	.12	.02	-1.0000	0.	.10	5.15	.10	.02	-1.0000	0.
0	0	0	0.	9.29	9.29	1.0000	0.	0.	*0.	0.	9.29	1.0000	0.
999	999	999	999.000	999.00	999.00	999.0000	999.0000	999.00	5.15	999.00			

* ZERO WEIGHTED DATA.

A= 5.077000
B= 6.267000
C= 5.397000
ALPHA= 90.000000
BETA=113.200000
GAMMA= 90.000000

APPENDIX B-2

These are the listings of the first and fifth cycles of the program LSLONG when hydrogen atoms are included into the calculation but not refined.

The notations are the same as described in Appendix B-1.

THIS IS CYCLE 1 OF SERIES 1
FOR BETA GLYCINE

F(0,0,0) = 9.29

H	K	L	SINL	KFOB	FCAL	COSA	SINA	DELF	FO/F	WTGRDFLF	FCALQ	COSAQ	SINAQ
1	-9	0	.726	.01	.12	-.2145	-.9767	-.11	.05	-.11	.12	-.2145	-.9767
1	-8	0	.647	.01	.17	-.9226	.3858	-.16	.04	-.16	.17	-.9226	.3858
1	-7	0	.569	.01	.11	.6382	-.7698	-.10	.08	-.10	.11	.6382	-.7698
1	-6	0	.491	.04	.55	-.9039	-.4278	-.51	.07	-.51	.55	-.9039	-.4278
1	-5	0	.413	.01	.33	.6465	.7629	-.32	.04	-.32	.33	.6465	.7629
1	-4	0	.337	.05	1.31	-.5246	-.8513	-1.26	.04	-1.26	1.31	-.5246	-.8513
1	-3	0	.262	.08	1.38	.2452	.9695	-1.30	.06	-1.30	1.38	.2452	.9695
1	-2	0	.192	.14	1.97	.1432	-.9897	-1.83	.07	-1.83	1.97	.1432	-.9897
1	-1	0	.134	.49	3.35	.1022	.9948	-2.86	.15	-2.86	3.35	.1022	.9948
1	0	0	.107	.06	1.56	1.0000	0.	-1.50	.04	-1.50	1.56	1.0000	0.
1	1	0	.134	.08	3.35	-.1022	.9948	-3.27	.02	-3.27	3.35	-.1022	.9948
1	2	0	.192	.05	1.97	.1432	.9897	-1.92	.03	-1.92	1.97	.1432	.9897
1	3	0	.262	.05	1.38	-.2452	.9695	-1.33	.04	-1.33	1.38	-.2452	.9695
1	4	0	.337	.05	1.31	-.5246	.8513	-1.27	.04	-1.27	1.31	-.5246	.8513
1	5	0	.413	.01	.33	-.6465	.7629	-.32	.04	-.32	.33	-.6465	.7629
-3	-2	0	.359	.00	.66	.3876	.9218	-.66	.01	-.66	.66	.3876	.9218
-3	-1	0	.331	.02	.74	-.0284	-.9996	-.72	.03	-.72	.74	-.0284	-.9996
-3	0	0	.321	.02	.26	1.0000	0.	-.25	.06	-.25	.26	1.0000	0.
-3	1	0	.331	.04	.74	.0284	-.9996	-.70	.06	-.70	.74	.0284	-.9996
-3	2	0	.359	.04	.66	.3876	-.9218	-.62	.05	-.62	.66	.3876	-.9218
-3	3	0	.401	.03	.51	.2502	-.9682	-.48	.06	-.48	.51	.2502	-.9682
-3	4	0	.453	.02	.60	.5244	-.8515	-.58	.04	-.58	.60	.5244	-.8515
-3	5	0	.512	.01	.22	.6675	-.7446	-.22	.03	-.22	.22	.6675	-.7446
-3	6	0	.577	.00	.28	.7024	-.7117	-.28	.01	-.28	.28	.7024	-.7117
-3	7	0	.644	.01	.09	.9910	.1340	-.08	.06	-.08	.09	.9910	.1340
-3	8	0	.715	.01	.07	.8120	-.5837	-.06	.08	-.06	.07	.8120	-.5837
-2	-3	0	.321	.02	.82	-.5423	.8402	-.80	.02	-.80	.82	-.5423	.8402
-2	-2	0	.267	.05	.40	-.0568	-.9984	-.35	.12	-.35	.40	-.0568	-.9984
-2	-1	0	.229	.04	.94	-.4225	.9064	-.90	.05	-.90	.94	-.4225	.9064
-2	0	0	.214	.04	.13	1.0000	0.	-.09	.28	-.09	.13	1.0000	0.
-2	1	0	.229	.05	.94	.4225	.9064	-.89	.05	-.89	.94	.4225	.9064
-2	2	0	.267	.05	.40	-.0568	.9984	-.35	.13	-.35	.40	-.0568	.9984
-2	3	0	.321	.05	.82	.5423	.8402	-.77	.06	-.77	.82	.5423	.8402
-2	4	0	.384	.04	.31	-.4850	.8745	-.27	.14	-.27	.31	-.4850	.8745
-2	5	0	.453	.02	.47	.7568	.6537	-.45	.04	-.45	.47	.7568	.6537
-2	6	0	.524	.00	.11	-.7927	.6097	-.10	.04	-.10	.11	-.7927	.6097
-1	-6	0	.491	.01	.55	-.9039	-.4278	-.54	.01	-.54	.55	-.9039	-.4278
-1	-5	0	.413	.00	.33	-.6465	-.7629	-.33	.01	-.33	.33	-.6465	-.7629
-1	-4	0	.337	.01	1.31	-.5246	-.8513	-1.30	.01	-1.30	1.31	-.5246	-.8513
-1	-3	0	.262	.04	1.38	-.2452	-.9695	-1.34	.03	-1.34	1.38	-.2452	-.9695
-1	-2	0	.192	.04	1.97	.1432	-.9897	-1.93	.02	-1.93	1.97	.1432	-.9897
-1	-1	0	.134	.08	3.35	-.1022	-.9948	-3.28	.02	-3.28	3.35	-.1022	-.9948
-1	0	0	.107	.04	1.56	1.0000	0.	-1.52	.03	-1.52	1.56	1.0000	0.
-1	1	0	.134	.25	3.35	.1022	-.9948	-3.10	.07	-3.10	3.35	.1022	-.9948
-1	2	0	.192	.19	1.97	.1432	.9897	-1.78	.10	-1.78	1.97	.1432	.9897
-1	3	0	.262	.10	1.38	.2452	-.9695	-1.28	.07	-1.28	1.38	.2452	-.9695
-1	4	0	.337	.08	1.31	-.5246	.8513	-1.23	.06	-1.23	1.31	-.5246	.8513
-1	5	0	.413	.05	.33	.6465	-.7629	-.28	.15	-.28	.33	.6465	-.7629
-1	6	0	.491	.01	.55	-.9039	.4278	-.54	.01	-.54	.55	-.9039	.4278
0	-6	0	.479	.01	.50	-.7628	-.6466	-.49	.02	-.49	.50	-.7628	-.6466
0	-4	0	.319	.02	1.48	.4134	-.9105	-1.46	.02	-1.46	1.48	.4134	-.9105
0	-2	0	.160	.22	5.54	.8767	-.4811	-5.32	.04	-5.32	5.54	.8767	-.4811
0	2	0	.160	.30	5.54	.8767	.4811	-5.24	.05	-5.24	5.54	.8767	.4811
0	4	0	.319	.05	1.48	.4134	.9105	-1.43	.04	-1.43	1.48	.4134	.9105
0	6	0	.479	.02	.50	-.7628	.6466	-.48	.04	-.48	.50	-.7628	.6466

5	-4	0	.624	.05	.19	.3643	.9313	-.14	.27	-.14	.19	.3643	.9313
5	-3	0	.587	.06	.33	-.3876	-.9218	-.27	.19	-.27	.33	-.3876	-.9218
5	-2	0	.559	.07	.23	-.3852	.9228	-.16	.31	-.16	.23	-.3852	.9228
5	-1	0	.542	.44	.66	-.1064	-.9943	-.22	.67	-.22	.66	-.1064	-.9943
5	0	0	.536	.05	.31	-1.0000	0.	-.27	.15	-.27	.31	-1.0000	0.
5	1	0	.542	.19	.66	.1064	-.9943	-.47	.29	-.47	.66	.1064	-.9943
5	2	0	.559	.07	.23	-.3852	-.9228	-.16	.31	-.16	.23	-.3852	-.9228
5	3	0	.587	.09	.33	.3876	-.9218	-.25	.25	-.25	.33	.3876	-.9218
5	4	0	.624	.08	.19	.3643	-.9313	-.11	.41	-.11	.19	.3643	-.9313
5	5	0	.668	.05	.10	.7206	-.6934	-.05	.50	-.05	.10	.7206	-.6934
5	6	0	.718	.05	.13	.9889	-.1486	-.07	.42	-.07	.13	.9889	-.1486
4	-8	0	.769	.05	.21	.7542	-.6566	-.17	.23	-.17	.21	.7542	-.6566
4	-7	0	.704	.05	.07	-.9578	.2873	-.02	.74	-.02	.07	-.9578	.2873
4	-6	0	.643	.07	.16	.7354	.6776	-.09	.44	-.09	.16	.7354	.6776
4	-5	0	.586	.06	.21	-.8492	.5280	-.15	.27	-.15	.21	-.8492	.5280
4	-4	0	.534	.12	.48	-.5651	.8250	-.36	.26	-.36	.48	-.5651	.8250
4	-3	0	.491	.08	.27	-.9842	.1770	-.19	.31	-.19	.27	-.9842	.1770
4	-2	0	.457	.75	1.02	-.8991	.4378	-.27	.73	-.27	1.02	-.8991	.4378
4	-1	0	.436	.26	.22	-1.0000	.0009	.04	1.20	.04	.22	-1.0000	.0009
4	0	0	.429	1.08	1.61	-1.0000	0.	-.53	.67	-.53	1.61	-1.0000	0.
4	1	0	.436	.07	.22	1.0000	.0009	-.15	.32	-.15	.22	1.0000	.0009
4	2	0	.457	.48	1.02	-.8991	-.4378	-.54	.47	-.54	1.02	-.8991	-.4378
4	3	0	.491	.07	.27	.9842	.1770	-.20	.27	-.20	.27	.9842	.1770
4	4	0	.534	.23	.48	-.5651	-.8250	-.25	.48	-.25	.48	-.5651	-.8250
4	5	0	.586	.06	.21	.8492	.5280	-.15	.29	-.15	.21	.8492	.5280
4	6	0	.643	.08	.16	.7354	-.6776	-.09	.47	-.09	.16	.7354	-.6776
4	7	0	.704	.05	.07	.9578	.2873	-.03	.64	-.03	.07	.9578	.2873
3	-8	0	.715	.07	.05	.5149	.8573	.02	1.30	.02	.05	.5149	.8573
3	-7	0	.644	.10	.08	.7610	-.6488	.03	1.35	.03	.08	.7610	-.6488
3	-6	0	.577	.20	.35	.6109	.7917	-.15	.56	-.15	.35	.6109	.7917
3	-5	0	.512	.11	.19	.8018	.5975	-.08	.56	-.08	.19	.8018	.5975
3	-4	0	.453	.50	.58	.4981	.8671	-.08	.36	-.08	.58	.4981	.8671
3	-3	0	.401	.46	.36	.1288	.9917	.09	1.26	.09	.36	.1288	.9917
3	-2	0	.359	.86	.76	.3256	.9455	.10	1.13	.10	.76	.3256	.9455
3	-1	0	.331	.83	.57	.1414	.9900	.31	1.54	.31	.57	.1414	.9900
3	0	0	.321	.45	.31	1.0000	0.	.13	1.43	.13	.31	1.0000	0.
3	1	0	.331	.52	.57	-.1414	.9900	-.05	.91	-.05	.57	-.1414	.9900
3	2	0	.359	.27	.76	.3256	-.9455	-.49	.35	-.49	.76	.3256	-.9455
3	3	0	.401	.29	.36	-.1288	.9917	-.08	.79	-.08	.36	-.1288	.9917
3	4	0	.453	.35	.58	.4981	-.8671	-.23	.60	-.23	.58	.4981	-.8671
3	5	0	.512	.09	.19	-.8018	.5975	-.10	.48	-.10	.19	-.8018	.5975
3	6	0	.577	.08	.35	.6109	-.7917	-.26	.24	-.26	.35	.6109	-.7917
3	7	0	.644	.05	.08	-.7610	-.6488	-.02	.67	-.02	.08	-.7610	-.6488
2	-9	0	.749	.05	.07	.9702	.2424	-.02	.70	-.02	.07	.9702	.2424
2	-8	0	.673	.08	.02	.8721	-.4894	.06	4.02	.06	.02	.8721	-.4894
2	-7	0	.598	.11	.15	.6608	-.7505	-.04	.60	-.08	.19	.6608	-.7505
2	-6	0	.524	.17	.13	-.3801	-.9249	.05	1.36	.05	.13	-.3801	-.9249
2	-5	0	.453	.26	.60	.7548	-.6560	-.34	.44	-.34	.60	.7548	-.6560
2	-4	0	.384	.37	.30	-.2785	-.9604	.07	1.22	.07	.30	-.2785	-.9604
2	-3	0	.321	.75	.83	.3748	-.9271	-.08	.90	-.08	.83	.3748	-.9271
2	-2	0	.267	1.19	.53	.3561	-.9344	.66	2.25	.66	.53	.3561	-.9344
2	-1	0	.229	1.03	1.42	.5716	-.8206	-.39	.73	-.39	1.42	.5716	-.8206
2	0	0	.244	.45	.22	1.0000	0.	.24	2.07	.24	.22	1.0000	0.
2	1	0	.229	.67	1.42	-.5716	-.8206	-.75	.47	-.75	1.42	-.5716	-.8206
2	2	0	.267	.48	.53	.3561	.9344	-.05	.93	-.05	.53	.3561	.9344
2	3	0	.321	.51	.83	-.3748	-.9271	-.32	.62	-.32	.83	-.3748	-.9271
2	4	0	.384	.32	.30	-.2785	.9604	.02	1.06	.02	.30	-.2785	.9604
2	5	0	.453	.33	.60	-.7548	-.6560	-.28	.54	-.28	.60	-.7548	-.6560
2	6	0	.524	.05	.13	-.3801	.9249	-.08	.38	-.08	.13	-.3801	.9249
2	7	0	.598	.05	.19	-.6608	-.7505	-.14	.24	-.14	.19	-.6608	-.7505
-5	0	1	.505	.32	.03	-1.0000	0.	.29	9.93	.29	.03	-1.0000	0.
-4	0	1	.430	1.61	1.09	-1.0000	0.	.72	1.65	.72	1.09	-1.0000	0.

-3	0	1	.297	.83	1.01	-1.0000	0.	-.13	.82	-.18	1.01	-1.0000	0.
-2	0	1	.198	.32	.70	-1.0000	0.	-.38	.46	-.38	.70	-1.0000	0.
-1	0	1	.115	.34	.17	1.0000	0.	.16	1.94	.16	.17	1.0000	0.
0	0	1	.101	.75	2.63	1.0000	0.	-1.87	.29	-1.87	2.63	1.0000	0.
1	0	1	.174	.96	2.74	1.0000	0.	-1.78	.35	-1.78	2.74	1.0000	0.
2	0	1	.270	.55	1.04	1.0000	0.	-.49	.53	-.49	1.04	1.0000	0.
3	0	1	.373	.23	.24	-1.0000	0.	.04	1.17	.04	.24	-1.0000	0.
4	0	1	.477	.08	.13	1.0000	0.	-.05	.64	-.05	.13	1.0000	0.
5	0	1	.583	.12	.26	-1.0000	0.	-.13	.48	-.13	.26	-1.0000	0.
-7	0	3	.680	.13	.06	1.0000	0.	.07	2.20	.07	.06	1.0000	0.
-6	0	3	.593	.23	.23	-1.0000	0.	-.00	.98	-.00	.23	-1.0000	0.
-5	0	3	.501	.23	.34	-1.0000	0.	-.10	.69	-.10	.34	-1.0000	0.
-4	0	3	.416	.21	.05	-1.0000	0.	.16	4.14	.16	.05	-1.0000	0.
-3	0	3	.344	.22	.03	-1.0000	0.	.19	7.24	.19	.03	-1.0000	0.
-2	0	3	.294	.25	.36	1.0000	0.	-.12	.67	-.12	.36	1.0000	0.
-1	0	3	.278	.49	.80	1.0000	0.	-.31	.61	-.31	.80	1.0000	0.
0	0	3	.302	.52	.24	-1.0000	0.	.28	2.16	.28	.24	-1.0000	0.
1	0	3	.358	.57	.42	-1.0000	0.	.15	1.37	.15	.42	-1.0000	0.
2	0	3	.434	.33	.45	-1.0000	0.	-.12	.74	-.12	.45	-1.0000	0.
3	0	3	.521	.06	.05	-1.0000	0.	.00	1.02	.00	.05	-1.0000	0.
4	0	3	.614	.05	.01	1.0000	0.	.05	6.94	.05	.01	1.0000	0.
5	0	3	.711	.05	.16	1.0000	0.	-.11	.34	-.11	.16	1.0000	0.
-1	0	-6	.654	.06	.11	-1.0000	0.	-.05	.51	-.05	.11	-1.0000	0.
0	0	-6	.605	.10	.52	-1.0000	0.	-.41	.20	-.41	.52	-1.0000	0.
1	0	-6	.571	.05	.11	1.0000	0.	-.07	.42	-.07	.11	1.0000	0.
2	0	-6	.556	.10	.01	1.0000	0.	.09	9.99	.09	.01	1.0000	0.
3	0	-6	.562	.03	.00	1.0000	0.	.09	9.99	.09	.00	1.0000	0.
4	0	-6	.584	.05	.58	1.0000	0.	-.53	.08	-.53	.58	1.0000	0.
5	0	-6	.630	.05	.04	-1.0000	0.	.01	1.15	.01	.04	-1.0000	0.
6	0	-6	.688	.05	.03	1.0000	0.	.03	2.04	.03	.03	1.0000	0.
7	0	-6	.756	.04	.15	1.0000	0.	-.11	.29	-.11	.15	1.0000	0.
-4	0	4	.458	.50	.81	-1.0000	0.	-.31	.62	-.31	.81	-1.0000	0.
-3	0	4	.435	.57	.60	1.0000	0.	-.04	.94	-.04	.60	1.0000	0.
-2	0	4	.375	.09	.10	1.0000	0.	-.01	.89	-.01	.10	1.0000	0.
-1	0	4	.374	.31	.36	-1.0000	0.	-.06	.85	-.06	.36	-1.0000	0.
0	0	4	.403	.47	.79	1.0000	0.	-.32	.60	-.32	.79	1.0000	0.
1	0	4	.456	.66	.55	-1.0000	0.	.12	1.21	.12	.55	-1.0000	0.
2	0	4	.526	.16	.36	-1.0000	0.	-.20	.44	-.20	.36	-1.0000	0.
-7	0	2	.696	.09	.21	1.0000	0.	-.12	.43	-.12	.21	1.0000	0.
-6	0	2	.593	.21	.06	-1.0000	0.	.14	3.21	.14	.06	-1.0000	0.
-5	0	2	.493	.43	.32	-1.0000	0.	.11	1.34	.11	.32	-1.0000	0.
-4	0	2	.395	.35	.39	1.0000	0.	-.04	.90	-.04	.39	1.0000	0.
-3	0	2	.305	.72	1.51	-1.0000	0.	-.79	.48	-.79	1.51	-1.0000	0.
-2	0	2	.229	.20	.74	-1.0000	0.	-.55	.26	-.55	.74	-1.0000	0.
-1	0	2	.187	.41	1.43	1.0000	0.	-1.02	.29	-1.02	1.43	1.0000	0.
0	0	2	.202	.70	2.39	-1.0000	0.	-1.70	.29	-1.70	2.39	-1.0000	0.
1	0	2	.263	.48	.98	1.0000	0.	-.50	.49	-.50	.98	1.0000	0.
2	0	2	.347	.33	.59	1.0000	0.	-.26	.56	-.26	.59	1.0000	0.
3	0	2	.442	.27	.32	-1.0000	0.	-.05	.85	-.05	.32	-1.0000	0.
4	0	2	.541	.27	.60	1.0000	0.	-.33	.45	-.33	.60	1.0000	0.
5	0	2	.642	.04	.06	1.0000	0.	-.02	.72	-.02	.06	1.0000	0.
-3	0	5	.479	.21	.00	-1.0000	0.	.20	9.99	.20	.00	-1.0000	0.
-2	0	5	.463	.12	.07	-1.0000	0.	.05	1.71	.05	.07	-1.0000	0.
-1	0	5	.472	.12	.26	-1.0000	0.	-.14	.47	-.14	.26	-1.0000	0.
0	0	5	.504	.08	.17	-1.0000	0.	-.09	.49	-.09	.17	-1.0000	0.
-6	0	6	.688	.03	.03	1.0000	0.	.05	3.09	.05	.03	1.0000	0.
-5	0	6	.633	.06	.04	-1.0000	0.	.02	1.42	.02	.04	-1.0000	0.
-4	0	6	.588	.21	.58	1.0000	0.	-.37	.36	-.37	.58	1.0000	0.
-3	0	6	.562	.12	.00	1.0000	0.	.12	9.99	.12	.00	1.0000	0.
-2	0	6	.555	.20	.01	1.0000	0.	.19	9.99	.19	.01	1.0000	0.
-1	0	6	.571	.05	.11	1.0000	0.	-.07	.40	-.07	.11	1.0000	0.
0	0	6	.605	.05	.52	-1.0000	0.	-.45	.10	-.45	.52	-1.0000	0.

1	0	6	.654	.14	.11	-1.0000	0.	.03	1.29	.03	.11	-1.0000	0.
-3	0	-4	.607	.05	.18	1.0000	0.	-.13	.27	-.13	.18	1.0000	0.
-2	0	-4	.526	.10	.36	-1.0000	0.	-.26	.29	-.26	.36	-1.0000	0.
-1	0	-4	.456	.94	.55	-1.0000	0.	.39	1.72	.39	.55	-1.0000	0.
0	0	-4	.403	.46	.79	1.0000	0.	-.32	.59	-.32	.79	1.0000	0.
1	0	-4	.374	.45	.36	-1.0000	0.	.09	1.24	.09	.36	-1.0000	0.
2	0	-4	.375	.34	.10	1.0000	0.	.24	3.43	.24	.10	1.0000	0.
3	0	-4	.405	.77	.60	1.0000	0.	.16	1.27	.16	.60	1.0000	0.
4	0	-4	.458	.58	.81	-1.0000	0.	-.23	.71	-.23	.81	-1.0000	0.
5	0	-4	.529	.06	.04	-1.0000	0.	.02	1.46	.02	.04	-1.0000	0.
0	0	-5	.504	.05	.17	-1.0000	0.	-.12	.29	-.12	.17	-1.0000	0.
1	0	-5	.472	.05	.26	-1.0000	0.	-.21	.20	-.21	.26	-1.0000	0.
2	0	-5	.463	.07	.07	-1.0000	0.	.00	1.02	.00	.07	-1.0000	0.
3	0	-5	.479	.49	.00	-1.0000	0.	.49	9.99	.49	.00	-1.0000	0.
4	0	-5	.517	.15	.21	-1.0000	0.	-.06	.73	-.06	.21	-1.0000	0.
5	0	-5	.573	.07	.08	1.0000	0.	-.01	.91	-.01	.08	1.0000	0.
-5	0	-1	.583	.21	.26	-1.0000	0.	-.05	.80	-.05	.26	-1.0000	0.
-4	0	-1	.477	.11	.13	1.0000	0.	-.02	.87	-.02	.13	1.0000	0.
-3	0	-1	.373	.10	.24	-1.0000	0.	-.14	.42	-.14	.24	-1.0000	0.
-2	0	-1	.270	.63	1.04	1.0000	0.	-.41	.60	-.41	1.04	1.0000	0.
-1	0	-1	.174	1.23	2.74	1.0000	0.	-1.50	.45	-1.50	2.74	1.0000	0.
0	0	-1	.101	.90	2.63	1.0000	0.	-1.73	.34	-1.73	2.63	1.0000	0.
1	0	-1	.115	.31	.17	1.0000	0.	.13	1.77	.13	.17	1.0000	0.
2	0	-1	.198	.11	.70	-1.0000	0.	-.59	.15	-.59	.70	-1.0000	0.
3	0	-1	.297	.52	1.01	-1.0000	0.	-.49	.51	-.49	1.01	-1.0000	0.
4	0	-1	.400	.56	1.09	-1.0000	0.	-.54	.51	-.54	1.09	-1.0000	0.
5	0	-1	.505	.08	.03	-1.0000	0.	.05	2.61	.05	.03	-1.0000	0.
-5	0	0	.536	.33	.31	-1.0000	0.	.02	1.06	.02	.31	-1.0000	0.
-4	0	0	.429	3.06	1.61	-1.0000	0.	1.45	1.93	1.45	1.61	-1.0000	0.
-3	0	0	.321	.15	.31	1.0000	0.	-.16	.49	-.16	.31	1.0000	0.
-2	0	0	.214	.12	.22	1.0000	0.	-.09	.57	-.09	.22	1.0000	0.
-1	0	0	.107	.85	1.39	1.0000	0.	-.53	.61	-.53	1.39	1.0000	0.
1	0	0	.107	.97	1.39	1.0000	0.	-.42	.70	-.42	1.39	1.0000	0.
2	0	0	.214	.12	.22	1.0000	0.	-.09	.57	-.09	.22	1.0000	0.
3	0	0	.321	.19	.31	1.0000	0.	-.12	.60	-.12	.31	1.0000	0.
4	0	0	.429	1.88	1.61	-1.0000	0.	.27	1.17	.27	1.61	-1.0000	0.
5	0	0	.536	.16	.31	-1.0000	0.	-.15	.51	-.15	.31	-1.0000	0.
-2	0	-3	.434	.13	.45	-1.0000	0.	-.32	.29	-.32	.45	-1.0000	0.
-1	0	-3	.358	.42	.42	-1.0000	0.	.00	1.00	.00	.42	-1.0000	0.
0	0	-3	.302	.39	.24	-1.0000	0.	.15	1.64	.15	.24	-1.0000	0.
1	0	-3	.278	.47	.80	1.0000	0.	-.33	.59	-.33	.80	1.0000	0.
2	0	-3	.294	.37	.36	1.0000	0.	.01	1.02	.01	.36	1.0000	0.
3	0	-3	.344	.12	.03	-1.0000	0.	.09	3.00	.09	.03	-1.0000	0.
4	0	-3	.416	.40	.05	-1.0000	0.	.35	7.72	.35	.05	-1.0000	0.
5	0	-3	.501	.51	.34	-1.0000	0.	.17	1.49	.17	.34	-1.0000	0.
-4	0	-2	.541	.30	.60	1.0000	0.	-.30	.50	-.30	.60	1.0000	0.
-3	0	-2	.442	.50	.32	-1.0000	0.	.18	1.57	.18	.32	-1.0000	0.
-2	0	-2	.347	.16	.59	1.0000	0.	-.43	.27	-.43	.59	1.0000	0.
-1	0	-2	.263	.40	.98	1.0000	0.	-.57	.41	-.57	.98	1.0000	0.
0	0	-2	.202	.97	2.39	-1.0000	0.	-1.42	.40	-1.42	2.39	-1.0000	0.
1	0	-2	.187	.49	1.43	1.0000	0.	-.94	.34	-.94	1.43	1.0000	0.
2	0	-2	.229	.22	.74	-1.0000	0.	-.52	.29	-.52	.74	-1.0000	0.
3	0	-2	.305	.56	1.51	-1.0000	0.	-.95	.37	-.95	1.51	-1.0000	0.
4	0	-2	.395	.15	.39	1.0000	0.	-.24	.39	-.24	.39	1.0000	0.
5	0	-2	.493	.12	.32	-1.0000	0.	-.20	.39	-.20	.32	-1.0000	0.
6	0	-2	.593	.07	.06	-1.0000	0.	.03	1.03	.03	.06	-1.0000	0.
0	0	0	0.	11.50	11.50	1.0000	0.	0.	*0.	0.	11.50	1.0000	0.
999	999	999	999.00	999.00	999.00	999.0000	999.0000	999.00	1.03	999.00			

* ZERO WEIGHTED DATA.

A= 5.07700

PARAMETER	E.S.D.	LAST SHIFT	SCALE
1	.061197	-.013255	
2	0.	0.	N
3	0.	0.	N
4	0.	0.	N
5	.915373	-.053609	N
6	.008833	.000045	01
7	.014473	-.003105	01
8	.009795	-.003586	01
9	.949672	-.138128	01
10	.011919	.001096	02
11	.016717	.003751	02
12	.014353	-.005992	02
13	1.431024	.523941	02
14	.006627	.000602	01
15	.014803	.004428	01
16	.010340	.004235	01
17	.841913	-.085618	01
18	.010835	-.000757	02
19	.014832	-.000931	02
20	.013184	.004933	02
21	1.281846	-.602183	02

1	-9	0	.726	.10	.16	.7659	-.6429	-.05	.66	-.05	.16	.7659	-.6429
1	-8	0	.647	.13	.44	.9945	-.1050	-.31	.30	-.31	.44	.9945	-.1050
1	-7	0	.569	.16	.07	.9922	.1245	.10	2.48	.10	.07	.9922	.1245
1	-6	0	.491	.75	.25	-.0651	.9979	.50	3.05	.50	.25	-.0651	.9979
1	-5	0	.413	.28	.52	.3413	.9399	-.24	.54	-.24	.52	.3413	.9399
1	-4	0	.337	.99	1.05	-.9632	-.2687	-.06	.94	-.06	1.05	-.9632	-.2687
1	-3	0	.262	1.56	1.37	.1163	.9932	.19	1.14	.19	1.37	.1163	.9932
1	-2	0	.192	2.70	2.21	-.2624	-.9650	.49	1.22	.49	2.21	-.2624	-.9650
1	-1	0	.134	9.43	3.46	.0559	.9984	5.97	2.72	5.97	3.46	.0559	.9984
1	0	0	.107	1.16	1.47	1.0000	0.	-.31	.79	-.31	1.47	1.0000	0.
1	1	0	.134	1.55	3.46	-.0559	.9984	-1.91	.45	-1.91	3.46	-.0559	.9984
1	2	0	.192	1.01	2.21	-.2624	.9650	-1.19	.46	-1.19	2.21	-.2624	.9650
1	3	0	.262	.99	1.37	-.1163	.9932	-.38	.72	-.38	1.37	-.1163	.9932
1	4	0	.337	.90	1.05	-.9632	.2687	-.15	.86	-.15	1.05	-.9632	.2687
1	5	0	.413	.28	.52	-.3413	.9399	-.24	.54	-.24	.52	-.3413	.9399
-3	-2	0	.359	.08	.71	.4199	.9076	-.62	.12	-.62	.71	.4199	.9076
-3	-1	0	.331	.38	.96	-.1476	-.9890	-.58	.39	-.58	.96	-.1476	-.9890
-3	0	0	.321	.33	.35	1.0000	0.	-.03	.92	-.03	.35	1.0000	0.
-3	1	0	.331	.81	.96	.1476	-.9890	-.15	.84	-.15	.96	.1476	-.9890
-3	2	0	.359	.69	.71	.4199	-.9076	-.02	.97	-.02	.71	.4199	-.9076
-3	3	0	.401	.55	.69	.3686	-.9296	-.14	.83	-.14	.69	.3686	-.9296
-3	4	0	.453	.44	.38	.4876	-.8731	.06	1.16	.06	.38	.4876	-.8731
-3	5	0	.512	.11	.40	.8508	-.5255	-.29	.27	-.29	.40	.8508	-.5255
-3	6	0	.577	.08	.26	-.4198	-.9076	-.19	.29	-.19	.26	-.4198	-.9076
-3	7	0	.644	.10	.18	.9999	-.0167	-.08	.55	-.08	.18	.9999	-.0167
-3	8	0	.715	.10	.39	-.7844	-.6202	-.29	.26	-.29	.39	-.7844	-.6202
-2	-3	0	.321	.32	.52	-.1367	.9906	-.19	.62	-.19	.52	-.1367	.9906
-2	-2	0	.267	.88	.77	.0866	-.9962	.11	1.14	.11	.77	.0866	-.9962
-2	-1	0	.229	.87	1.26	-.5093	.8606	-.39	.69	-.39	1.26	-.5093	.8606
-2	0	0	.214	.70	.48	1.0000	0.	.22	1.46	.22	.48	1.0000	0.
-2	1	0	.229	.98	1.26	.5093	.8606	-.28	.78	-.28	1.26	.5093	.8606
-2	2	0	.267	.96	.77	.0866	.9962	.19	1.24	.19	.77	.0866	.9962
-2	3	0	.321	.92	.52	.1367	.9906	.41	1.78	.41	.52	.1367	.9906
-2	4	0	.334	.83	.41	-.7945	.6073	.43	2.05	.43	.41	-.7945	.6073
-2	5	0	.453	.33	.33	.9935	.1142	.01	1.02	.01	.33	.9935	.1142
-2	6	0	.524	.08	.04	-.9388	.3444	.04	2.08	.04	.04	-.9388	.3444
-1	-6	0	.491	.10	.25	-.0651	.9979	-.15	.40	-.15	.25	-.0651	.9979
-1	-5	0	.413	.59	.52	-.3413	-.9399	-.43	.17	-.43	.52	-.3413	-.9399
-1	-4	0	.337	.19	1.05	-.9632	-.2687	-.86	.18	-.86	1.05	-.9632	-.2687
-1	-3	0	.262	.73	1.37	-.1163	-.9932	-.64	.54	-.64	1.37	-.1163	-.9932

-1	-2	0	.192	.81	2.21	-.2624	-.9650	-1.40	.37	-1.40	2.21	-.2624	-.9650
-1	-1	0	.134	1.45	3.46	-.0559	-.9984	-2.01	.42	-2.01	3.46	-.0559	-.9984
-1	0	0	.107	.78	1.47	1.0000	0.	-.68	.53	-.68	1.47	1.0000	0.
-1	1	0	.134	4.78	3.46	.0559	-.9984	1.31	1.38	1.31	3.46	.0559	-.9984
-1	2	0	.192	3.75	2.21	-.2624	.9650	1.54	1.76	1.54	2.21	-.2624	.9650
-1	3	0	.262	1.87	1.37	.1163	-.9932	.50	1.36	.50	1.37	.1163	-.9932
-1	4	0	.337	1.57	1.05	-.9632	.2687	.53	1.50	.53	1.05	-.9632	.2687
-1	5	0	.413	.92	.52	.3413	-.9399	.40	1.78	.40	.52	.3413	-.9399
-1	6	0	.491	.13	.25	-.0651	-.9979	-.12	.53	-.12	.25	-.0651	-.9979
0	-6	0	.479	.17	.30	.5755	.8178	-.13	.57	-.13	.30	.5755	.8178
0	-4	0	.319	.46	.94	.6568	-.7541	-.49	.49	-.49	.94	.6568	-.7541
0	-2	0	.160	4.22	5.13	.8307	-.5567	-.90	.82	-.90	5.13	.8307	-.5567
0	2	0	.160	5.59	5.13	.8307	.5567	.56	1.11	.56	5.13	.8307	.5567
0	4	0	.319	1.06	.94	.6568	.7541	.11	1.12	.11	.94	.6568	.7541
0	6	0	.479	.42	.30	.5755	-.8178	.13	1.42	.13	.30	.5755	-.8178
5	-4	0	.624	.10	.19	.9994	-.0359	-.10	.50	-.10	.19	.9994	-.0359
5	-3	0	.587	.12	.50	-.2758	-.9612	-.37	.25	-.37	.50	-.2758	-.9612
5	-2	0	.559	.14	.31	-.0183	.9998	-.17	.45	-.17	.31	-.0183	.9998
5	-1	0	.542	.85	.94	-.1153	-.9933	-.10	.90	-.10	.94	-.1153	-.9933
5	0	0	.536	.09	.43	-1.0000	0.	-.34	.21	-.34	.43	-1.0000	0.
5	1	0	.542	.36	.94	.1153	-.9933	-.58	.39	-.58	.94	.1153	-.9933
5	2	0	.559	.14	.31	-.0183	-.9998	-.17	.45	-.17	.31	-.0183	-.9998
5	3	0	.587	.16	.50	.2758	-.9612	-.33	.33	-.33	.50	.2758	-.9612
5	4	0	.624	.15	.19	.9994	.0359	-.05	.76	-.05	.19	.9994	.0359
5	5	0	.668	.10	.23	.1538	-.9881	-.13	.43	-.13	.23	.1538	-.9881
5	6	0	.718	.10	.21	-.2056	.9786	-.11	.49	-.11	.21	-.2056	.9786
4	-8	0	.769	.09	.11	.2118	-.9773	-.02	.83	-.02	.11	.2118	-.9773
4	-7	0	.704	.10	.18	-.9689	-.2476	-.07	.59	-.07	.18	-.9689	-.2476
4	-6	0	.643	.14	.11	-.9414	.3372	.03	1.22	.03	.11	-.9414	.3372
4	-5	0	.586	.11	.22	-.9610	.2766	-.11	.49	-.11	.22	-.9610	.2766
4	-4	0	.534	.24	.47	-.6760	.7369	-.23	.51	-.23	.47	-.6760	.7369
4	-3	0	.491	.16	.30	-.9597	.2809	-.14	.53	-.14	.30	-.9597	.2809
4	-2	0	.457	1.44	1.30	-.8614	.5080	.14	1.11	.14	1.30	-.8614	.5080
4	-1	0	.436	.50	.25	-.9972	.0751	.24	1.96	.24	.25	-.9972	.0751
4	0	0	.429	2.08	2.10	-1.0000	0.	-.02	.99	-.02	2.10	-1.0000	0.
4	1	0	.436	.13	.25	.9972	.0751	-.12	.52	-.12	.25	.9972	.0751
4	2	0	.457	.93	1.30	-.8614	-.5080	-.37	.72	-.37	1.30	-.8614	-.5080
4	3	0	.491	.14	.30	.9597	.2809	-.16	.46	-.16	.30	.9597	.2809
4	4	0	.534	.45	.47	-.6760	-.7369	-.02	.96	-.02	.47	-.6760	-.7369
4	5	0	.586	.12	.22	.9610	.2766	-.10	.53	-.10	.22	.9610	.2766
4	6	0	.643	.15	.11	-.9414	-.3372	.04	1.31	.04	.11	-.9414	-.3372
4	7	0	.704	.09	.18	.9689	-.2476	-.09	.51	-.09	.18	.9689	-.2476
3	-8	0	.715	.14	.39	-.7844	.6202	-.25	.35	-.25	.39	-.7844	.6202
3	-7	0	.644	.20	.18	.9999	.0167	.02	1.10	.02	.18	.9999	.0167
3	-6	0	.577	.33	.26	-.4198	.9076	.11	1.43	.11	.26	-.4198	.9076
3	-5	0	.512	.20	.40	.8508	.5255	-.19	.51	-.19	.40	.8508	.5255
3	-4	0	.453	.97	.38	.4876	.8731	.58	2.53	.58	.38	.4876	.8731
3	-3	0	.401	.88	.69	.3686	.9296	.19	1.27	.19	.69	.3686	.9296
3	-2	0	.359	1.66	.71	.4199	.9076	.95	2.34	.95	.71	.4199	.9076
3	-1	0	.331	1.70	.96	.1476	.9890	.74	1.77	.74	.96	.1476	.9890
3	0	0	.321	.36	.35	1.0000	0.	.51	2.43	.51	.35	1.0000	0.
3	1	0	.331	1.30	.96	-.1476	.9890	.64	1.04	.04	.96	-.1476	.9890
3	2	0	.359	.52	.71	.4199	-.9076	-.19	.73	-.19	.71	.4199	-.9076
3	3	0	.401	.55	.69	-.3686	.9296	-.14	.80	-.14	.69	-.3686	.9296
3	4	0	.453	.67	.38	.4876	-.8731	.29	1.76	.29	.38	.4876	-.8731
3	5	0	.512	.13	.40	-.8508	.5255	-.22	.45	-.22	.40	-.8508	.5255
3	6	0	.577	.16	.26	-.4198	-.9076	-.10	.62	-.10	.26	-.4198	-.9076
3	7	0	.644	.13	.18	-.9999	.0167	-.08	.55	-.08	.18	-.9999	.0167
2	-9	0	.749	.37	.61	.6709	.7415	-.52	.15	-.52	.61	.6709	.7415
2	-8	0	.673	.15	.09	.9548	-.2971	.06	1.62	.06	.09	.9548	-.2971
2	-7	0	.598	.22	.36	.4982	.8670	-.14	.61	-.14	.36	.4982	.8670
2	-6	0	.524	.33	.64	-.9338	-.3444	.30	4.13	.33	.64	-.9338	-.3444

2	-5	0	.453	.51	.33	.9935	-.1142	.18	1.56	.18	.33	.9935	-.1142
2	-4	0	.384	.71	.41	-.7945	-.6073	.31	1.75	.31	.41	-.7945	-.6073
2	-3	0	.321	1.44	.52	.1367	-.9906	.92	2.79	.92	.52	.1367	-.9906
2	-2	0	.247	2.29	.77	.0866	-.9962	1.52	2.57	1.52	.77	.0866	-.9962
2	-1	0	.229	1.98	1.26	.5093	-.8606	.72	1.57	.72	1.26	.5093	-.8606
2	0	0	.214	.88	.48	1.0000	0.	.40	1.82	.40	.48	1.0000	0.
2	1	0	.229	1.28	1.26	-.5093	-.8606	.02	1.02	.02	1.26	-.5093	-.8606
2	2	0	.267	.92	.77	.0866	.9962	.15	1.19	.15	.77	.0866	.9962
2	3	0	.321	.98	.52	-.1367	-.9906	.47	1.90	.47	.52	-.1367	-.9906
2	4	0	.384	.62	.41	-.7945	.6073	.21	1.52	.21	.41	-.7945	.6073
2	5	0	.453	.63	.33	-.9945	-.1142	.30	1.92	.30	.33	-.9935	-.1142
2	6	0	.524	.39	.04	-.5388	.3444	.06	2.39	.06	.04	-.5388	.3444
2	7	0	.598	.39	.36	-.4982	.8670	-.27	.25	-.27	.36	-.4982	.8670
-5	0	1	.505	.62	.22	-1.0000	0.	.40	2.77	.40	.22	-1.0000	0.
-4	0	1	.400	3.49	1.55	-1.0000	0.	1.94	2.25	1.94	1.55	-1.0000	0.
-3	0	1	.297	1.60	1.02	-1.0000	0.	.58	1.57	.58	1.02	-1.0000	0.
-2	0	1	.198	.61	.59	-1.0000	0.	.02	1.04	.02	.59	-1.0000	0.
-1	0	1	.115	.65	.27	1.0000	0.	.38	2.39	.38	.27	1.0000	0.
0	0	1	.101	1.45	2.60	1.0000	0.	-1.15	.56	-1.15	2.60	1.0000	0.
1	0	1	.174	1.54	2.86	1.0000	0.	-1.02	.64	-1.02	2.86	1.0000	0.
2	0	1	.270	1.06	1.15	1.0000	0.	-.09	.92	-.09	1.15	1.0000	0.
3	0	1	.373	.53	.39	-1.0000	0.	.15	1.38	.15	.39	-1.0000	0.
4	0	1	.477	.16	.16	1.0000	0.	-.01	.96	-.01	.16	1.0000	0.
5	0	1	.583	.24	.38	-1.0000	0.	-.15	.62	-.15	.38	-1.0000	0.
-7	0	3	.649	.26	.04	1.0000	0.	.22	6.19	.22	.04	1.0000	0.
-6	0	3	.593	.44	.45	-1.0000	0.	-.00	.99	-.00	.45	-1.0000	0.
-5	0	3	.501	.45	.46	-1.0000	0.	-.00	.99	-.00	.46	-1.0000	0.
-4	0	3	.416	.41	.27	1.0000	0.	.14	1.52	.14	.27	1.0000	0.
-3	0	3	.344	.42	.23	1.0000	0.	.18	1.78	.18	.23	1.0000	0.
-2	0	3	.294	.47	.50	1.0000	0.	-.03	.94	-.03	.50	1.0000	0.
-1	0	3	.278	.94	.60	1.0000	0.	.34	1.57	.34	.60	1.0000	0.
0	0	3	.302	1.01	.53	-1.0000	0.	.48	1.91	.48	.53	-1.0000	0.
1	0	3	.358	1.10	.87	-1.0000	0.	.23	1.27	.23	.87	-1.0000	0.
2	0	3	.434	.64	.83	-1.0000	0.	-.19	.77	-.19	.83	-1.0000	0.
3	0	3	.521	.11	.10	-1.0000	0.	.01	1.06	.01	.10	-1.0000	0.
4	0	3	.614	.11	.05	-1.0000	0.	.06	2.19	.06	.05	-1.0000	0.
5	0	3	.711	.10	.43	1.0000	0.	-.33	.24	-.33	.43	1.0000	0.
-1	0	-6	.654	.11	.14	-1.0000	0.	-.03	.76	-.03	.14	-1.0000	0.
0	0	-6	.605	.23	.90	-1.0000	0.	-.71	.22	-.71	.90	-1.0000	0.
1	0	-6	.571	.09	.18	1.0000	0.	-.09	.52	-.09	.18	1.0000	0.
2	0	-6	.556	.19	.01	-1.0000	0.	.17	9.99	.17	.01	-1.0000	0.
3	0	-6	.562	.17	.04	1.0000	0.	.13	4.24	.13	.04	1.0000	0.
4	0	-6	.588	.09	.09	1.0000	0.	-.89	.09	-.89	.09	1.0000	0.
5	0	-6	.630	.10	.08	-1.0000	0.	.02	1.29	.02	.08	-1.0000	0.
6	0	-6	.683	.10	.03	1.0000	0.	.07	3.83	.07	.03	1.0000	0.
7	0	-6	.756	.09	.23	1.0000	0.	-.14	.34	-.14	.23	1.0000	0.
-4	0	4	.458	.96	.78	-1.0000	0.	.18	1.23	.18	.78	-1.0000	0.
-3	0	4	.405	1.09	1.21	1.0000	0.	-.12	.90	-.12	1.21	1.0000	0.
-2	0	4	.375	.17	.52	1.0000	0.	-.35	.33	-.35	.52	1.0000	0.
-1	0	4	.374	.59	.47	-1.0000	0.	.12	1.26	.12	.47	-1.0000	0.
0	0	4	.423	.90	.80	1.0000	0.	.10	1.12	.10	.80	1.0000	0.
1	0	4	.456	1.28	1.06	-1.0000	0.	.22	1.20	.22	1.06	-1.0000	0.
2	0	4	.526	.31	.71	-1.0000	0.	-.41	.43	-.41	.71	-1.0000	0.
-7	0	2	.696	.17	.36	1.0000	0.	-.19	.48	-.19	.36	1.0000	0.
-6	0	2	.593	.40	.12	-1.0000	0.	.28	3.35	.28	.12	-1.0000	0.
-5	0	2	.493	.84	.61	-1.0000	0.	.22	1.36	.22	.61	-1.0000	0.
-4	0	2	.395	.67	.52	1.0000	0.	.15	1.29	.15	.52	1.0000	0.
-3	0	2	.305	1.39	1.62	-1.0000	0.	-.24	.85	-.24	1.62	-1.0000	0.
-2	0	2	.229	.38	.42	-1.0000	0.	-.44	.46	-.44	.82	-1.0000	0.
-1	0	2	.187	.79	1.35	1.0000	0.	-.55	.59	-.55	1.35	1.0000	0.
0	0	2	.202	1.34	2.77	-1.0000	0.	-1.43	.48	-1.43	2.77	-1.0000	0.
1	0	2	.263	.93	.98	1.0000	0.	-.65	.94	-.65	.98	1.0000	0.

2	0	2	.347	.63	.44	1.0000	0.	.19	1.44	.19	.44	1.0000	0.
3	0	2	.442	.52	.52	-1.0000	0.	.00	1.01	.00	.52	-1.0000	0.
4	0	2.	.541	.52	.84	1.0000	0.	-.32	.62	-.32	.84	1.0000	0.
5	0	2	.642	.08	.10	1.0000	0.	-.02	.80	-.02	.10	1.0000	0.
-3	0	5	.479	.40	.34	1.0000	0.	.06	1.18	.06	.34	1.0000	0.
-2	0	5	.463	.23	.14	1.0000	0.	.09	1.64	.09	.14	1.0000	0.
-1	0	5	.472	.24	.15	-1.0000	0.	.09	1.62	.09	.15	-1.0000	0.
0	0	5	.504	.16	.31	-1.0000	0.	-.15	.52	-.15	.31	-1.0000	0.
-6	0	6	.688	.15	.03	1.0000	0.	.13	5.80	.13	.03	1.0000	0.
-5	0	6	.630	.12	.08	-1.0000	0.	.04	1.58	.04	.08	-1.0000	0.
-4	0	6	.583	.40	.09	1.0000	0.	-.59	.40	-.59	.09	1.0000	0.
-3	0	6	.562	.23	.04	1.0000	0.	.19	5.79	.19	.04	1.0000	0.
-2	0	6	.556	.39	.01	-1.0000	0.	.37	9.99	.37	.01	-1.0000	0.
-1	0	6	.571	.09	.18	1.0000	0.	-.09	.49	-.09	.18	1.0000	0.
0	0	6	.605	.10	.90	-1.0000	0.	-.80	.11	-.80	.90	-1.0000	0.
1	0	6	.654	.28	.14	-1.0000	0.	.13	1.94	.13	.14	-1.0000	0.
-3	0	-4	.607	.09	.16	1.0000	0.	-.07	.59	-.07	.16	1.0000	0.
-2	0	-4	.526	.20	.71	-1.0000	0.	-.51	.28	-.51	.71	-1.0000	0.
-1	0	-4	.456	1.81	1.06	-1.0000	0.	.75	1.70	.75	1.06	-1.0000	0.
0	0	-4	.403	.89	.90	1.0000	0.	.09	1.11	.09	.80	1.0000	0.
1	0	-4	.374	.87	.47	-1.0000	0.	.40	1.85	.40	.47	-1.0000	0.
2	0	-4	.375	.66	.52	1.0000	0.	.14	1.27	.14	.52	1.0000	0.
3	0	-4	.405	1.48	1.21	1.0000	0.	.26	1.22	.26	1.21	1.0000	0.
4	0	-4	.458	1.11	.78	-1.0000	0.	.33	1.42	.33	.78	-1.0000	0.
5	0	-4	.529	.11	.04	1.0000	0.	.07	2.57	.07	.04	1.0000	0.
0	0	-5	.504	.10	.31	-1.0000	0.	-.21	.31	-.21	.31	-1.0000	0.
1	0	-5	.472	.10	.15	-1.0000	0.	-.04	.71	-.04	.15	-1.0000	0.
2	0	-5	.463	.14	.14	1.0000	0.	-.00	.97	-.00	.14	1.0000	0.
3	0	-5	.479	.94	.34	1.0000	0.	.60	2.79	.60	.34	1.0000	0.
4	0	-5	.517	.29	.13	-1.0000	0.	.16	2.26	.16	.13	-1.0000	0.
5	0	-5	.573	.14	.08	1.0000	0.	.06	1.65	.06	.08	1.0000	0.
-5	0	-1	.583	.40	.38	-1.0000	0.	.01	1.04	.01	.38	-1.0000	0.
-4	0	-1	.477	.21	.16	1.0000	0.	.05	1.32	.05	.16	1.0000	0.
-3	0	-1	.373	.19	.39	-1.0000	0.	-.20	.49	-.20	.39	-1.0000	0.
-2	0	-1	.270	1.21	1.15	1.0000	0.	.06	1.05	.06	1.15	1.0000	0.
-1	0	-1	.174	2.37	2.86	1.0000	0.	-.49	.83	-.49	2.86	1.0000	0.
0	0	-1	.101	1.72	2.60	1.0000	0.	-.88	.66	-.88	2.60	1.0000	0.
1	0	-1	.115	.59	.27	1.0000	0.	.32	2.17	.32	.27	1.0000	0.
2	0	-1	.198	.21	.59	-1.0000	0.	-.39	.35	-.39	.59	-1.0000	0.
3	0	-1	.297	1.00	1.02	-1.0000	0.	-.02	.98	-.02	1.02	-1.0000	0.
4	0	-1	.400	1.07	1.55	-1.0000	0.	-.48	.69	-.48	1.55	-1.0000	0.
5	0	-1	.515	.16	.22	-1.0000	0.	-.06	.72	-.06	.22	-1.0000	0.
-5	0	0	.536	.64	.43	-1.0000	0.	.21	1.50	.21	.43	-1.0000	0.
-4	0	0	.429	5.88	2.10	-1.0000	0.	3.78	2.80	3.78	2.10	-1.0000	0.
-3	0	0	.321	.29	.35	1.0000	0.	-.06	.83	-.06	.35	1.0000	0.
-2	0	0	.214	.24	.48	1.0000	0.	-.24	.50	-.24	.48	1.0000	0.
-1	0	0	.107	1.64	1.47	1.0000	0.	.17	1.12	.17	1.47	1.0000	0.
1	0	0	.107	1.86	1.47	1.0000	0.	.39	1.27	.39	1.47	1.0000	0.
2	0	0	.214	.24	.48	1.0000	0.	-.24	.50	-.24	.48	1.0000	0.
3	0	0	.321	.36	.35	1.0000	0.	.01	1.02	.01	.35	1.0000	0.
4	0	0	.429	3.61	2.10	-1.0000	0.	1.51	1.72	1.51	2.10	-1.0000	0.
5	0	0	.536	.31	.43	-1.0000	0.	-.12	.72	-.12	.43	-1.0000	0.
-2	0	-3	.434	.25	.83	-1.0000	0.	-.58	.30	-.58	.83	-1.0000	0.
-1	0	-3	.358	.80	.87	-1.0000	0.	-.07	.92	-.07	.87	-1.0000	0.
0	0	-3	.302	.76	.53	-1.0000	0.	.23	1.44	.23	.53	-1.0000	0.
1	0	-3	.278	.91	.60	1.0000	0.	.31	1.52	.31	.60	1.0000	0.
2	0	-3	.294	.72	.50	1.0000	0.	.21	1.42	.21	.50	1.0000	0.
3	0	-3	.344	.22	.23	1.0000	0.	-.01	.96	-.01	.23	1.0000	0.
4	0	-3	.416	.77	.27	1.0000	0.	.50	2.83	.50	.27	1.0000	0.
5	0	-3	.501	.98	.46	-1.0000	0.	.52	2.15	.52	.46	-1.0000	0.
-4	0	-2	.541	.53	.84	1.0000	0.	-.26	.69	-.26	.84	1.0000	0.
-3	0	-2	.442	.96	.52	-1.0000	0.	.44	1.85	.44	.52	-1.0000	0.

-2	0	-2	.347	.31	.44	1.0000	0.	-.13	.70	-.13	.44	1.0000	0.
-1	0	-2	.263	.78	.98	1.0000	0.	-.20	.79	-.20	.98	1.0000	0.
0	0	-2	.202	1.87	2.77	-1.0000	0.	-.90	.67	-.90	2.77	-1.0000	0.
1	0	-2	.187	.94	1.35	1.0000	0.	-.40	.70	-.40	1.35	1.0000	0.
2	0	-2	.229	.42	.82	-1.0000	0.	-.40	.51	-.40	.82	-1.0000	0.
3	0	-2	.305	1.08	1.62	-1.0000	0.	-.55	.66	-.55	1.62	-1.0000	0.
4	0	-2	.395	.29	.52	1.0000	0.	-.23	.56	-.23	.52	1.0000	0.
5	0	-2	.493	.24	.61	-1.0000	0.	-.37	.39	-.37	.61	-1.0000	0.
6	0	-2	.593	.13	.12	-1.0000	0.	.01	1.07	.01	.12	-1.0000	0.
0	0	0	0.	11.50	11.50	1.0000	0.	0.	*0.	0.	11.50	1.0000	0.
999	999	999	999.000	999.00	999.00	999.0000	999.0000	999.00	1.07	999.00			

* ZERO WEIGHTED DATA.

A= 5.077000
B= 6.267000
C= 5.397000
ALPHA= 90.000000
BETA=113.200000
GAMMA= 90.000000

ACKNOWLEDGMENTS

Special appreciation is expressed to Dr. Robert Glaeser who accepted the student and suggested the problem and to Drs. Cornelius Tobias and Gareth Thomas who, as members of the thesis committee offered many valuable suggestions and comments. I would also like to thank Dr. Peter Fisher for his patient and careful reading of the manuscript and for his enlightening comments, and to Dr. Allan Zalkin whose programs I have used and whose comments I have found helpful. The suggestions and collaboration of many others have contributed substantially to my efforts. In particular, I wish to thank Miss Susan Daniels, Mr. Edward Dowling, Mr. John C. Lee, Mr. Terrance Owyang, Mr. Siddharth Ray, Mrs. Helena Ruben, Mr. Arnold Steinman, Miss Ka Yee Shi, Mr. Frank Upham and Mr. Alfred Windsor for their assistance. The facilities provided by the Lawrence Radiation Laboratory greatly aided my research. I would also thank Mrs. Julia Hess for her expert typing.

This research was supported in part by the Biophysics Training Grant of the National Institute of Health, Grant No. 5 T01 GM00829.

LEGAL NOTICE

This report was prepared as an account of Government sponsored work. Neither the United States, nor the Commission, nor any person acting on behalf of the Commission:

A. Makes any warranty or representation, expressed or implied, with respect to the accuracy, completeness, or usefulness of the information contained in this report, or that the use of any information, apparatus, method, or process disclosed in this report may not infringe privately owned rights; or

B. Assumes any liabilities with respect to the use of, or for damages resulting from the use of any information, apparatus, method, or process disclosed in this report.

As used in the above, "person acting on behalf of the Commission" includes any employee or contractor of the Commission, or employee of such contractor, to the extent that such employee or contractor of the Commission, or employee of such contractor prepares, disseminates, or provides access to, any information pursuant to his employment or contract with the Commission, or his employment with such contractor.

TECHNICAL INFORMATION DIVISION
LAWRENCE RADIATION LABORATORY
UNIVERSITY OF CALIFORNIA
BERKELEY, CALIFORNIA 94720